Microstructure-Assisted Particle Pattern Generation for High Density Peptide Arrays

Zur Erlangung des akademischen Grades
Doktor der Ingenieurswissenschaften
der Fakultät für Maschinenbau des
Karlsruher Instituts für Technologie (KIT)
genehmigte **Dissertation**
von
Valentina Bykovskaya

Tag der mündlichen Prüfung: 5.04.2016
Hauptreferent: Prof. Dr. Alexander Nesterov-Müller
Korreferenten: Prof. Dr. Volker Saile

Abstract

"Smart" particles, which can carry different compounds and release them on command, are becoming the focus of various modern industrial applications. One of the impressive examples is the particle-based combinatorial synthesis of peptides arrays, where polymer particles transfer amino acids to the synthesis areas. Peptides are small fragments of proteins that can be selectively bound with antibodies.

Peptides synthesized in spots on a solid support are used to develop early disease diagnostics with a patient's sera containing antibodies. Therefore, peptide arrays are incubated with the blood sera, and the binding results are read with fluorescent methods to analyze immune responses of individuals.

With this work, we developed particle patterning processes on microstructured surfaces for the combinatorial synthesis of high density peptide arrays. The higher the density of the peptide spots, the greater the amount of information that could be obtained from the blood samples with a single readout. We worked with polymer microparticles with embedded amino acids derivatives and solid substrates with cylindrical microcavities. First, we used pulsed Nd:YAG-laser radiation to remove the particles from microstructures and transferred them to another microstructured substrate suitable for peptide synthesis. In this case, the position of each particle is determined by the laser scanning pattern. Using this method, we demonstrated combinatorial particle patterning with a pitch of $10\,\mu m$, which corresponds to 1 million spots per cm^2.

Then, we investigated the random filling of microcavities with particles to synthesize the so-called stochastic peptide arrays. In this approach, the position of the resulting peptides is decoded by optical analysis of particle deposition patterns. In a proof-of-principle experiment, we synthesized a dipeptide array with a density of 25 million peptide spots per cm^2, which is an unreachable resolution for other state-of-the-art array synthesis methods.

Kurzfassung

In die Gruppe der "smart" materials reihen sich smarte Partikel ein, die als Träger unterschiedlicher Substanzen agieren und diese unter definierten Bedingungen wieder frei lassen können. Solche Partikel schieben sich mehr und mehr in den Fokus moderner industrieller Anwendungen. Eines der eindrucksvollsten Beispiele ist die Partikel-basierte kombinatorische Synthese von Peptidarrays. Hier transportieren die Polymerpartikel Aminosäuren zu unterschiedlichen Syntheseorten.

Peptide sind kleine Fragmente von Proteinen, die selektiv durch Antikörper gebunden werden können. Die auf einem festen Träger in Spots synthetisierten Peptide werden zur Entwicklung neuer Methoden zur Früherkennung von Krankheiten auf Basis der charakteristischen Bindungsmuster der Antikörper aus Patientenseren eingesetzt. Hierbei werden Peptidarrays mit den Blutseren inkubiert und die Bindungsereignisse mit Fluoreszenz-Verfahren ausgelesen.

In dieser Arbeit wurden Prozesse zur Partikelstrukturierung für die kombinatorische Synthese von hochdichten Peptidarrays mit Hilfe mikrostrukturierter Oberflächen entwickelt. Je höher die Dichte der Peptidspots ist, umso mehr Krankheits-relevante Information kann aus den Blutproben ermittelt werden. Wir verwenden Polymermikropartikeln mit eingebetteten Aminosäuren-Derivaten und feste Substrate mit zylindrischen Mikrokavitäten. Im Zuge der Arbeit wurde der Übertrag der Partikel aus den Mikrokavitäten und deren Transport zu anderen Mikrokavitäten mit Hilfe von gepulster Nd:YAG-Laserstrahlung untersucht. In diesem Fall wird die Position jedes Partikels und somit die Position der Aminosäuresequenzen durch das Lasserscanningmuster definiert.

Mit dieser Methode ist es gelungen, kombinatorische Partikelmuster mit einem Pitch von 10 μm zu erzeugen, was einer Spotdichte von einer Million Spots pro cm^2 entspricht. AnschlieÃend wurde eine weitere Methode-die so genannten stochastischen Arrays ermittelt, die auf der zufälligen Füllung der Mikrokavitäten mit Aminosäurepartikeln basiert. Bei diesem Ansatz werden die Positionen der resultierenden Peptide durch die optische Analyse der Partikelmuster decodiert. In einem Proof-of-Principle Experiment synthetisieren wir ein Peptidarray mit einer Dichte von 25

Millionen Spots pro cm^2, die für die State-of-the-Art-Peptidarrays nicht erreichbar ist.

Contents

1 Introduction

1.1 Peptides

Peptides are molecules which can be found in any living organism on Earth, from simple bacterial strains to complex life forms.[1] In the 19th century, Emil Fischer, the German chemist and recipient of the Nobel Prize in chemistry proved that proteins and peptides are chains of amino acids.[2] Amino acids are organic molecules, which consist of amine ($-NH_2$) and carboxylic acid (-COOH) functional groups. In nature amino acids are most commonly found in the α-configuration shown in Figure 1.1, where carboxylic (also called C-terminal) and amino groups (N-terminal) are bound to the same carbon atom. Each amino acid has a special side chain R, which determines its chemical property. Up to twenty different amino acids (different side chains) can be found in natural proteins.
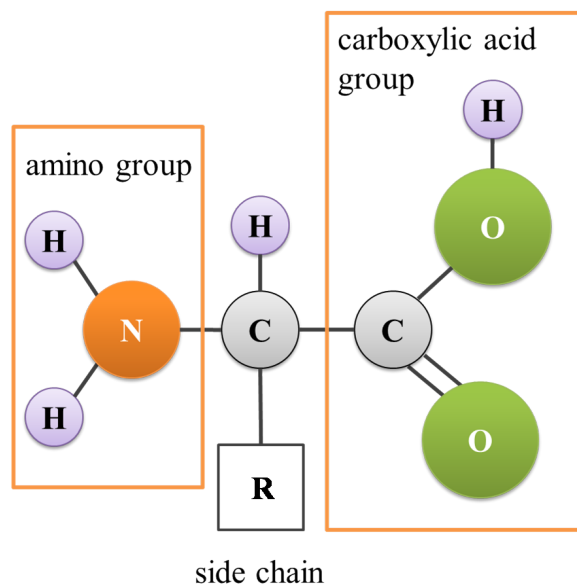
Figure 1.1: Schematic representation of amino acid molecule.

Amino acids bind together through a peptide bond, which is created through the reaction between a carboxylic group of one amino acid and an amino group of another amino acid (Figure 1.2). The result of this synthesis is joined amino acids, also called

a dipeptide, and a water molecule. The chemical properties of each peptide depend on the combination and sequence of different amino acid molecules.
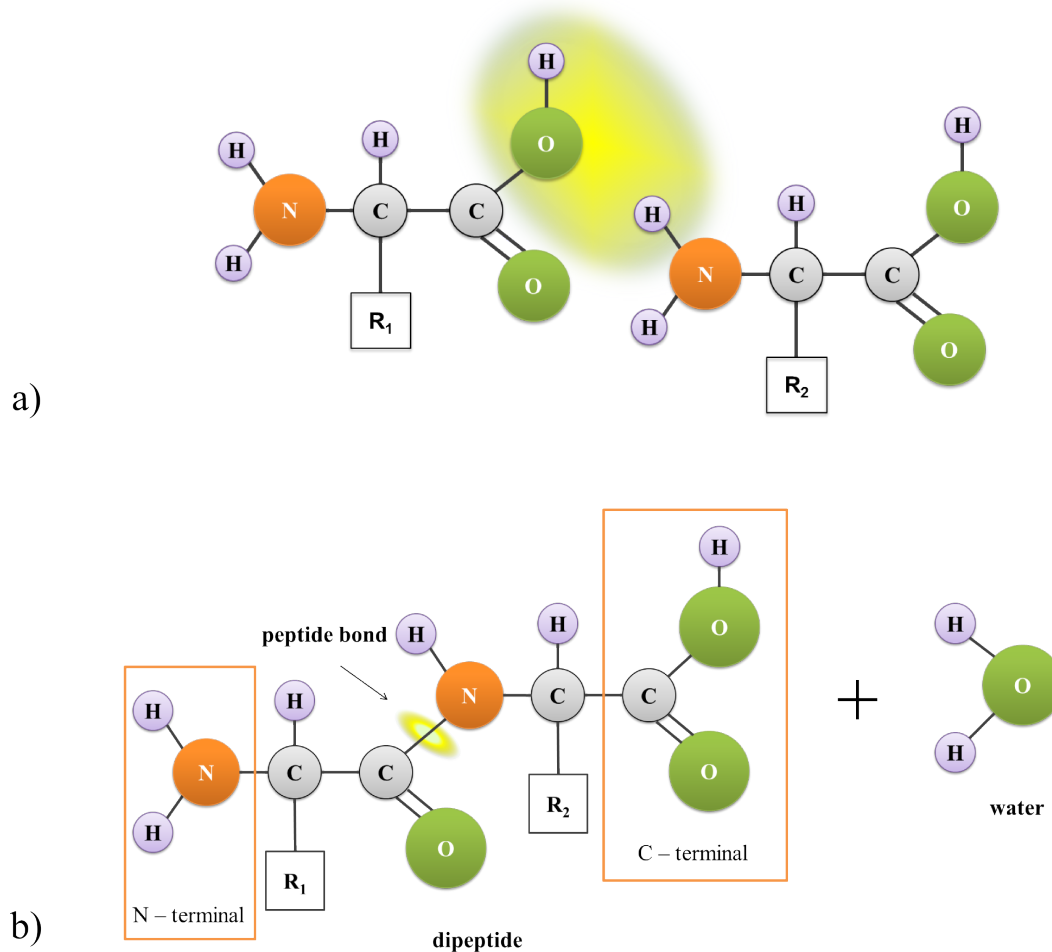
Figure 1.2: Schematic representation of the peptide bond formation. a) reaction between carboxylic group of one amino acid and amino group of another amino acid, b) the result of the synthesis is a dipeptide and a water molecule.

1.2 Peptide Arrays

Solid supports with spatially arranged peptides are called peptide arrays (Figure 1.3). This arrangement is achieved by synthesizing peptides on the spatially-defined spots on the substrate. Large varieties of peptides can be produced with the combination of 20 amino acids. Moreover, if the sequence of amino acids varies from one spot to another, the synthesis is referred to as combinatorial. If the number of spots per area (in other words, resolution) is up to 10.000 per cm^2, the arrays are called high density arrays.[3]
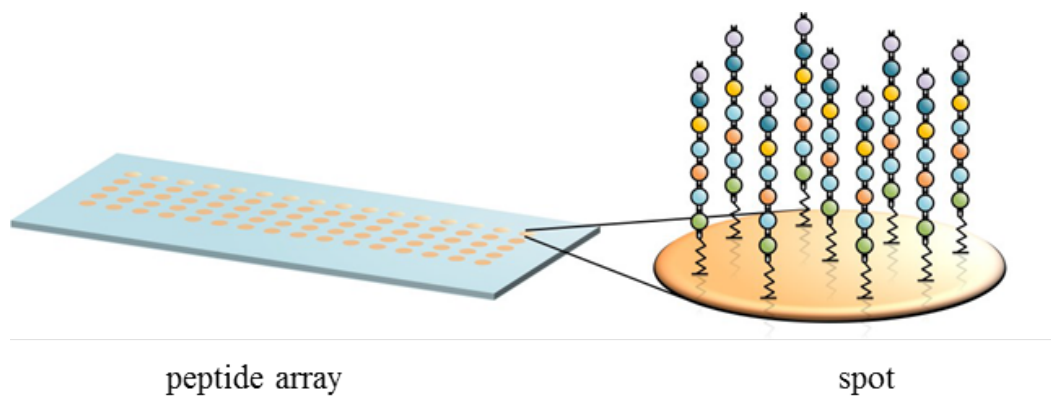
Figure 1.3: Schematic representation of peptide arrays synthesized as spatially defined spots on the solid support.[4]

High density peptide arrays are of great interest nowadays, as their use can accelerate medical research by providing the technical basis for high throughput screening of drugs, vaccines[5] or for studying of protein-protein interactions.[6] One of the examples of characterization of the interaction between antibodies and peptides is epitope mapping. For instance, bacterial cells are micromolecules, which are recognized by a human immune system as a foreign microorganism. As a response from the body, the antibodies are produced to 'attack' the alien bacterial cell. However, each individual antibody cannot neutralize the whole molecule, but can only specifically bind to a small protein fragment called epitope which consists, as a rule, of 6-12 amino acids (Figure 1.4). The identification of these epitopes, especially the amount and sequence of these amino acids, provides important information for developing therapeutic molecules and vaccines.[7]
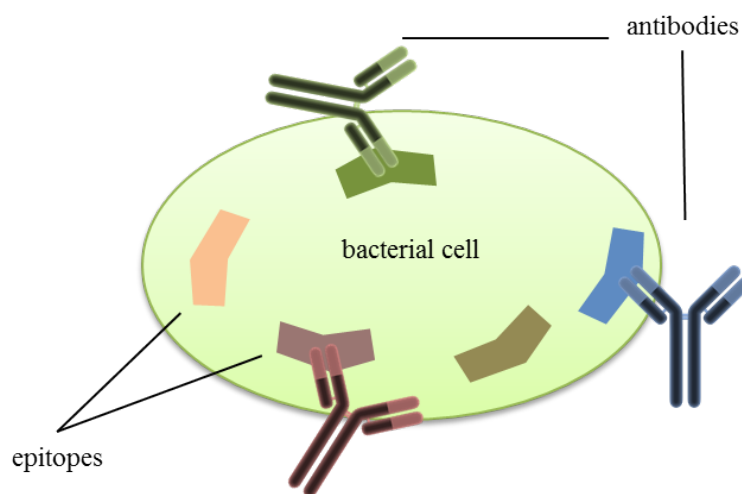
Figure 1.4: Schematic representation of bacterial cell with bounded antibodies to specific epitopes.

To analyze the response of the humoral immune system (antibody response), the library of the overlapping peptides can be used (Figure 1.5). For this, the proteins of a foreign organism, or bacteria in this case, can be considered as a long chain of amino acids. This long chain is represented by short fragment peptides, which then can be synthesized in array format. Thus the higher the spot density of peptides, the higher the amount of information that can be obtained from the screening of a single peptide array. Furthermore, using arrays with higher density significantly reduces the volume of applied reagents, as well as the costs and the amount of time required for the analysis.
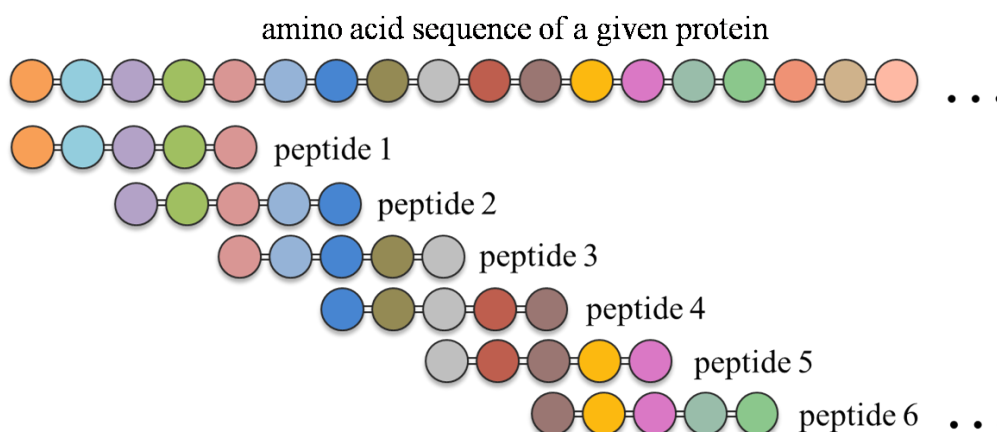
Figure 1.5: Schematic representation of amino acid sequence of a protein and overlapping linear epitopes.

1.3 Peptide Arrays Synthesis

Since the first dipeptide synthesis by E. Fischer in 1901,[8] it took more than 60 years to develop a method, with which it was only possible to synthesize longer chains of amino acids, but also to atomize the process.[9] This revolutionary solid phase synthesis technique was suggested by Merrifield in 1963 and presented two main features that automated the peptide synthesis process, namely, synthesis of peptides on the solid support (not in solution as before) and the protection of amino acid groups.
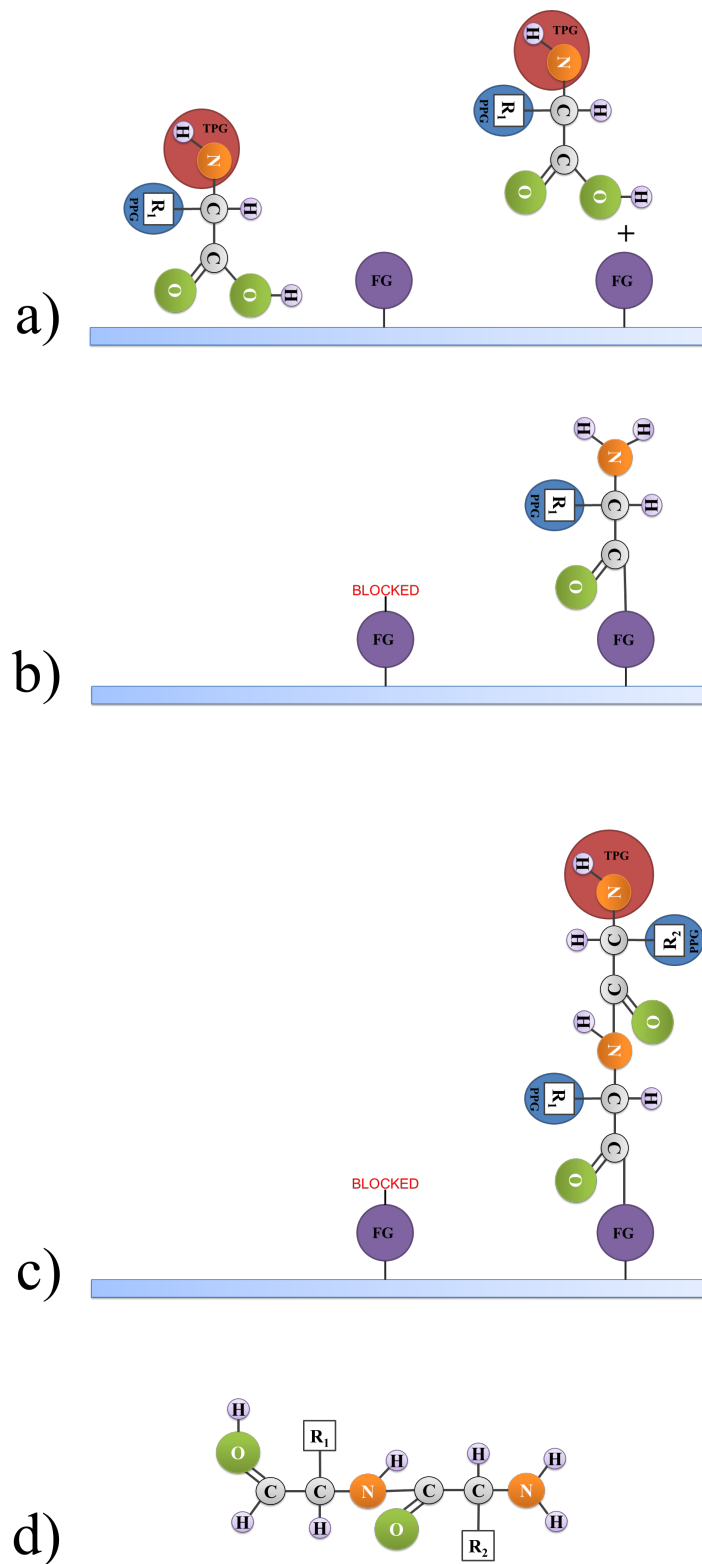
1.3.1 Solid Phase Peptide Synthesis

The main features of the solid phase peptide synthesis (SPPS) method are the introduction of a solid surface, where the synthesis of peptides takes place[10] and the use of amino acids modified with protecting groups. The surface of the solid support has

free functional groups, to which amino acids couple via their C-terminal (Figure 1.6 a).

At the time of the first coupling reaction, the N-terminals are temporarily protected, while the side chains are permanently protected for the duration of the synthesis process. This is prevent amino acids from interacting with each other and they only can couple to functional groups on the solid support. In the case, when not all of the functional groups on the support are bound with amino acids, they are deactivated through the blocking step in order to avoid synthesis of unwanted sequences. Subsequently, the temporary protection groups are removed. The washing step allows all uncoupled reagents to be removed, while the synthesis products remain covalently bound to the surface (Figure 1.6 b). Such purification of the synthesis products is technically easier than the one performed in solution. Repetition of these coupling steps results in the synthesis of the required amino acid sequences (Figure 1.6 c). At the final stage of the synthesis the side chains are cleaved and the peptide is released from the surface (Figure 1.6 d).

This method became widely known and was a starting point for peptide array synthesis. Since then, many techniques based on SPPS have been introduced, which can be divided into two main blocks - liquid-based and particle-based methods. In all of these approaches, synthesis occurs on a solid support with washing and deprotecting cycles. The main difference between the different fabrication methods is the deposition of amino acids. They can be deposited from a liquid state or in a hard matrix polymer onto a flat or structured surface. Such variety in the methods is a result of the goal to achieve the highest possible density of peptides.

Figure 1.6: Schematic representation of solid phase peptide synthesis. a) deposition of amino acids and their coupling to the functional groups on the surface, b) removal of temporary protection groups (TPG) and blocking of uncoupled functional groups, c) deposition of another layer of amino acids, d) deprotection of amino groups and side chains (PPG - permanent protection group), and release of peptide.

1.3.2 SPOT Synthesis of Peptide Arrays

SPOT synthesis on cellulose membrane was based on SPPS and was developed by Ronald Frank in 1993. It was the first method of synthesizing peptide arrays.[10] In this approach, amino acids are deposited on the functionalized surface from a liquid state. Different amino acids are separately dissolved in solutions and applied as drops on a functionalized cellulose membrane. The resulting spots have a round shape and do not overlap with each other. The cycle described in Chapter 1.3.1 then follows, it takes place at each individual spot and includes the coupling of amino acids with the functionalized groups on the membrane, washing off extra amino acid molecules and deprotecting amino groups. After that, the second layer of the amino acids is spotted precisely on the previously deposited layer and new cycle starts. This procedure is repeated until the required length of amino acid chain is reached. At first, the drops were pipetted by hand, and later this method was automated and was performed by a robot[11] (Figure 1.7). The main advantage of SPOT synthesis is the possibility to synthesize peptide arrays without using complicated setups.
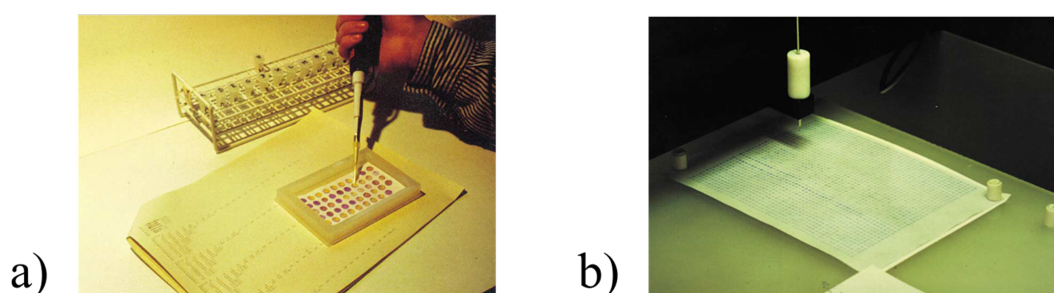
Figure 1.7: SPOT synthesis performed by a) hand and b) robot.[11]

By applying SPOT synthesis, it is possible to obtain a large amount of peptides of a good quality. However, the density of the spots is only 25 per cm^2.[12] The resolution is limited by the spot size. A further decrease in the size of the droplet means using a smaller amount of the liquid suspension with the amino acids, which leads to its faster evaporation and makes the deposition impossible. Moreover, the speed of mechanical movements of the robot limit the speed of the method.

1.3.3 Particle-Based Synthesis of Peptide Arrays

Another method for the fabrication of peptide arrays is particle-based synthesis. The main difference between the particle-based synthesis and the SPOT method (Chapter 1.3.2) is that the amino acids are deposited not from a liquid state, but as particles.[13]

In this case, amino acid derivatives are embedded into the inert polymer, which is solid at room temperature. As the amino acid molecules are protected, they do not interact with each other inside the particles. Furthermore, the amino acids in this case are more stable.[14],[15] During the synthesis process, the particles are deposited onto the functionalized surface (Figure 1.8). By applying heat, the matrix polymer melts and becomes viscous. This allows amino acids to diffuse and couple to functional groups on the solid support. In the next steps, uncoupled amino acids and matrix material are washed off. The next deprotecting step makes the first layer of coupled amino acids ready for the subsequent cycles of the synthesis. Particle-based synthesis became a basic principle for several methods, such as bioxerographic printer[15] and combinatorial laser fusing.[16]
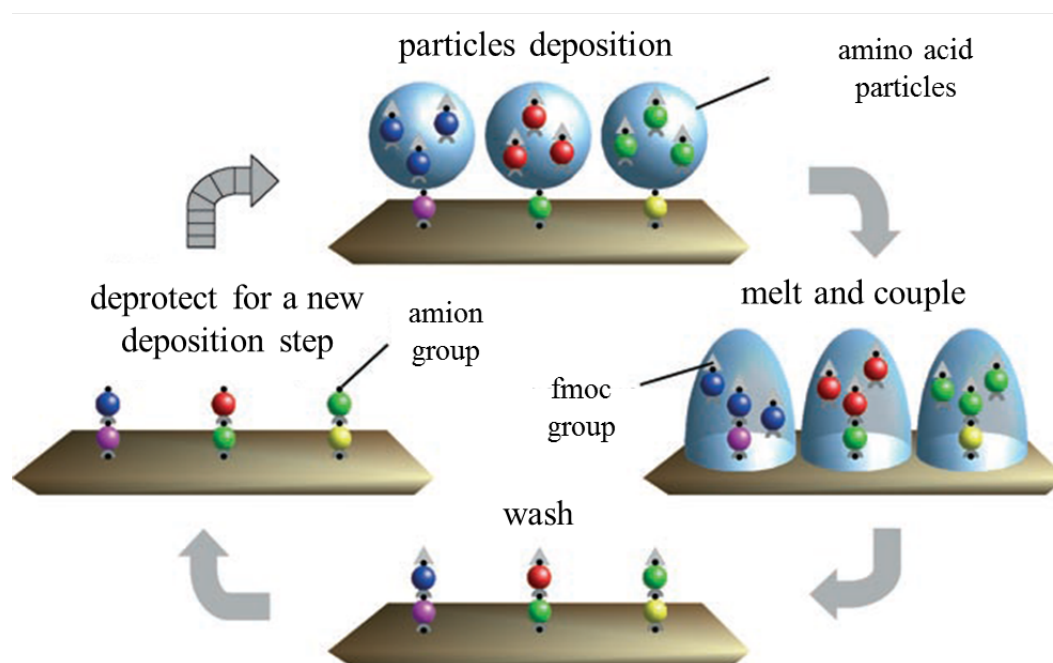
Figure 1.8: Schematic representation of particle-based method of peptide array synthesis.[15]

1.3.4 Peptide Arrays Synthesis by Xerographic Printing

Xerographic printing is a particle-based method for peptide arrays synthesis, based on the working principle of the laser color printer.[15] However, instead of toner particles the pattern is printed by charged polymer microparticles with embedded amino acid derivatives. Thus in the specially designed printer, the four color cartridges were replaced by twenty, the number of different amino acid particles required for the synthesis (Figure 1.9). The particle pattern is printed on the functionalized glass surface with the precise position of each kind of amino acid. This method of deposition

increases the flexibility and speed of the peptide array fabrication, while allowing the peptides to be synthesized on a larger scale. The particle-based synthesis cycles (Chapter 1.3.1) with heating, coupling, deprotecting and washing steps follow the deposition of amino acid particles. The next layer of amino acids should be printed on exactly the same position as the previous one. But due to mechanical alignment for each cycle of twenty, the resolution is limited to 800 spots per cm^2.[17]
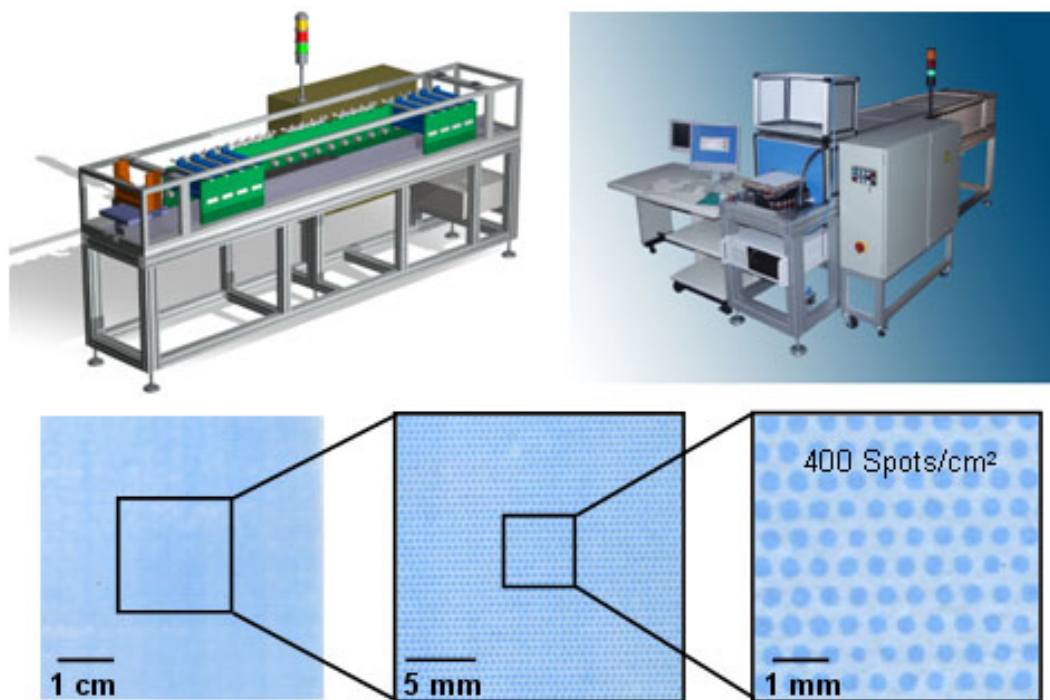
Figure 1.9: Laser printer with 20 aligned cartridges filled with amino acid particles and glass slide with amino acids printed and coupled to the glass substrate.[15]

1.3.5 Combinatorial Laser Fusing

Another particle-based method for peptide arrays synthesis is combinatorial laser fusing of amino acid particles. This technique dramatically increases the resolution of the synthesis spots up to 40.000 per cm^2.[16] In this case, particles are deposited on the functionalized synthesis substrate as a homogeneous thin layer[18] (Figure 1.10 a). Combinatorial patterning occurs via laser irradiation. A focused laser beam illuminates well-defined spots on the substrate, thereby selectively melting and fusing the amino acid particles. The liquefied matrix material forms a droplet, which, after the cooling, has much higher adhesion on the surface than the loose particles (Figure 1.10 b). These loose unfixed particles are subsequently removed by a compressed air stream or by an ultrasonic bath (Figure 1.10 c). After that, the second kind of amino acid particles is deposited on the functionalized substrate (Figure 1.10 d). When the

required pattern for the first layer is finished (Figure 1.10 f), the sample is placed in the oven, where the coupling step occurs for all kinds of amino acids simultaneously. The chemical steps described in Chapter 1.3.1 then follow. The resolution of the laser fusing method, as well as the size of the spots, depends on the thickness of the layer and thermal diffusion, which limit this technique. Moreover, removing unfixed particles after each deposition step increases the amount of used material and, as a result, raises the cost for the peptide arrays.
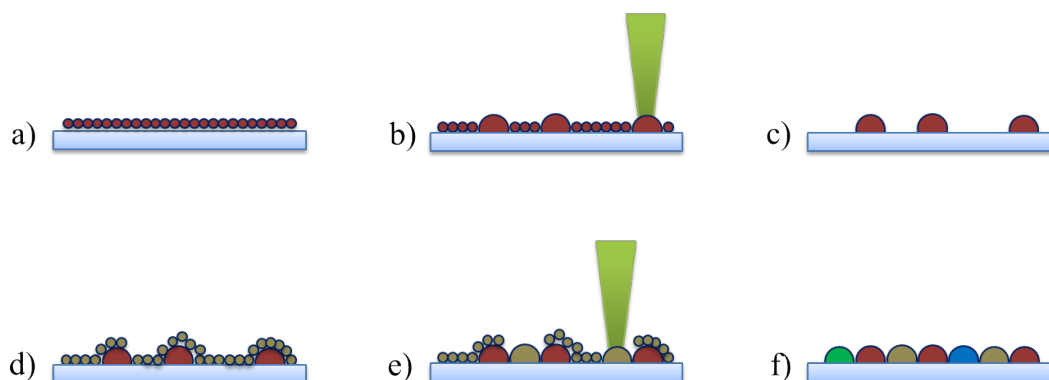
Figure 1.10: Schematic representation of laser fusing method. a) and d) deposition of the thin layer of the particles onto the functionalized glass substrate, b) and e) melting and fusing the particles at specific spots via laser irradiation, c) removing of the loose particles, f) combinatorial pattern of fused amino acid particles.

1.4 Developing New Methods for Peptide Array Synthesis

As mentioned above, all of the approaches considered for peptide array syntheses are limited in resolution. Due to technical reasons, further improvement of these methods will not significantly increase the amount of synthesized peptides. Therefore, the main goal of this work is to develop and characterize new techniques which allow combinatorial particle patterns to be generated with a higher array density, that are also suitable for peptide synthesis and which can be automated. In order to develop new methods, other techniques for particle patterning were analyzed.

### 1.4.1 Analysis of Existing Particle Patterning Methods

There are a lot of different techniques, that allow microparticles to be manipulated and structured, for example, using femtosecond laser irradiation[19] or optically induced dielectrophoretic devices.[20] However, using most of these methods, it would be impossible to synthesize high density peptide arrays on a big scale, as they allow only

small amount of the particles to be manipulated at once. Therefore, only approaches which are relevant for combinatorial peptide synthesis were considered.

Laser Induced Forward Transfer (LIFT)

Laser induced forward transfer method allows combinatorial patterns to be made with different kinds of materials, including metals,[21]–[24] polymers,[25]–[27] DNA,[28],[29] proteins[30],[31] and other biological samples.[32]–[35] Following this technique, material is transferred from one substrate to another in a specified size and shape via laser irradiation. The sample is prepared from two slides (Figure 1.11). One of them is a donor slide, which is transparent for the laser irradiation and covered with the material to be transferred. It is placed on top of another slide, called an acceptor. Subsequently, a pulsed laser beam is applied to the rear side of the donor slide with sufficient energy to transfer the material to the acceptor slide. The direct application of this method for biological materials is not possible, because of the high laser energy and resulting high temperatures can damage the sample.[36],[37] In this case, an additional layer is required, deposited between the donor surface and the material to be transferred. This intermediate layer absorbs the energy and generates localized vapor due to the ablation process. The vapor gas propagates towards the acceptor slide and, at the same time, propels the material.[38],[39]

It is possible to apply laser induced forward transfer not only for the transfer from the thin films, but also for generating particle pattern on the acceptor slide (Figure 1.11). The resolution achieved for particle printing following this approach is a 200 μm x 200 μm spot size.[40] However, during the transfer process the particles are spread around, which will lead to contamination when applied to the peptide array synthesis.
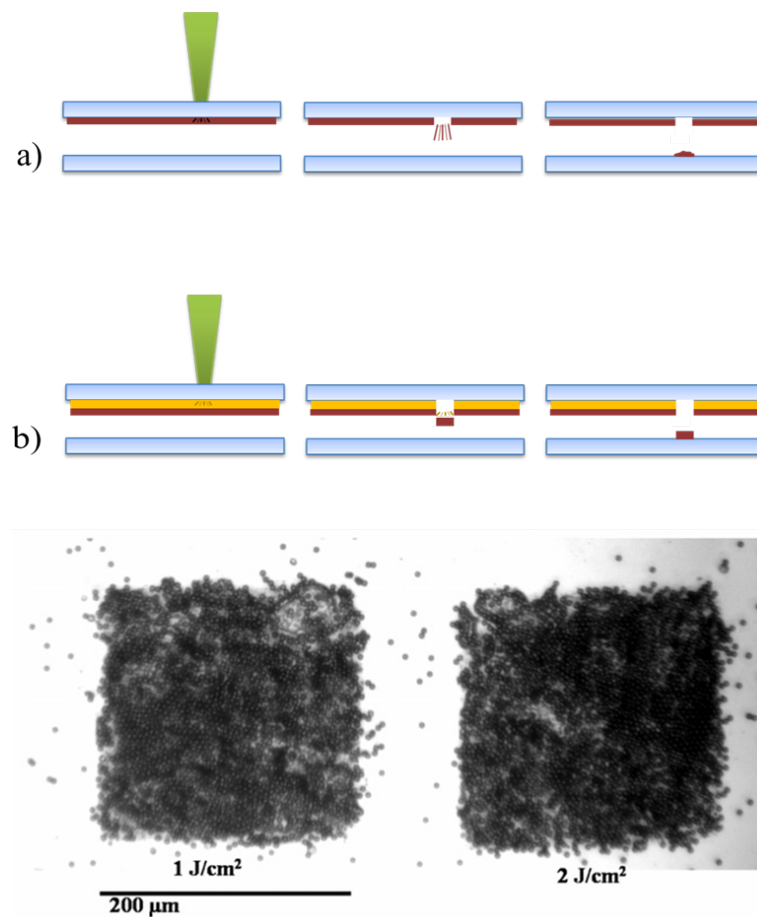
Figure 1.11: Schematic representation of laser induced forward transfer method a) without and b) with absorption layer and the optical image of the particles transferred to the acceptor slide.[40]

Self-Assembly of the Particles

One of the most efficient methods for transferring a disordered system of particles to a well-organized structure on the surface is based on the self-assembly of spherical beads. This process is realized when the initially chaotic system of the particles self-organizes into the ordered pattern due to external forces. By applying electrostatic[41] surface tension or capillary forces,[42] it is possible to achieve two or three dimensional particle structures.[43] There are several ways to generate these self-organized patterns.[44]–[47] One of them is based on a chemical templating of the surface.[48]–[50] In this case, the substrate is patterned with the charged multilayer. Oppositely charged particles are trapped by the electric force exactly on the patterned regions, but not on the rest of the substrate.[51],[52] The size and the shape of the particle clusters can be controlled by the size and shape of the printed multilayer (Figure 1.12).
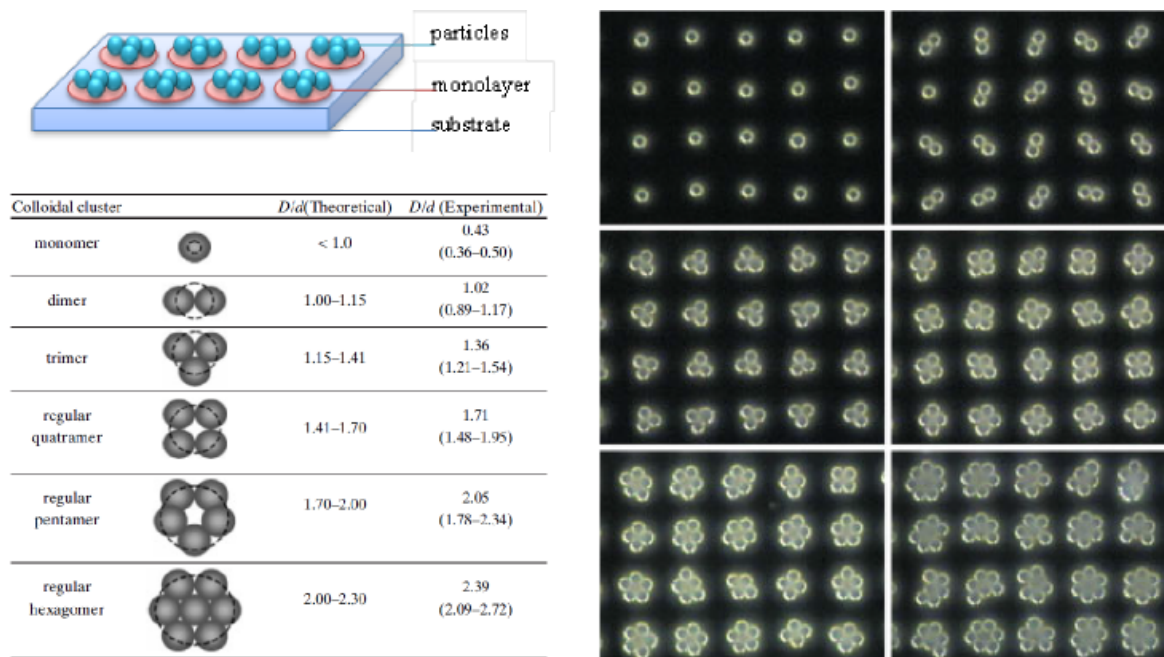
Figure 1.12: Schematic representation of chemical templating method and the optical image of the 2D particle clusters. Deposited particles (diameter d) onto the circular patterned polyelectrolyte templates were controlled by the size and shape of the multilayer (diameter D), pitch 18 μm.[51]

Another method for particle pattern generation is physical patterning, where particles self-organize inside a pre-structured substrate. In this approach, it is also possible to filter the shape and size of the spherical beads and, as a result, to obtain a well-controlled form of particle clusters. For deposition of the beads into the template, a fluidic cell is usually used.[53] It is fabricated from two parallel glass slides, where the lower substrate is previously structured via the lithography process with the required pattern (Figure 1.13). Another plane substrate is placed on the top to seal the fluidic cell. The beads in this cell are drawn with the suspension flow and fall into the structured holes due to the gravitation force. As the solution dries, the particles stay trapped inside the templates by capillary force. The amount of the beads inside each cavity is determined by the ratio between the size of the structure and diameter of the particles. It is possible to change the form of the clusters by varying the template pattern, so that the particles will form rings, lines or zigzag chains. The filtering of the beads occurs at the same time, as by choosing the appropriate size of the template only well-defined sizes of the particles can be trapped inside the structures.[54]
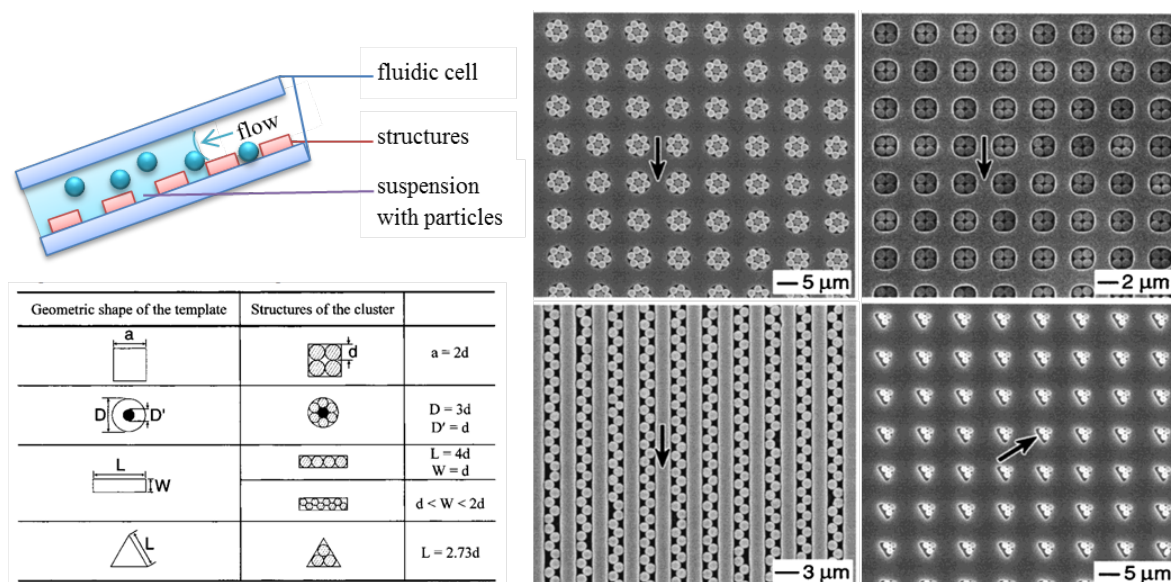
Figure 1.13: Schematic representation of physical templating method and images of the 2D particle clusters. Deposited into the pre-structured template particles were controlled by the size and shape of the structures. Arrow indicates the direction of the flow.[54]

To improve and optimize the stability and selectivity of the generated pattern, it is possible to combine chemical and physical templating methods.[55]–[57] In this case, the first step is fabrication of the structured substrate. Subsequently, chemical templating is performed by depositing the positively charged polymer on the whole surface of the substrate. Later another negatively charged layer is applied only to the top of the structures, forming a blocking layer. As a result, negatively charged particles are trapped by the electrostatic force only inside the templates (Figure 2.1).
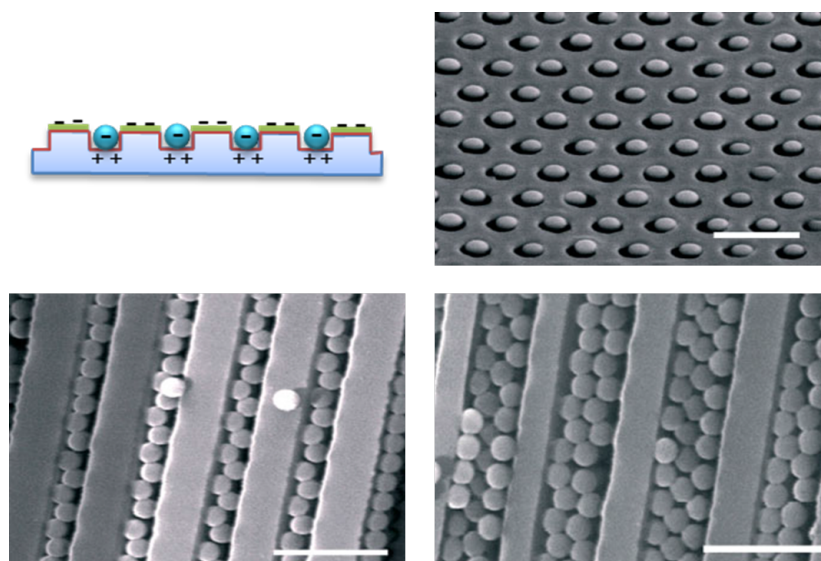
Figure 1.14: Schematic representation of combined physical and chemical templating method and optical images of the 2D particle clusters. Scale bars = 1 μm.[55]

Methods based on self-assembly of the particles can be performed with different materials and parameters. Another advantage of these techniques is the possibility of generating particle patters in micro- and nanoscales.[58],[59] However, for combinatorial peptide synthesis, the direct application of the self-assembly approach is not suitable, because when using this approach, the structured substrate will be filled with only one kind of particles. Thus, it will not be possible to synthesis the peptides with different amino acid sequences in neighboring spots or cavities.

1.4.2 Outline

The direct application of any methods described in Chapter 1.4.1, namely, laser induced forward transfer and self-assembly of the particles, would not solve the limitation problems in resolution of array density. In case of the LIFT approach, the resolution is not high enough, though it is possible to make combinatorial patterns. The main advantage of self-assembly, however, is a predefined resolution by the structures on the surface. The fixed and separated spots inside the templates would also lead to a reduction of contamination during the synthesis process. Nonetheless, the difficulty in self-assembly methods is the generation of combinatorial patterns.

Thus in order to obtain combinatorial peptide arrays with highly dense of the spots, novel methods are developed based on the combination of the advantages and modifications of the self-assembly property of the particles and the LIFT approach. In all techniques developed in this work, the particle pattering is generated on the prestructured with microwells glass substrate, which determines the resolution of the method. The filling of the microcavities occurs due to the self-assembly of the microbeads on the physically patterned template. In order to generate the combinatorial pattern on the structured surface two main techniques have been developed. One of them is a laser-based approach, where some of the particles are removed from the microwells by laser irradiation (particle pattern generation method) or by transferring the microbeads from one structured substrate to another (material transfer method). By applying laser-based methods for combinatorial peptide synthesis, the density of the arrays is increased up to 1 million spots per cm^2. A detailed description of the particle pattern generation and material transfer methods is given in Chapter 3.

The second approach for combinatorial particle patterning on the structured substrate is called the stochastic method. This technique does not require the laser irradiation to be applied to generate the pattern, but is mainly based on the self-assembly property of the microbeads. The major difference between stochastic and laser-based

methods is in the deposition of the particles on the substrate. For the particle pattern generation and material transfer techniques all the microwells on one substrate are filled with one kind of particles in one step, while in the stochastic approach, several deposition steps are required in order to generate a random combinatorial pattern. In the first step, one kind of microbeads is used to fill only the required percentage of microcavities. During the second deposition step, the defined amount of another kind of particles is applied to the structured surface. This process is repeated until all the microwells are filled with different microbeads. The method is described in more detail in Chapter 4. By applying the stochastic method, it is possible to synthesize ultra-high density peptide arrays with the record resolution of 25 million spots per cm^2 .

2 Materials and Fabrication Techniques

To increase the density of peptide arrays synthesized on a solid support, the surfaces structured with cylindrical microcavities are introduced. Therefore, Chapter 2.1 describes the fabrication process of microstructures, which would be suitable for the peptide array synthesis. The particle pattern on these structured surfaces can be generated by applying various kinds of microbeads. In this work, silica, polystyrene and amino acid micropspheres are used, all characteristics of which are presented in Chapter 2.2.1 and Chapter 2.2.2. In order to generate combinatorial patterns on the substrates with microcavities, some of the microbeads are removed from the microwells by applying laser irradiation. This removal process is performed by using the laser system described in Chapter 2.3.

2.1 Fabrication of Microstructured Substrates

The main requirement for the structured substrate in the particle generation and material transfer methods is its transparency to the laser irradiation. For this purpose, fused silica wafers purchased from Siegert Wafer GmbH (Germany, Aachen) are used. In this work, two kinds of microstructured surfaces are introduced. One of them involves microwells made of photoresist via a photolithography process. In general, photoresist micropatterns are used as molds for fabricating metallic microstructures, mainly of nickel, copper, or gold.[60]–[62] However, in our case, microwells made of photoresist itself are used for studying the self-assembling properties of the microbeads. The second kind of microstructures is obtained by the plasma etching of fused silica substrates. Both kinds of microstructured surfaces are fabricated based on the expertise of the Institute of Microstructure Technology, where the processes are mostly optimized for silica wafers. Therefore, the adjustment of the parameters for microstructures fabrication on the glass surface is required.

2.1.1 Microstructure Fabrication via Photolitography Process

First microstructured substrates were made of SU-8 photoresist via the photolithography process. SU-8 is an epoxy-based negative resist, which mainly consists of resin,

solvent and photosensitive component. Variation to the amount of the solvent in the composition gives variation in the resist viscosity, which determines the resist layer thickness. SU-8 photoresist is chosen due to its excellent properties for coating and planarization.[63] Moreover, the cross-linked SU-8 polymer is chemically and mechanically stable,[64] which is an important property for synthesizing peptide arrays on resist microstructures. Using this photoresist, it is possible to coat the substrates with a film thickness ranging from 0.5 μm to 200 μm.[65]–[67]

Therefore, substrates are fabricated via the photolithography process, which consists of several steps and is described in more detail in [68], [69] and [70]:

1. *Substrate Preparation*

Substrate preparation is the first step of the microstructures fabrication process. It is required to improve the resist adhesion on the substrate surface.[71] This step is also one of the most important ones in the lithography process, because in case of resist failure, no further steps are possible. Thus first of all, air dust, any particles, oils or other kind of contaminants should be cleaned from the substrate, as they prevent the resist from contacting the substrate surface. There are several ways to clean the wafer surface, among them are chemical, plasma and vapor cleaning.[70] In our case, fused silica wafers were delivered from the manufacturer in hermetically closed packages; therefore, it was sufficient to rinse them for 5 minutes in isopropanol.

2. *Photoresist Coating*

After cleaning, the substrate is covered with a uniform layer of the photoresist by spin-coating.[72] In this approach, the wafer is placed on the holder (spinner chuck) and kept there by vacuum. The small amount of resist is applied into the center of the substrate. Subsequently, the wafer starts to rotate at the required speed to distribute the photoresist on the surface. The speed of the rotation, time and acceleration are the important parameters in obtaining a uniform layer with the desired thickness.[73] They should be adjusted properly, depending on the viscosity of the resist and the surface of the substrate. Other external parameters which influence the resist adhesion and quality of the layer are humidity and temperature, as they are critical for the resist stability.[74]

In our case, a layer of SU-8 photoresist is added to the glass substrate by spin-coating. The resulting thickness of 10 μm is achieved with the parameters presented in Table 2.1.

During the first experimental fabrication, all the structures delaminated from the surface after the development step due to weak resist adhesion on the glass surface. However, it was possible to further improve the resist adhesion by modifying the

Table 2.1: Parameters for spincoating SU-8 photoresist with thickness of 10 μm on fused silica wafer

Time, s	Speed, rpm	Ramp rate, rpm/s
30	500	500
60	100	0
60	1500	2800

substrate surface. The adhesion promoters (primers) react chemically with the surface, thereby making it possible for the resist to bond with the top of the substrate.[75] The primers are usually applied on the surface and spin-coated just before the resist is deposited. To improve adhesion of SU-8 photoresist on glass wafers, the organic polymer solution, OmniCoat, was used.[76] It was spin-coated on the substrate with the parameters presented in the Table 2.2 before applying the photoresist.

Table 2.2: Parameters for spincoating of the OmniCoat on a fused silica wafer

Time, s	Speed, rpm	Ramp rate, rpm/s
5	500	100
30	3000	300

As a result of using the OmniCoat primer, the adhesion of the resist was significantly improved. However, as was previously the case, not all the microstructures stayed on the glass surface. Another way to improve adhesion of the resist to the glass substrate is silanization.[77] The main principle of this chemical process is to create a covalent bonding between an organic polymer and inorganic mineral surface by applying silane coupling agents.[78] The first step of this method is to clean and etch the substrate with KOH in order to generate hydroxyl groups (-OH) on the surface of the wafer. For this, the wafer is placed for three hours in the solution, made of 5.6 g of potassium hydroxide dissolved in 100 ml of isopropanol. After washing the substrate in distilled water and drying it with pressurized air, it is placed overnight in a trimethoxysilane solution in a chamber filled with argon gas to complete the silanization procedure. To prepare this solution, 650 μL of 3-Glycidyloxypropyl reagent is mixed with 100 ml of dichloromethane (DCM). During this chemical reaction, hydroxyl groups on the top of the substrate bind with silane groups and create a well-aligned molecular film on the surface. As a result, this functionalized surface provided

better adhesion to an SU-8 polymer photoresist.

3. *Soft-Baking*

After the spin-coating, the resist still contains a certain percentage of the solvent. By storing the substrate at room temperature, the solvent will gradually evaporate and thereby the properties of the film will be changed with time.[79] In order to stabilize the resist film, the solvent is removed from the deposited layer by soft-baking.[80] During this step, the substrate is placed into the oven or over a hotplate. The temperature and the time of the backing are defined by the resist properties and thickness of the layer. It should be taken into account that, after soft backing, the thickness of the resist layer is usually decreased by 0.4-0.7%.[70],[81] In our case, the sample was baked for 25 minutes at 95° C on a hot plate.

4. *Photoresist Exposure*

In order to obtain the microstructures, the photoresist layer should be exposed to light. During the exposure process, the molecular structure and solubility of the resist is modified.[71] In the case of SU-8 photoresist, after the exposure and a post-exposure bake, the exposed spots become insoluble to the photoresist developer, whereas the other parts are washed away. There are several methods to expose resist, for example, with x-rays,[82] or e-beam.[83] The chosen method depends on the type of the resist and on the size of the required structures. In our case, to fabricate microstructures on glass substrate coated with SU-8 resist, both samples with OmniCoat and functionalized surface were exposed to the UV light using HeCd laser with a wavelength of 442 nm, which was a part of the DWL 66FS laser lithography system (Heidelberg Instruments GmbH (Heidelberg, Germany)). That system allowed any pattern to be written on the resist directly according to the layout, without mask usage.[84] To obtain good quality structures of the microcavities on the glass surface, it was important to determine the exposure dose in order not to over- or under-expose the resist. Therefore, several experiments with dose variation were performed. For this, the layout was designed with four horizontal lines with different size of the microwells, where the pitch was varied from 10 to 40 μm at increments of 10 μm. Each line was divided into 27 fields for 27 different exposure doses from 10 to 155 mW (Figure 2.1).

After the experiment, it was found that the exposure dose influenced the adhesion, as well as the quality of the microstructures. The fabricated samples with adhesion promoters were checked under the light microscope and the results are presented in Figure 2.2.
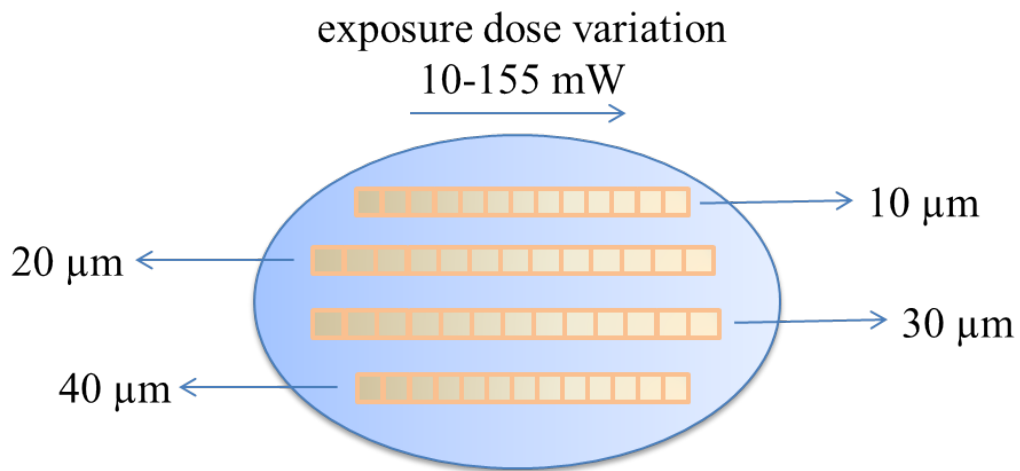
Figure 2.1: Schematic representation of the wafer layout, which was designed to adjust the exposure dose.

Figure 2.2: Variation of the laser power from 10 mW to 155 mW for the structures with the pitch of 10 μm, 20 μm, 30 μm and 40 μm for two different surface modifications applied as adhesion promoters.

Red color in the table indicates that the resist did not adhere to the glass surface. In the case of the OmniCoat, the adhesion was not sufficient with the low and high exposure doses. Moreover, it is observed that the quality of the structures depends on the laser power as well, where, in the range of 40- 60 mW, a significant amount of cracks appeared on the resist surface. By increasing the exposure dose from 80 mW to 105 mW, the micro structures became clear and the resist had a smooth surface. By increasing the laser energy further, the resist was over-exposed and, as a result, the microwells became smaller in size and were partly filled with the resist. (Figure 2.3). The best exposure dose to achieve good quality microstructures was 85 mW for all the fields on the sample.
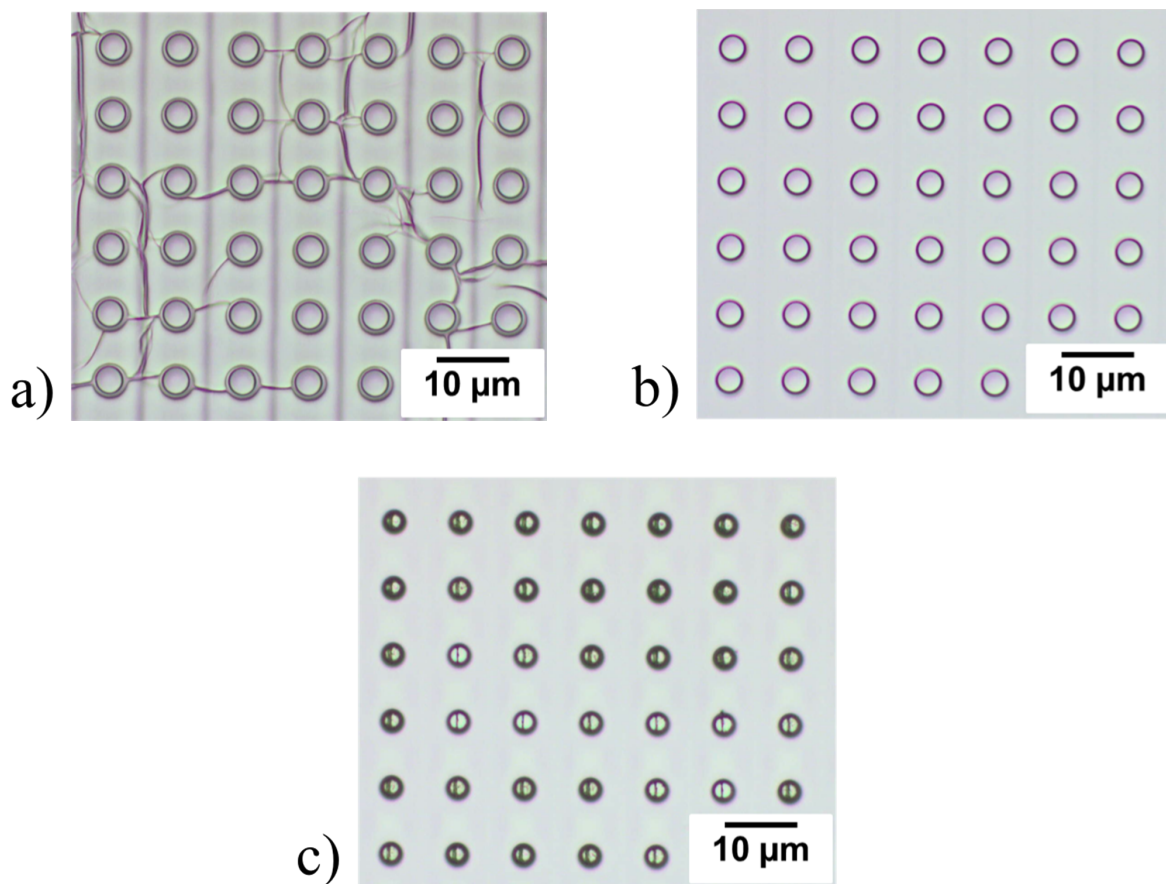
Figure 2.3: Light microscope images of the fabricated structures of microcavities with the pitch of 10 μm, made of negative photoresist and exposed to the different exposure doses. a) under exposed fields with laser power of 45 mW, b) sufficient laser power of mW for the exposure, c) laser power for the exposure is 115 mW.

In case of the silanization of the surface for the low exposure doses, the range where the resist did not adhere to the surface is increased relative to the result, with OmniCoat as adhesion promoter. However, the quality of the structures fabricated on the surface with silanization is dramatically improved. In this case, independent of

the laser power and the pitch of the microcavities, there were no cracks in the resist and no undeveloped resist inside the structures. Thus for this surface modification, the energy of the laser for the resist exposure can be chosen in the range from 100 to 155 mW. In Figure 2.4, the microcavities with different diameters fabricated on functionalized surface are presented. All of the microstructures were exposed to the same laser energy of 135 mW.
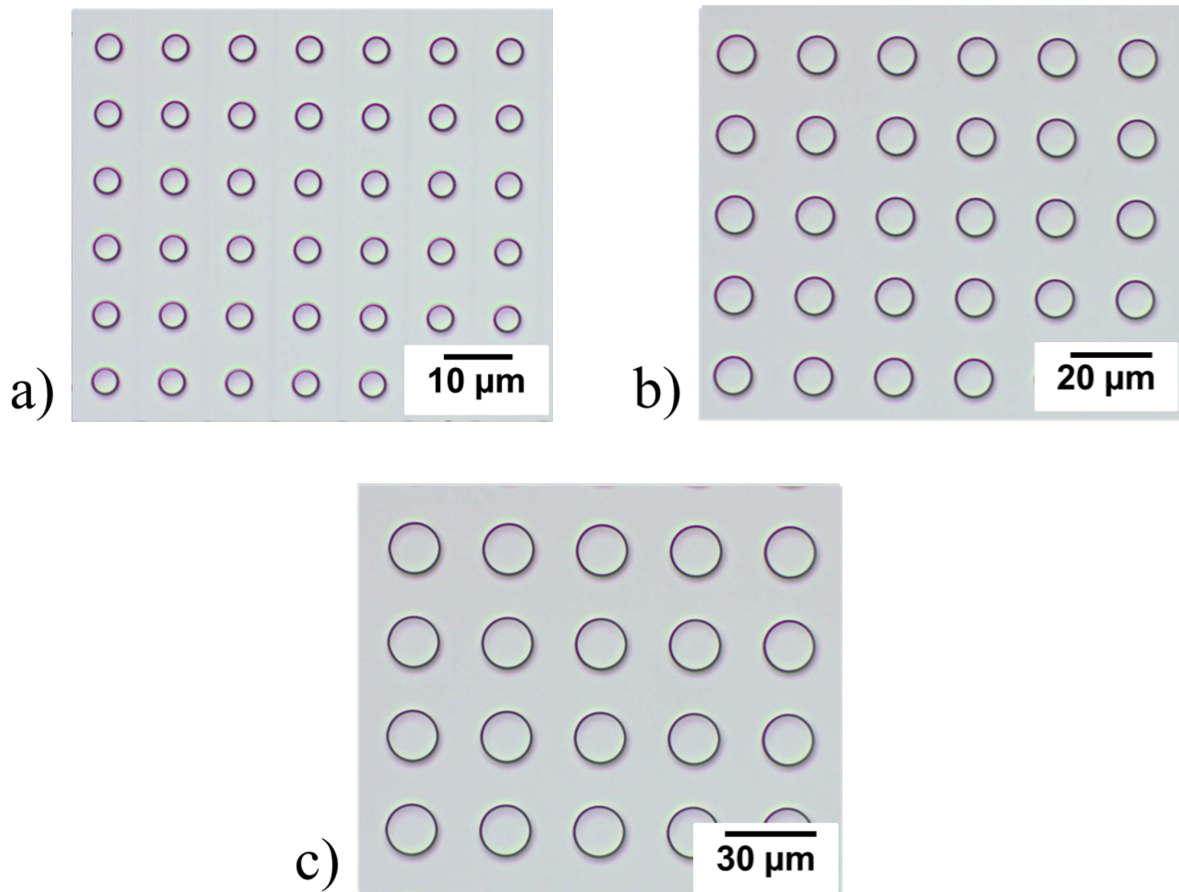
Figure 2.4: Light microscope images of the fabricated microcavity arrays with the pitch of 10 µm with the silanization of the surface and exposed with the laser power of 135 mW. a) pitch 10 µm, b) pitch 20 µm, c) pitch 30 µm.

For further microstructure fabrication, the silanization of the surface was chosen, as the quality of the resist layer did not depend on the exposure dose.

5. *Post-Exposure Bake*

Post exposure bake is required for several reasons. First, during the exposure the small variation of the exposure dose occurs at the depth of the resist layer. While heating, photoproducts created by light defuse and make this variation smoother.[69] Second, during the exposure chemical reactions take place in the resist layer resulting in a change to the polymer solubility.[71] The heat is required to continue the process

of cross-linking, which creates the bonds between the chains in polymer.[85] In our case, the sample with SU-8 resist on the glass substrate was baked at 75° C for 40 minutes and at 55° C for 60 minutes.

6. *Photoresist Development*

During the SU-8 photoresist development process, the sample was placed into the special chemical reagents, which were dissolving the unexposed pats of the resist layer (in case of negative resist). The hardened polymer, which was cross-linked during the exposure process and post-exposure bake, stayed on the substrate.[85] For the development of SU-8 resist, propyleneglycol monomethylether acetate (PGMEA) was used. The sample was placed in the developer for 90 minutes. After that it was rinsed in isopropanol for 30 min.

7. *Post-Develop Bake*

During the post-develop bake of the photoresist, further cross-linking of the polymer and evaporation of the solvent from the resist occur.[71] This step is required mostly when the structures are used as a final product, especially in high temperature applications. Otherwise, the resist can change its shape and properties. For this purpose, the substrate with developed SU-8 structures was placed in the oven for the post-develop bake for two hours at 30° C.

As previously mentioned, the main requirement for the microstructured samples was the ability to use them for the peptide array synthesis. This means that the fabricated SU-8 templates should be stable in the solvents during the chemical process of the synthesis. However, SU-8 did not fulfill this requirement. In Figure 2.5, the result is shown of placing SU-8 structured substrate to dichloromethane (DCM) - which is used during the peptide synthesis - for five minutes. Due to chemical reactions, the adhesion between the resist and the surface was deteriorated and caused the displacement of some parts of the structures. Moreover, the shape and the quality of the template were also changed. Therefore, further use of the SU-8 structures was no longer possible. Thus there was a need to find other ways to fabricate the templates. Another option was to fabricate the microstructures not from the resist, but to structure the glass wafer itself. In this case, the template would always remain on the sample, and stay stable in any chemical solutions used during the synthesis.
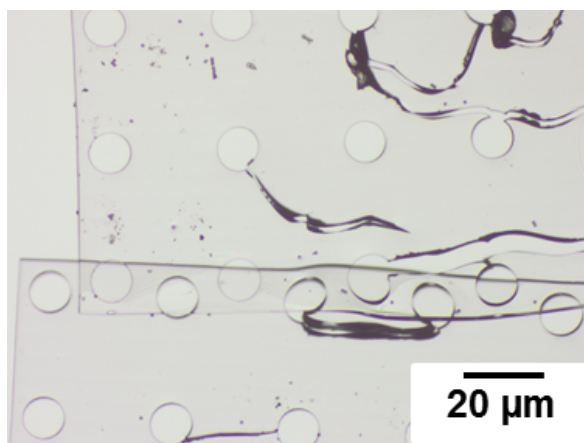
Figure 2.5: Light microscope image of SU-8 structures of micro cavities which were placed in dichloromethane for 5 minutes.

2.1.2 Microstructure Fabrication via Plasma Etching

Another way to fabricate microstructures to apply the plasma etching process.[68], [69] Plasma is a partially ionized gas, which consists of radicals, neutral atoms and equal amount of electrons and ions.[86] The etching process occurs when the ions that accelerate towards the substrate chemically react with the material to be etched and/or when the atoms are knocked out off the material by high energy ions, which are bombarding the surface.[87], [88] Plasma etching is a complex task with many parameters to be adjusted, such as flow rate, etch time and applied power. Therefore, before starting fabrication of microstructures via etching process at the institute, it should be ensured, that these templates would be suitable for combinatorial peptide arrays synthesis. The test microstructures were purchased from Microglass Chemtech GmbH (Mainz, Germany) with the layout presented in Figure 2.6.

After realizing that the glass microstructures fulfill all the requirements for the combinatorial peptide arrays synthesis, we developed our own fabrication procedure. Moreover, making similar structures on a fused silica wafer adds flexibility in the choice of layout as required and an opportunity to obtain the samples on time and at the right quantity. The general principle of the etching process consists of two steps. First, fabrication of the mask and, second, structuring of the fused silica surface itself.

Field 1 : 3 µm diameter, 10 µm pitch
Field 2 : 4 µm diameter, 10 µm pitch
Field 3 : 5 µm diameter, 10 µm pitch
Field 4 : 6 µm diameter, 10 µm pitch
Field 5 : 7 µm diameter, 10 µm pitch
Field 6 : 10 µm diameter, 14 µm pitch
10 µm depth
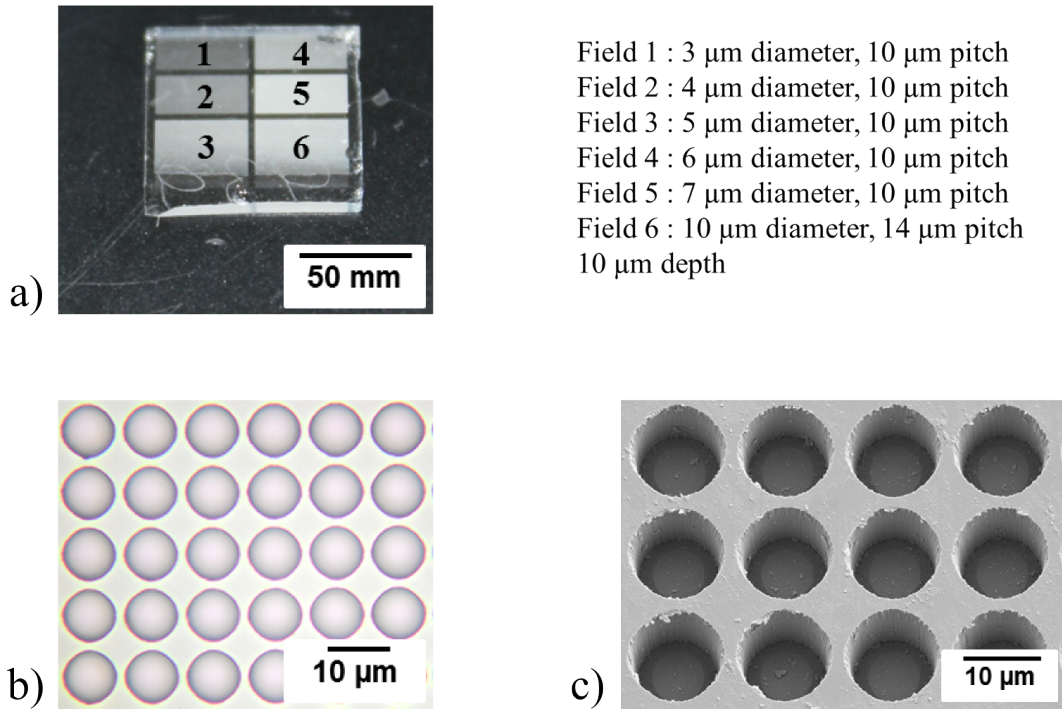
Figure 2.6: Images of the sample with microcavities, which was ordered at mikroglas chemtech GmbH. a) the layout of the sample, b) image taken under the light microscope, c) SEM picture of the micro cavities.

The main part of the mask is fabricated via the photolithography process described above (Chapter 2.1.1), where the pattern of microcavities is generated first on the photoresist layer. However, in this case, before resist spincoating, an additional chrome layer was deposited on the surfaces of the wafer. The thickness of the additional chrome layer depends on the required depth of the final structures. In our experiments, to fabricate 5 µm deep microcavities, a layer of 350 nm was chosen. The next step was spin-coating the wafer with the positive photoresist AZ 150 (thickness = 1.5 µm) and parameters presented in the Table 2.3.

Table 2.3: Parameters for spincoating of positive resist AZ 150

Time, s	Speed, rpm	Ramp rate, rpm/s
60	1500	500

The spin-coating is followed by soft-bake for 5 min at 95° C. The sample was then exposed to UV light with the wavelength of 405 nm and a dose of 80 mJ, using a UV-lithography mask with a required pattern of the structures, purchased from Delta Mask (Enschede, Netherlands). Subsequently, the wafer was placed in the AZ developer to

remove exposed parts of the polymer (positive photoresist) for 15 seconds, followed by post-baking at 200 ° C for two minutes.

The pattern generated on the resist was transferred into the chrome layer by reactive ion etching process (RIE). In the RIE technique, the atoms of the etched material are removed through the chemical reaction and mechanical ion bombarding of the surface.[88] During this process, the chrome layer was selectively etched, with the removal of the metal only occurring in the openings on the photoresist mask (Figure 2.7).
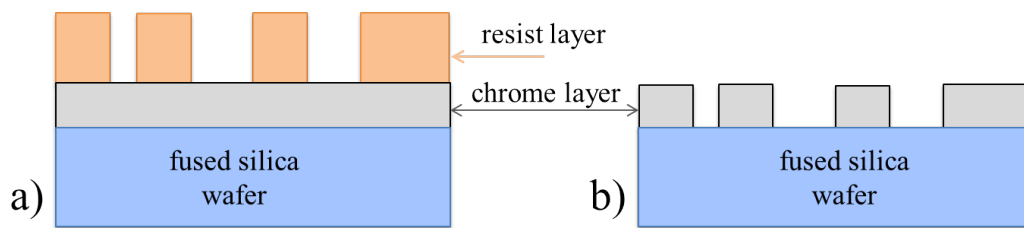
Figure 2.7: Illustration of chrome mask fabrication. a) positive resist structured with the required pattern, b) pattern transferred to chrome layer by RIE etching process.

For this step, the wafer was set for 25 minutes in a processing chambers of Oxford Plasmalab System 100 (Oxford Instruments (Abingdon, United Kingdom)), filled with the plasma of the mixture of gases Cl_2, O_2 and He. The etching occurred when oxygen and chlorine ions bound with chrome at the surface, resulting in product that was volatile at room temperature.[89]

$$Cr + 2O + 2Cl \rightarrow CrO_2Cl_2$$

Helium was added as a buffer gas to improve the etching process. After the selective chrome removal, the rest of the resist was striped.

The result for RIE etching is the patterned chrome layer, also called chrome mask. To obtain the pattern on the glass surface, a similar etching process is required. In this case, both chrome layer and fused silica surface were etched parallel to one another in CHF_3 plasma using the same Plasmalab System (Figure 2.8).

$$3SiO2 + 4CHF_3 \rightarrow 3SiF_4 + 4CO + 2H_2O$$
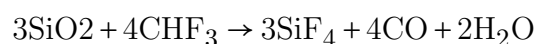
The etching process was continued for 60 minutes, and after that the required depth of the structures was obtained. The last step was to remove the remaining chrome

mask by wet aching in a mixture of perchloric acid ($HClO_4$) and ceric ammonium nitrate $(NH_4)_2[Ce(NO_3)_6]$.
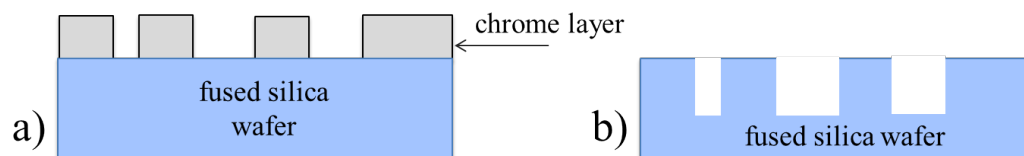
Figure 2.8: Schematic representation of micro wells fabrication on a fused silica surface via etching process. a) chrome mask on the glass surface, b) etched micro cavities.

During the work, several different layouts with microwells were made in order to find proper parameters for the peptide arrays fabrication. The diameter of the cavities was varied from 1 µm to 15 µm and the pitch from 2 µm to 20 µm, respectively. One of the samples with microstructured surface is presented in Figure 2.9.
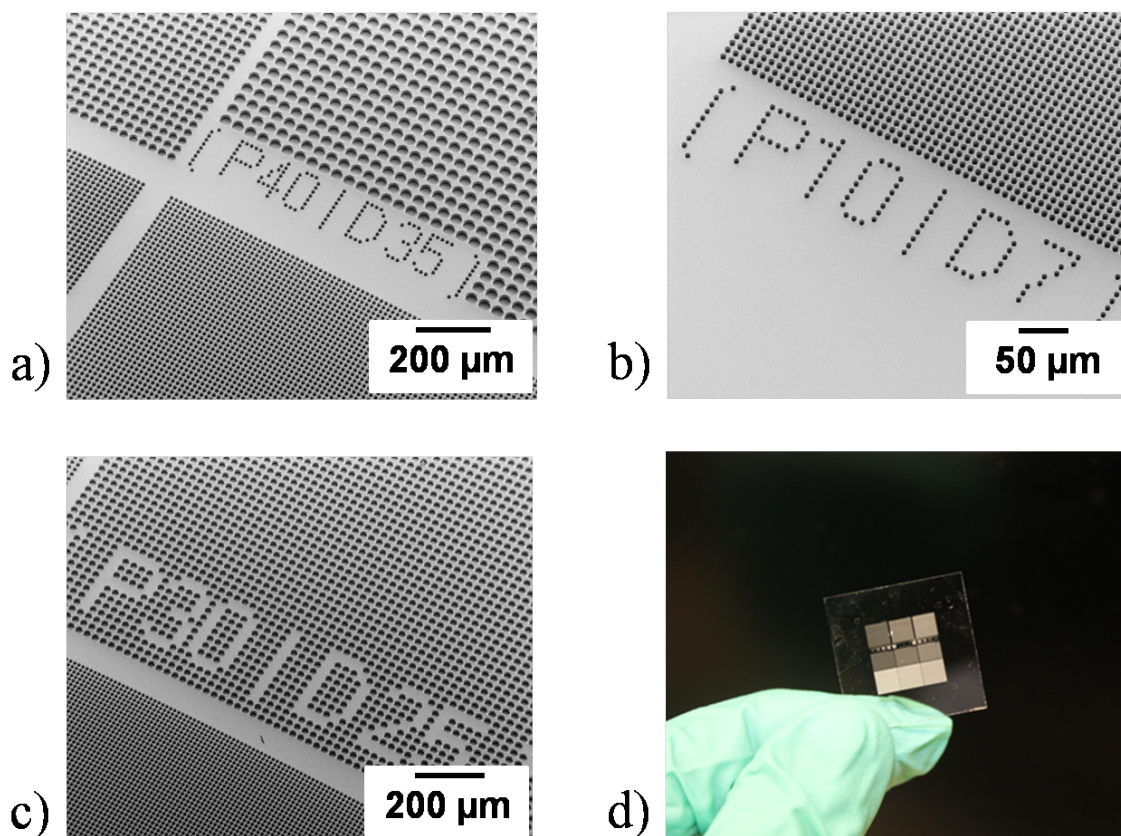
Figure 2.9: Glass substrate structured with microcavities via plasma etching process. a), b) and c) SEM pictures of the microcavities with different diameters and pitches (SEM image by P. Abbafy, RIE operator Dr. D. Häringer), d) photograph of the glass sample.

Apart from flexibility in the choice of layout of microcavities, the advantage of custom fabrication of the structured surfaces is the possibility to adjust the fabrication

parameters to obtain the desired properties of the sample. Figure 2.10 shows the example of two substrates made with smooth and rough surfaces. For the experiments, the microstructures with smooth surface were used. However, microwells with rough surface can be used to increase the covering area for the amino acid coupling.
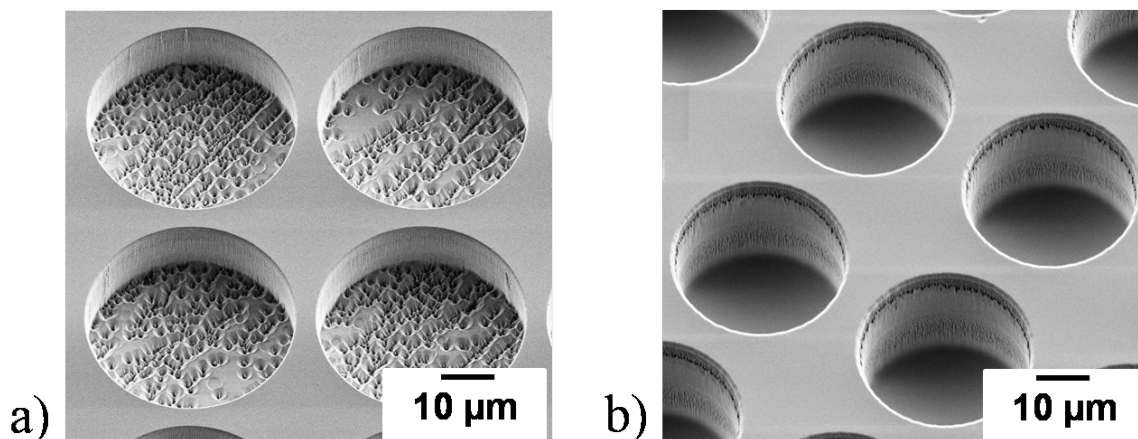
Figure 2.10: SEM images of microstructured glass substrates fabricated via etching process. a) rough surface of the substrate after the etching, b) smooth surface of the substrate after the etching.

2.2 Microparticles

2.2.1 Comercialy Available Microparticles

The main goal of the development of the new methods was to achieve a combinatorial pattern of the particles. To understand the behavior of the microbeads during their deposition and further manipulations, colored microspheres were used (Fig. 2.11). The monodispersed polymer microparticles were purchased in different sizes and colors in aqueous suspension. The polystyrene $3\,\mu m$ particles in red, yellow and blue were ordered from Polysciences, Inc (Warrington, USA). Other polystyrene microbeads in blue, with a variety of diameters from 1 to $7\,\mu m$ were purchased at microParticles GmbH (Berlin, Germany), as well as fluorescent melamine particles with a diameter of $2.65\,\mu m$ and excitation wavelengths of 510 and 636 nm. $10\,\mu m$ dark red and $10\,\mu m$ dark blue polystyrene micro particles were bought from Sigma-Aldrich (St. Louis, USA).

The process of particle deposition on microstructures is described in Chapter 3.1. During the experiments, it was found that the mechanical stability of the polymer microspheres that were purchased did not depend on the manufacturer of the particles, but depends on the size of the microbeads. So the particles with a diameter of $10\,\mu m$ are more stable in shape while mechanical force is applied. The smaller the diameter

of the particles, the 'softer' they become, and the more likely they will be destroyed under pressure during the deposition. Thus in order to reduce contamination during the deposition, the microbeads with a diameter smaller than 3 μm should be treated with more care.

Apart from the polystyrene particles, 3 μm silica microbeads and 1 μm hydrophobized silica microspheres from Kisker Biotech GmbH Co. KG (Steinfurt, Germany) were used.
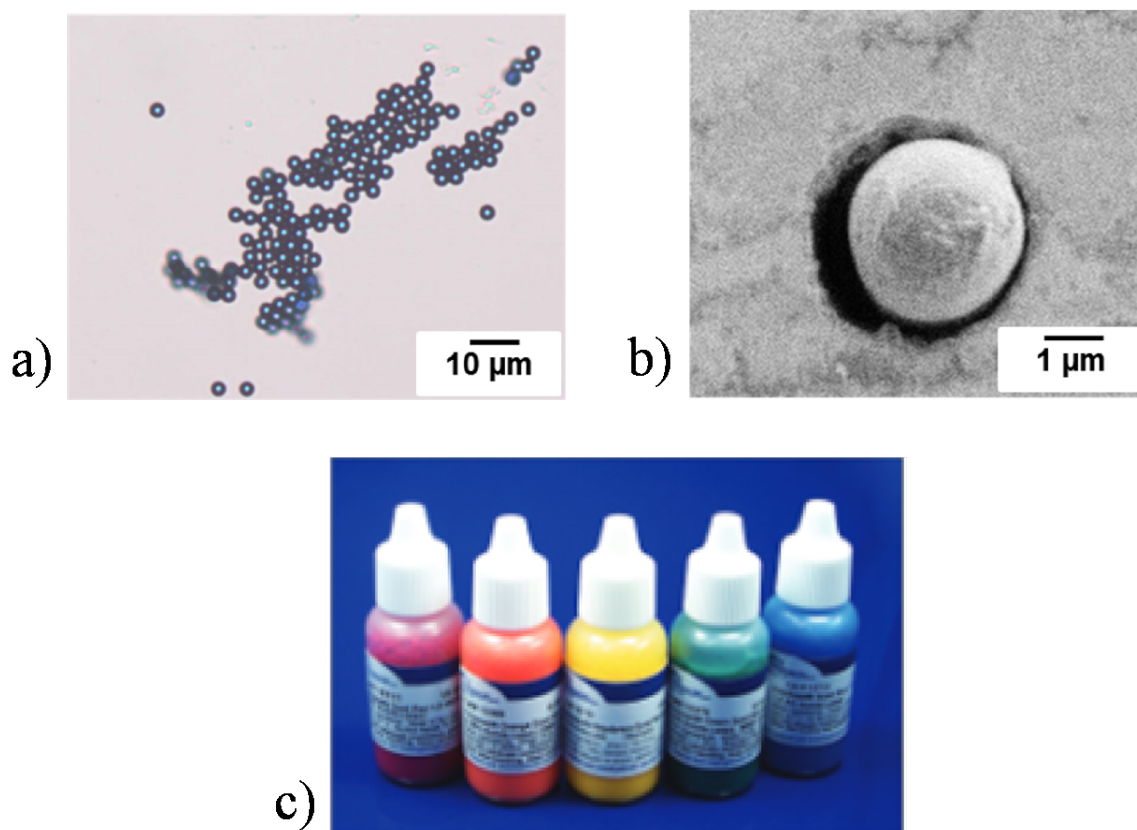
Figure 2.11: Polystyrene particles. a) 3 μm blue polystyrene particles on a glass surface under the light microscop, b) SEM picture of a 3 μm polystyrene particle deposited into the 3.5 μm cavity, c) colored polystyrene particles in a water suspension.[90]

2.2.2 Amino Acid Microparticles

The polymer microparticles with embedded amino acids (amino acid particles) used in this work were fabricated through the spray drying process. Spray drying allows the particle powder to be obtained from liquids. The required solution was dispersed in a small amount through the nozzle of the spray dryer device (Mini Spray Dryer B-290, Buchi Labortechnik AG (Essen, Germany)). The small droplets from the nozzle dry quickly in the spray gas, thereby taking spherical shape. A detailed description of the particle fabrication process could be found in PhD thesis of Dr. B. Muenster [91].

The solution for the spray was made from resin (matrix material, SLEC PLT-7552, Sekisui Chemical GmbH (Dusseldorf, Germany)) and amino acid derivatives dissolved in dichloromethane (DMF). After the fabrication, the size of the particles was determined by using the Malvern Mastersizer 2000 (Malvern Instruments Ltd (Malvern, UK)) particle size analyzer. The working principle of the device is based on analyzing the intensity of light scattered by the particles, which are dispersed in the chamber. The resulting size distribution curve and scanning electron microscope (SEM) picture are presented in Figure 2.12. The particles have a round shape, but are not monodispersed, and they have a size distribution of $0.2\,\mu m$ to $10\,\mu m$ and a mean diameter of $3.1\,\mu m$. This characteristic puts limitations on the development of new approaches, as it increases contamination during the deposition. Nevertheless, newly developed techniques were adapted to this issue, as discussed in Chapters 3, 4 and 5.
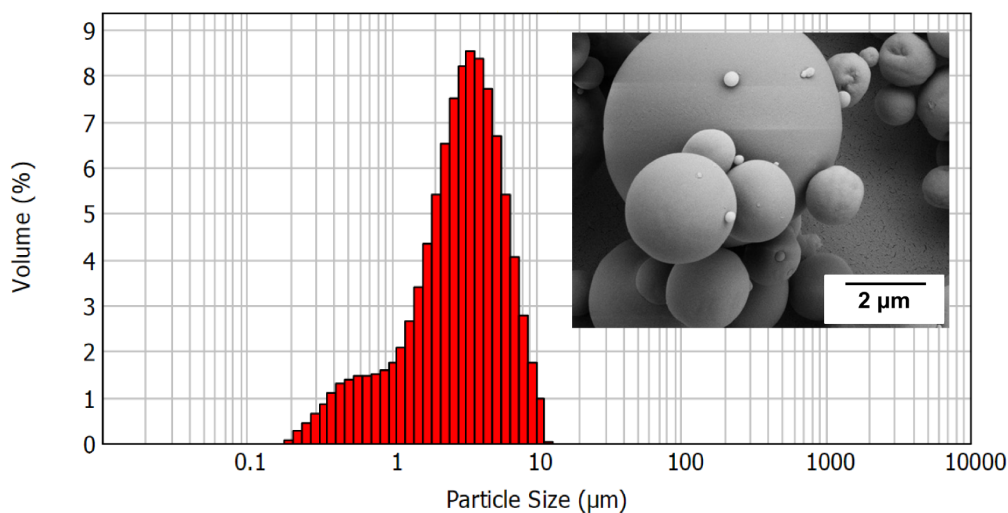
Figure 2.12: The size distribution curve and SEM picture of the particles which were fabricated via spray drying process.[91]

2.3 Laser System

For particle pattern generation and material transfer methods described in Chapter 3 the microbeads should be removed from the structured substrate. It is possible to achieve this by applying laser irradiation with short pulses and sufficient energy. For this purpose, the laser system was developed with the Nd:YAG nanosecond pulsed laser operated at a wavelength of 532 nm (Matrix 532-7-30, Coherent Inc.). The technical details of the laser are presented in Table 2.4. A more detailed description of the development and parameters of the laser system can be found in Master Thesis of C. von Bojničić-Kninski [92] and PhD Thesis of Dr. F. Maerkle [93].

Table 2.4: laser specifications for MATRIX 532-7-30, Coherent Inc.

wavelength	average power	pulse duration	pulse duration	beam parameters
532 nm	7 W at 30 kHz	5-60 kHz	<20 ns	230 µm

The laser system used for combinatorial particle patterning is presented in Figure 2.13. The laser is fixed on the movable support, which allows its position to be adjusted in X and Y directions. The laser beam's intensity is attenuated using density filters and is guided by reflecting mirrors to the microscope objective with 20 times magnification, focusing the laser on the substrate (Figure 2.13 a). The substrate is placed on XY-stage, which allows scanning with the laser across the sample. Additionally, the system is equipped with a specially designed holder for precise positioning of two substrates on top of each other, namely, for adjusting their relative X and Y coordinates and angular position (Figure 2.13 b). The sample was constantly monitored using the CMOS camera.
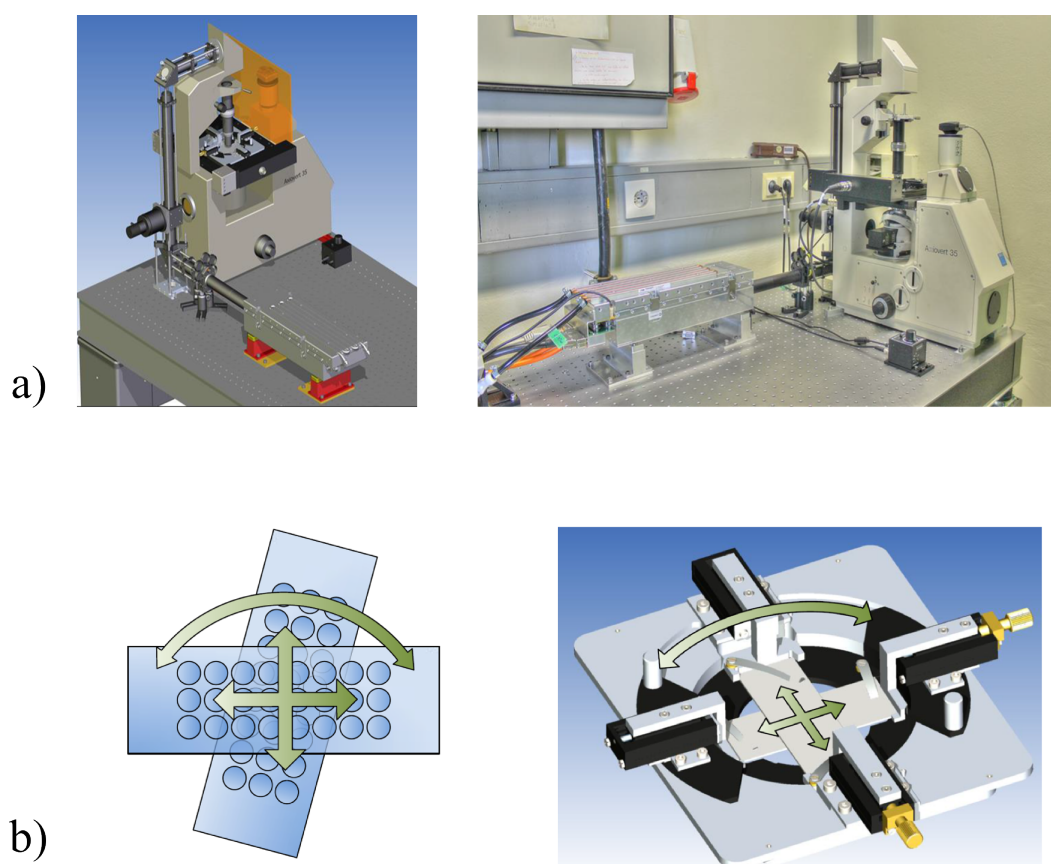
Figure 2.13: The laser system used for laser-based techniques for combinatorial peptide array synthesis. a) CAD picture and photograph of the laser system, b) custom-designed sample holder.[92]

3 Laser-Based Methods for Particle Patterning

Two novel techniques were developed during this work for the high density peptide arrays synthesis. Both of them are based on the laser induced forward transfer approach and self-assembly of the particles inside the structured surface. In both cases substrates structured with cylindrical cavities are used, which can be filled with microbeads by applying a specially developed particle deposition method described in Chapter 3.1. The new laser-based methods allow combinatorial particle patterns to be obtained with a high resolution up to 1 million spots per cm^2. One of the techniques is particle pattern generation (Chapter 3.2), where the combinatorial pattern is realized by removal of the material from the microstructures. Material transfer is another possible method (Chapter 3.3), based on the transfer of the particles between two substrates.[94],[95]

3.1 Particle Deposition Method

The particle deposition method was developed based on the self-assembly properties of the microspheres. The main difference from deposition techniques described in Chapter 1.4.1 is that it is not required to build a fluidic chamber or chemically pattern the substrate with electrically charged monolayers. In this approach, the structured substrate can be filled with the microbeads by applying soft paper tissue and mechanical force. In this case, for the deposition, a small drop of particle suspension is poured on the top of the structured surface and distributed all over it. After the solution evaporates, a thin film of self-assembled particles stays on the substrate. Some of the beads are guided into the microwells by capillary forces and trapped inside, while some remain on the surface. By applying a soft paper tissue and gently wiping the structured surface, it is possible not only to remove the extra particles from the top of the sample, but also to fill the empty microwells. The schematic representation of this procedure is shown in Figure 3.1 .
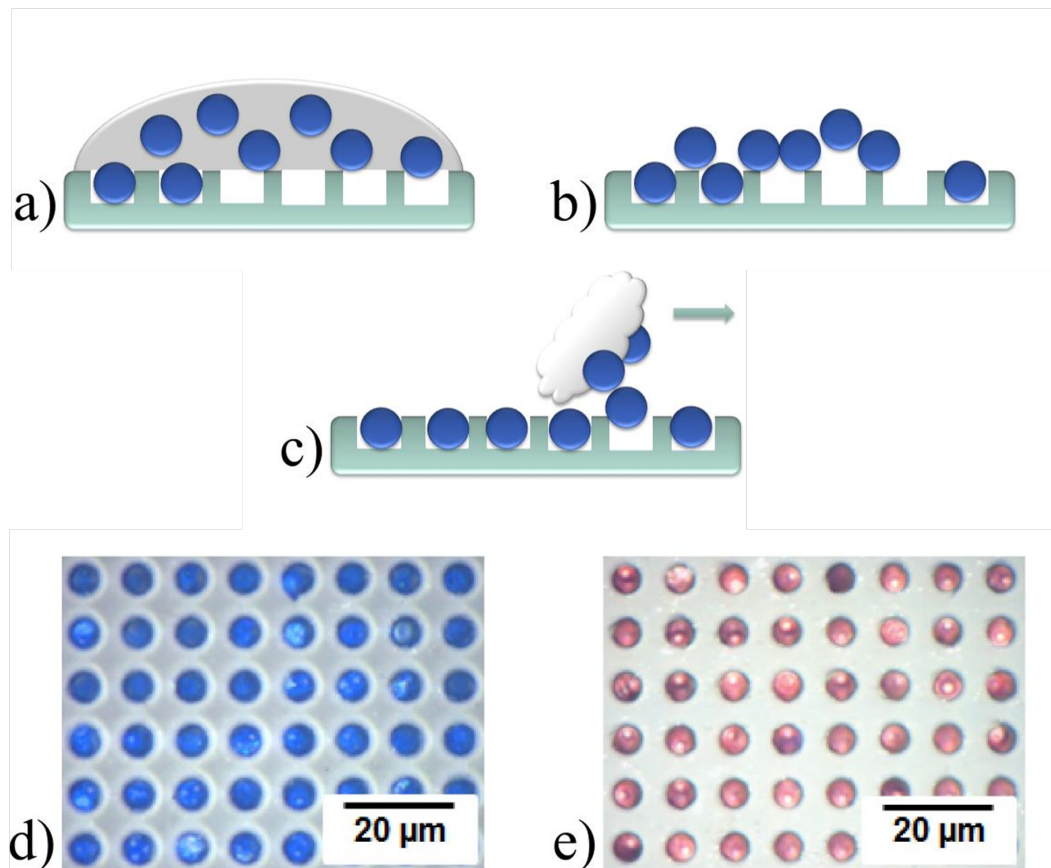
Figure 3.1: Schematic representation of particle deposition method. a) a required amount of solution with particles is applied onto the structured surface, b) self-assembling of the particles after solution evaporation, c) particles distribution and cleaning of the surface by applying a soft tissue, d), e) and f) structured substrate with $10\,\mu m$ pitch filled with $3\,\mu m$ polystyrene particles.

The amount of the deposited particles inside one micro well can vary depending on the ratio between the microbead size and the diameter of the cavity. It is possible to achieve one particle per microwell (Figure 3.2 a) . Therefore, the diameter and the depth of the structures should be approximately the same as the diameter of the microbead. In other cases, the particles can self-assemble to the different patterns in the cavities (Figure 3.2 b and 3.2 c). There are always small deviations in shape and the size of the polystyrene particles, however, the microbeads with diameters larger than the microcavity will be filtered away by the structures. Only microspheres with appropriate shape would fit and fill in the microwells, and the rest would be wiped away during the cleaning step (Figure 3.2 d).
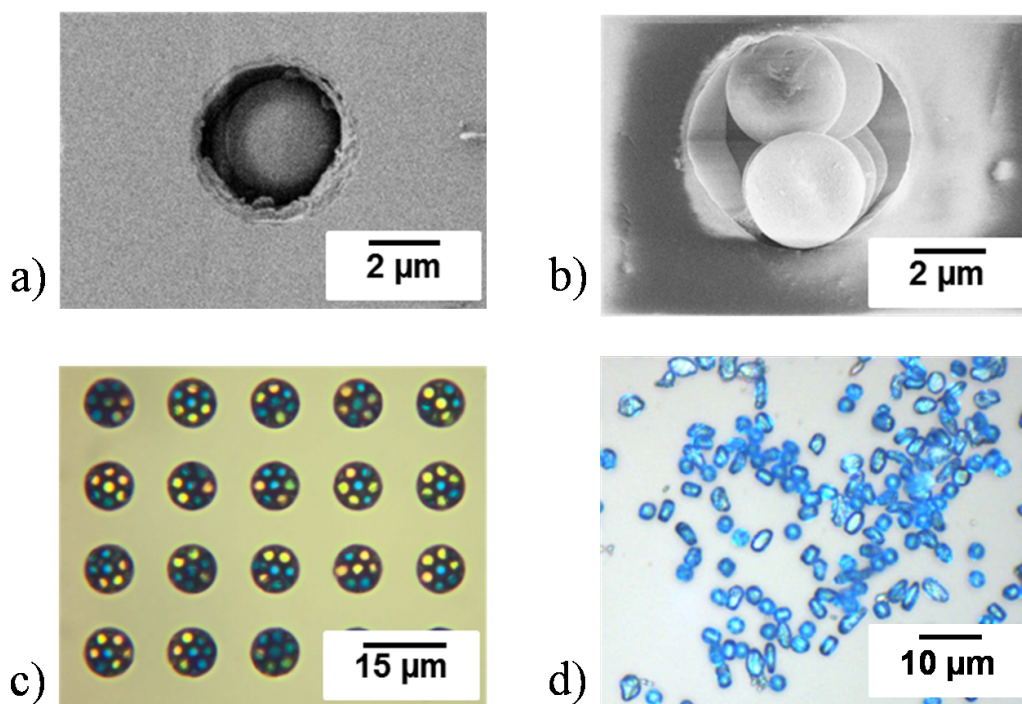
Figure 3.2: Particle deposition. The SEM images of the structures with a) microwell diameter of 4 μm filled with 3 μm polystyrene particle, b) microwell with diameter of 6 μm filled with 3 μm polystyrene particles. Optical microscope images of c) self-assembled pattern of 3 μm polystyrene particles in 9 μm microwells, pitch 15 μm, d) particles with the size deviation, filtered away by the structured surface.
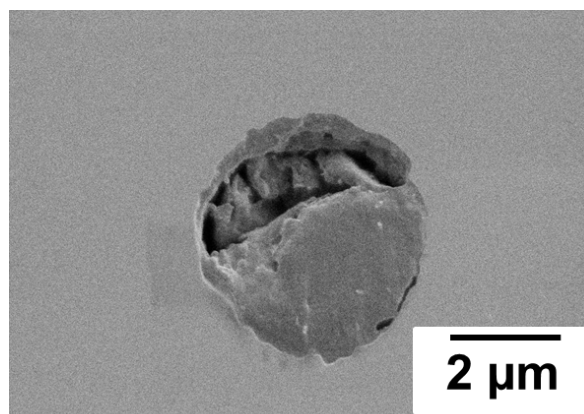
Figure 3.3: The SEM images of 4 μm micro well filled with a 3 μm polystyrene particle, which acts as a paste.

This particle deposition approach allows the structures to be filled with microbeads made from organic or inorganic materials, which could be found in the solution or as a powder. Moreover, unlike the methods where the deposition occurs in fluidic chambers, this new technique requires significantly smaller amount of particles. However, if the material from which the particles are made is soft, due to mechanical force

during the wiping step, some of the microbeads behave as a paste and plaster over another kind of microbead which was deposited earlier (Figure 3.3). Thus, this kind of soft particles should be deposited with more care, otherwise it will lead to contamination and will not be possible to make a pattern with different kind of materials on the same substrate.

Spin-coating the particle suspension over the structured substrate is a possible solution for particle deposition, whereby instead of mechanical impact, the particles would be pushed inside the structures by the centrifugal and capillary forces. Therefore, the possibility of destroying the shape of the soft particles would be reduced. However, it was not sufficient to fill all the microwells independently on the particles concentration in the suspension, as some of the microcavities were blocked by the air inside. As shown in Figure 3.4 a large amount of the particles stayed on the surface and needed to be removed. Moreover, spin-coating required more microbeads, than during the deposition technique with soft tissue.
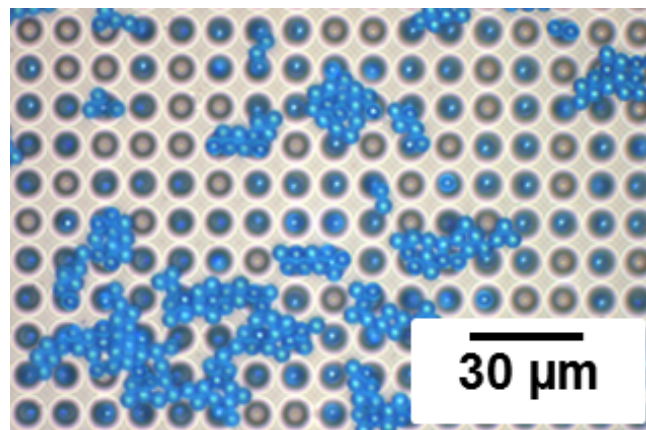
Figure 3.4: Optical image of the structured substrate after spin-coating with microparticle suspension, particle diameter is 5 μm, 7 μm diameter of microwells, pitch 10 μm.

3.1.1 Deposition of Amino Acid Particles

Amino acid particles used in this work are hydrophobic, which means they cannot be mixed with water and it is impossible to make a suspension for the deposition. Therefore, amino acid microparticles are applied on the surface as a powder. In this case, a small amount of the microbeads are spread on the top of the micro structures with a spatula. Subsequently, the soft tissue is applied to push the particles inside the micro cavities and remove the rest of them from the surface. The result of the particle deposition from the powder is shown in Figure 3.5.
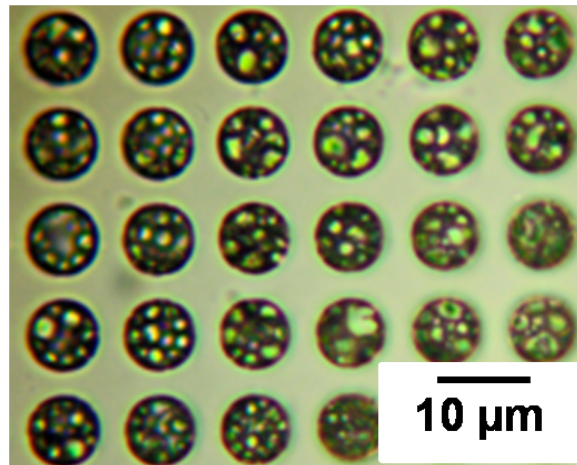
Figure 3.5: Optical image of the structured substrate with the diameter of microwells of 7 μm and pitch 10 μm filled with amino acid particles, which were deposited from the powder.

Both of the described deposition methods, from the liquid and the powder, allow the micro cavities to be filled equally. However, in first case, when the particles are mixed with a solvent, their distribution over the structured surface is more homogenous. Therefore, by applying the particles in a solution it is easier to control the amount of the deposited icrobeads in order to minimize their loss.

3.2 Particle Pattern Generation Method

3.2.1 Pattern Generated with Polystyrene Particles

The particle pattern generation method is based on the laser ablation process,[96], [97] where material is removed from the surface by irradiating it with the laser pulses. Laser ablation is a complex process which strongly depends on the ability of the material to absorb the light. The general case can be described as absorption of the laser energy by the electrons inside the material. The electrons subsequently transfer their energy to the lattice vibration. With enough energy supply, the strong lattice vibration weakens the bonds between molecules, causing the material to melt.[98]–[100] Further energy absorption leads to vaporization and sublimation, and subsequently to plasma formation. The hot expanding plasma interacts with surrounding gases and creates a shockwave, propelling the material.[101]

By applying the mechanism of laser ablation it is possible to obtain a combinatorial particle patterning with different kind of particles on one substrate. In addition, the position of each particle on the structured surface is well-defined. Schematic representation of particle pattern generation method is shown in Figure 3.6. First, all

micro cavities on the substrate are filled with one kind of microbeads by applying the deposition method described in Chapter 3.1. To generate the required combinatorial particle pattern, some of the microparticles are selectively removed from specific microwells (Figure 3.6 a) by irradiating them with focused laser beam. Afterwards, the sample is ready for deposition of another type of particles (Figure 3.6 b). The required combinatorial pattern is generated by repeating these steps of removal and deposition of different microbeads (Figure 3.6 c).
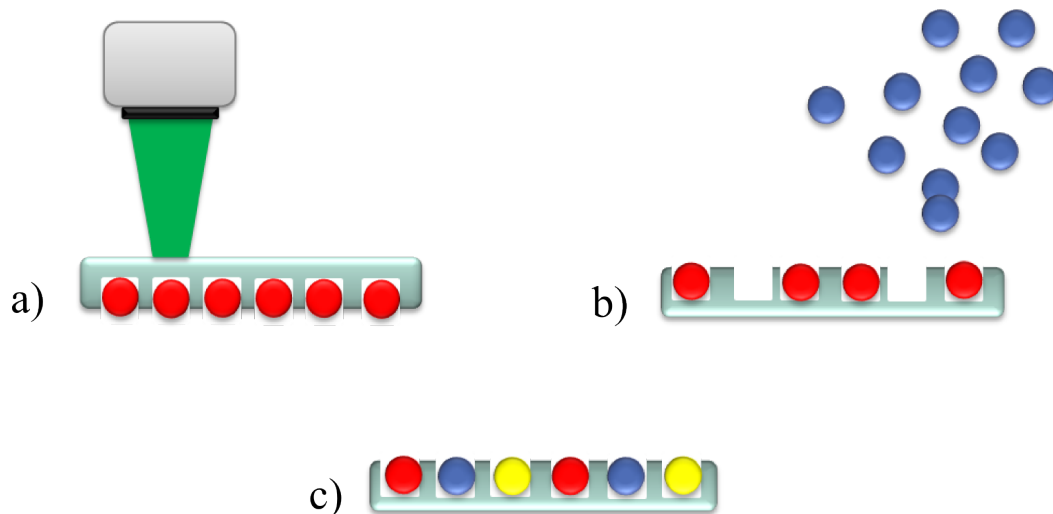
Figure 3.6: Schematic representation of the particle pattern generation method. a) removing the particular particles out of the microwells by laser irradiation, b) deposition of another kind of particle, c) by repeating the removal and deposition process the required amount of times, the particle pattern is generated.
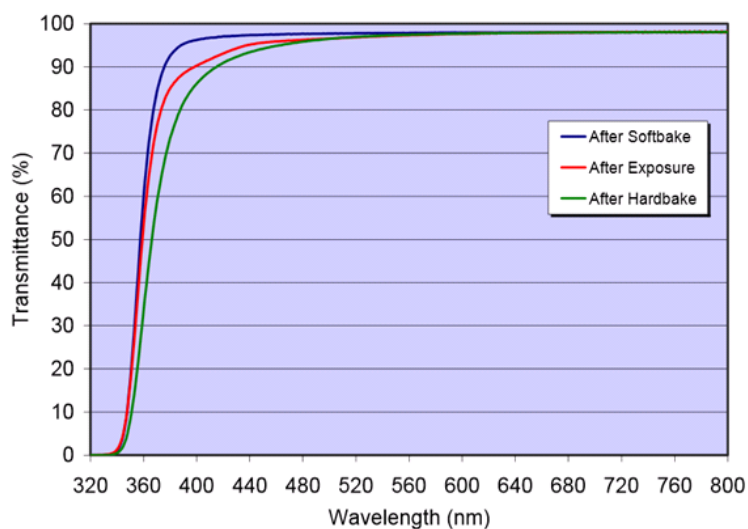
Figure 3.7: The transmittance of SU8 resist over a wavelenght range.[65]

The development of combinatorial particle patterning process was started with experiments on SU-8 microstructures. For this, we used the laser system described in Chapter 2.3 with Nd:YAG laser (532 nm). According to the transmission curve presented in Figure 3.7, the SU-8 resist transmission coefficient for the used wavelength is over 98%. Thus due to weak light absorption, SU-8 would not disturb the removal of the particles by laser beam intensities below its damage threshold.

First of all, laser parameters that were sufficient for the particle removal from the microcavities were determined. The pulse intensity was optimized in such a way that it was enough to remove the material from the cavities and, at the same time, not to destroy the SU-8 structures itself. For this, the series of the experiments was performed, where the laser irradiation from the laser system was applied to the substrate filled with microparticles.

During the adjustment of the laser parameters, its intensity was varying, starting at 30% with 2% increments at a constant number of five pulses. The minimum laser intensity at which particle removal took place was 48%. This value was fixed for further experiments, where the number of pulses varied from one till ten pulses with the repetition frequency of 1 kHz. The result of particle removal with different laser intensity is presented in Figure 3.8. The best parameters for the particle removal were achieved at a laser intensity of 48% and 10 pulses.
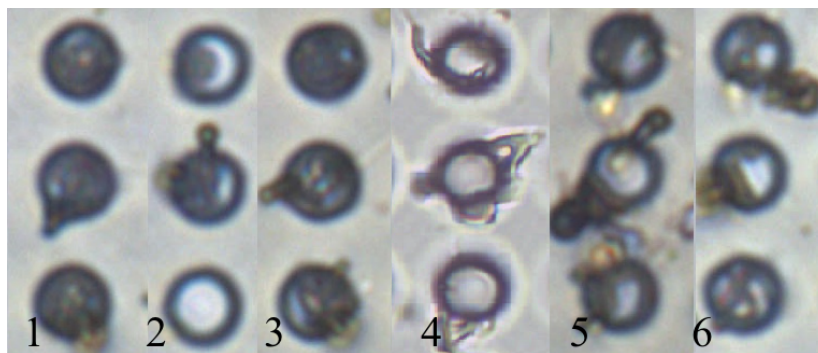
Figure 3.8: Light microscope image of particle removal from the microcavities with variation of laser parameters. 1) 46% and 5 pulses, 2) 48% and 5 pulses, pulse adjustment: 3) 48% and 1 pulse, 4) 48% and 10 pulses. 5) 50% and 10 pulses, 6) 48% and 15 pulses. Microwell diameter of 4 μm.

However, the particles were not removed completely from the structures even with the sufficient parameters. In addition, the trace of melted polystyrene micro beads was still on the top of the substrate. Further increasing of the laser intensity or the amount of pulses led to the melting of the particles and SU-8 resist, thus leaving even

more residue (Figure 3.8 5 and 6). This drawback is especially unacceptable for the peptide array synthesis, as it would lead to contamination.

The direct application of the pulsed laser irradiation to the sample causes the damage and melting of the polymer. To overcome this problem, the sacrificial layer, also called the dynamic release layer (DRL), was introduced. In this case, this additional layer absorbs the laser energy and due to its ablation propels the contents of the micro cavities without damage them.[102]

The material for the DRL and its thickness was chosen depending on its ability to absorb the light in the wavelength range of the laser. One of the most suitable materials for additional layers, at wavelength of 532 nm, is gold.[103] It is preferable to choose the DRL thickness below the penetration depth for gold. With a thicker additional layer, the laser irradiation would not penetrate the whole depth of the gold film and, as a result, the light absorption in the release layer and its ablation becomes inhomogeneous.[104],[105] The penetration depth of different metals is presented in Figure 3.9. For sufficient particle removal from the microcavities, the thickness of the gold layer should not exceed 20 nm.
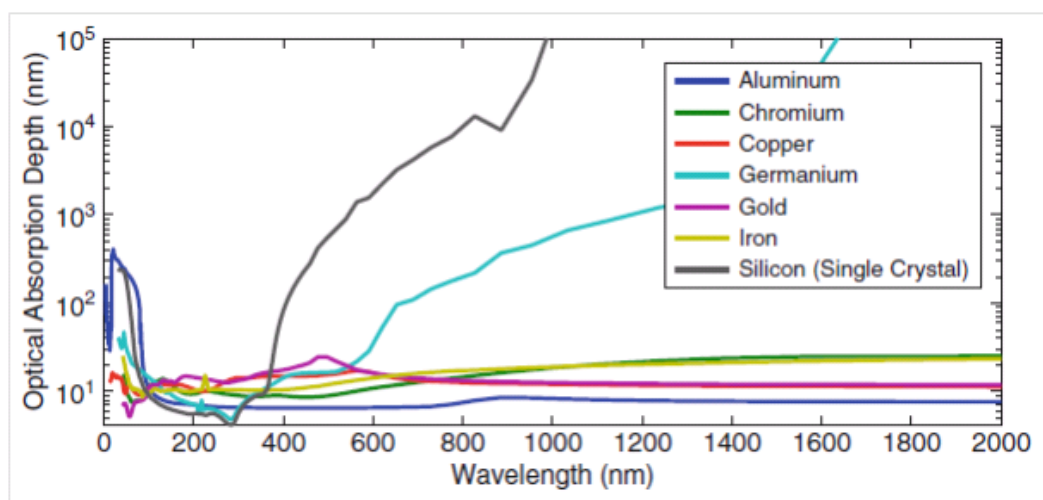
Figure 3.9: Optical absorption depth for different metals in a range of wavelengths.[106]

To realize the advantage of using the dynamic release layer, gold was sputtered only onto one half of the glass sample with SU-8 structures, with the thickness of 15 nm (Figure 3.10 c). Subsequently, both parts of the sample with and without DRL were irradiated with the same laser parameters used to remove the microparticles from the microcavities. The results of the comparison experiment are shown in Figure 3.10. On the side without the sacrificial layer, the particles were destroyed and were not completely removed from the microwells (Figure 3.10 a). However, on the side with

the gold layer, the microcavities were emptied without any remainings (Figure 3.10 b). Moreover, further experiments showed that using gold as dynamic release layer required less laser intensity. The sufficient parameters for particle pattern generation were 47% and one pulse.
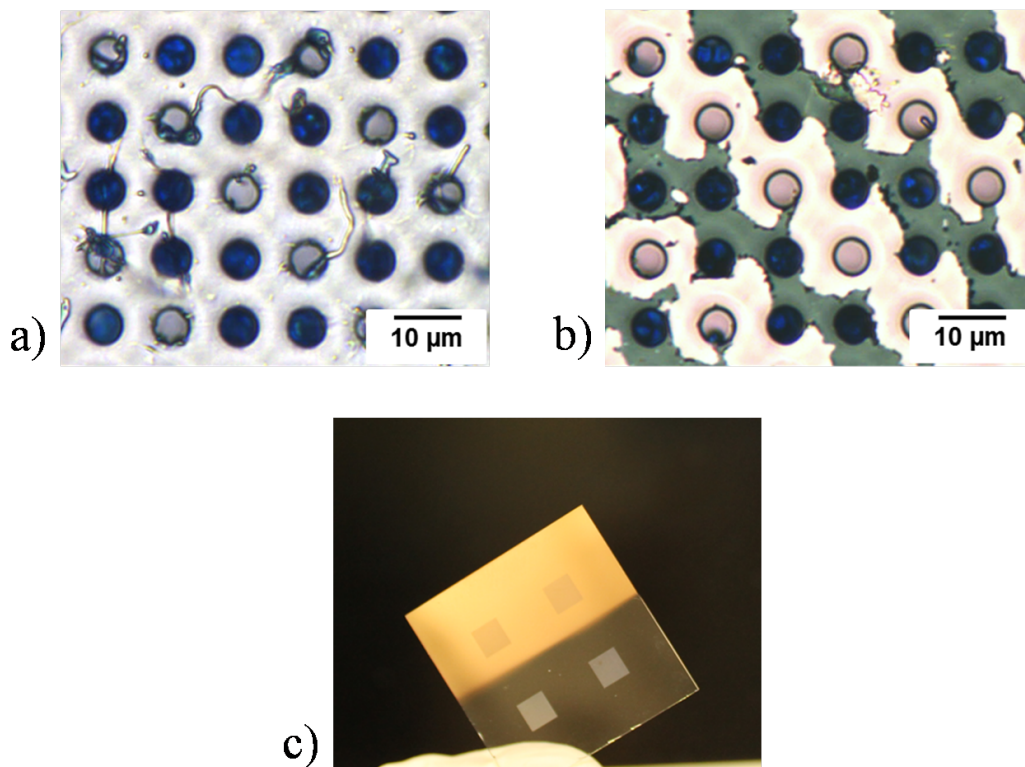
Figure 3.10: Particle pattern generation method performed on SU8 structures of micro wells with the diameter of 6 μm with and without sacrificial layer, filled with 3 μm polystyrene particles. a) glass chip with SU-8 structures, half covered with 15 nm gold layer, b) the removal of the microparticles without sacrificial layer, c) the removal of the microparticles with sacrificial layer.

As already described in Chapter 2.1.2, SU-8 structures were not suitable for peptide synthesis, because they were not stable in such chemical solution as dichloromethane (DCM). Thus the glass substrates fabricated via the plasma etching process described in Chapter 2.1 were used for the further experiments.

Therefore, the same series of experiments were performed on the etched glass substrates in order to find the sufficient laser parameters for particle removal. First of all, the sample without the gold layer was proceeded with laser intensity varying from 44% to 48% and one pulse. Despite the residuals on the top of the structures, the most sufficient parameters were obtained with the laser intensity of 47% (Figure 3.11 2). A further increase in laser power destroyed the glass substrate. However, this also removed material completely from the cavities without any residue on the surface, meaning that, in the case of SU-8 structures with increases to the intensity, the traces

of the material inside and on the top of the structured substrate could be explained by melting of the resist itself.
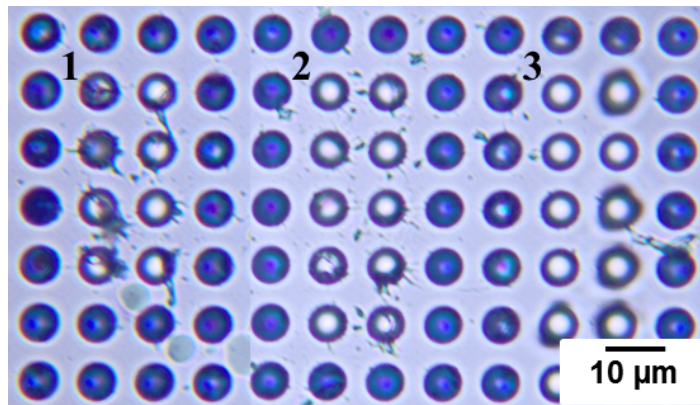
Figure 3.11: Optical microscope image of the result for the experiment with variation of the laser intensity for particle removal from the glass substrate structured with the micro cavities. 1) 46% and 1 pulse, 2) 47% and 1 pulse, 3) 48% and 1 pulse.
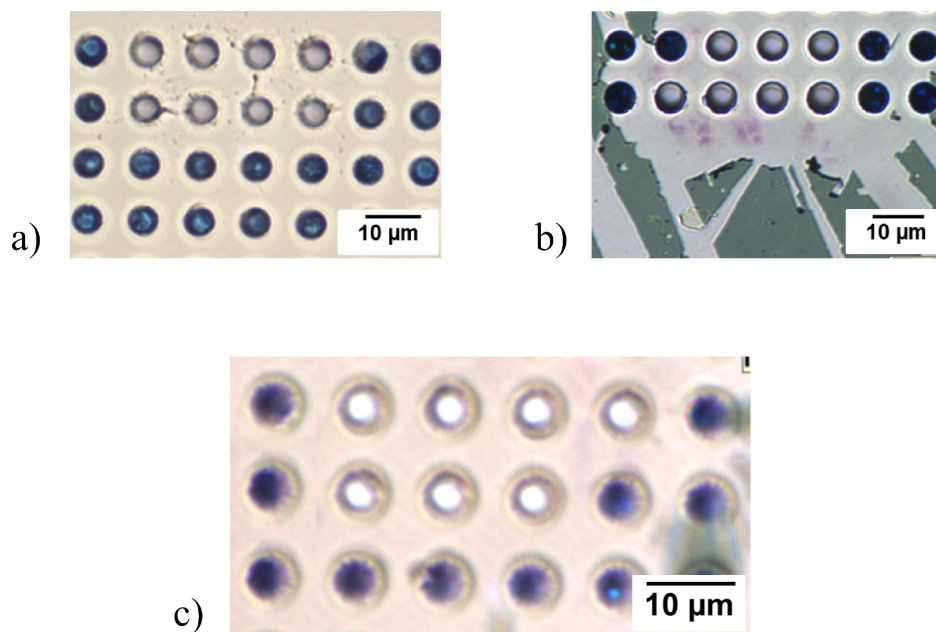
Figure 3.12: Optical microscope images of particle pattern generation performed on a glass structures with microwells with a diameter of 6 µm, filled with 3 µm polystyrene particles. a) the removal of the particle without DRL, b) and c) the removal of the particle with DRL layer.

To check the necessity of using a sacrificial layer for the glass substrates, half of the sample was covered with the gold layer of 15 nm. After particle deposition, particle removal was performed at 47% of laser energy and 1 pulse. The results for glass substrate are the same as previously with SU-8 structures and are shown in Figure 3.12. Without the dynamic release layer microwells were not completely empty, with

some residues left on the surface (Figure 3.12 a). In contrast, Figures 3.12 b and 3.12 c show total removal of the particles from the microcavities on the side where the gold layer was sputtered. Thus later in this work, all the experiments were performed on the glass substrates with gold release layer.
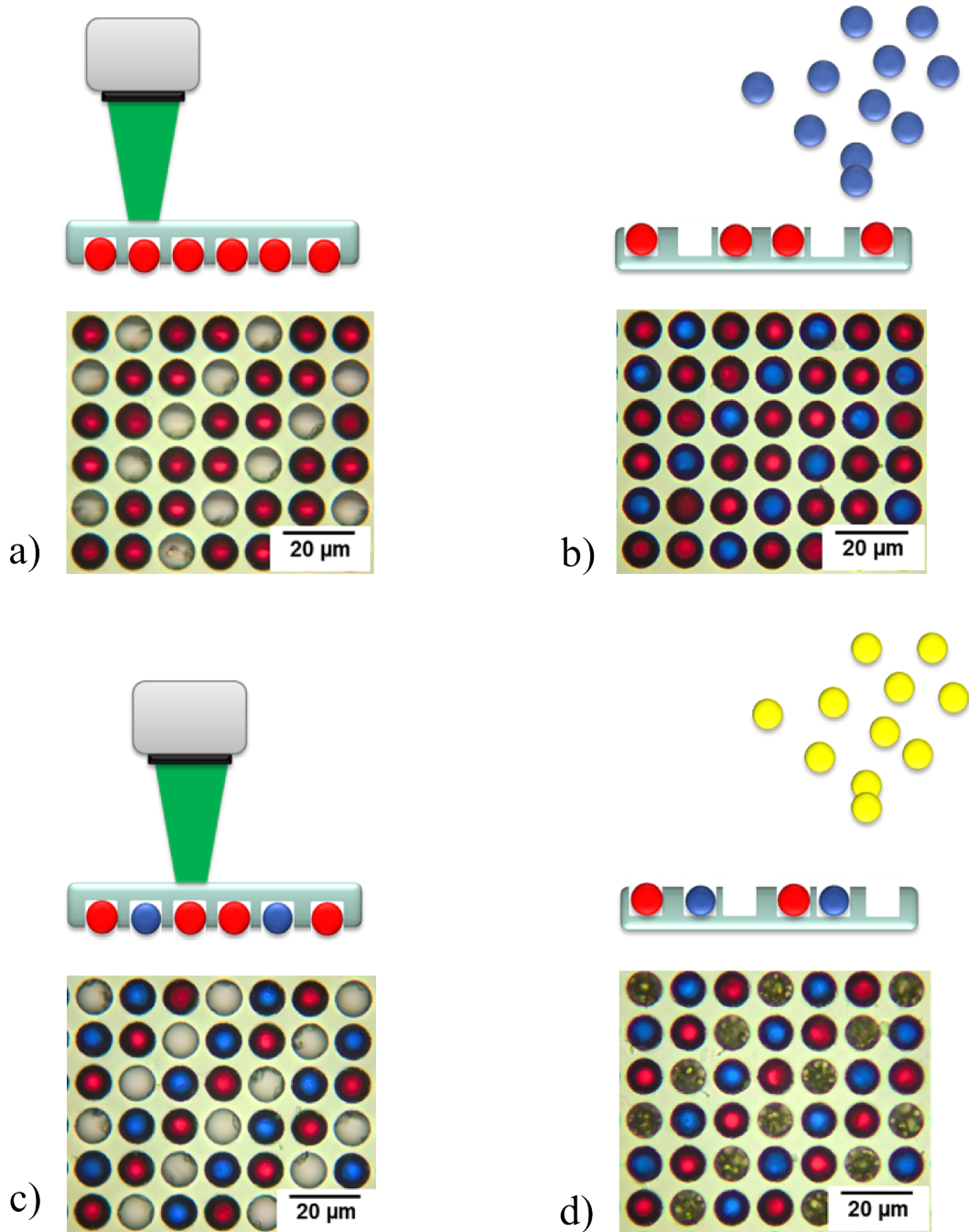
Figure 3.13: Schematic and optical images of particle patter generated on 10 μm cavities with a pitch of 14 μm with 10 μm blue, red and 3 μm yellow particles. a) a d c) removal of the particles from the micro wells by applying laser irradiation, b) and d) deposition of another kind of particles into emptied micro wells.

Using laser parameters suitable for particle removal, combinatorial patterns were

generated on the microstructured substrate. The proof-of-principle experiment was performed with 10 μm red and blue color particles and 3 μm yellow particles on the structures with cylindrical microcavities with a diameter of 10 μm and depth of 10 μm.

First, 10 μm red microbeads were deposited on the structured surface (Figure 3.13 a). Subsequently, the microwells defined by the pattern were irradiated with the laser. After the removal of red microbeads, 10 μm blue beads were deposited into the emptied microcavities (Figure 3.13 b). Subsequently, the next removal step was repeated again and 3 μm yellow particles were deposited (Figure 3.13 d). The result from the deposition of yellow microbeads shows that even with a smaller microsphere diameter, it is possible to generate a pattern without contamination. However, the important requirement for the deposition of smaller microbeads is when other microparticles are tightly fill microwells, preventing particle mix.

The same particle pattern generation technique can be applied for the microstructures with smaller pitch. However, in that case, it is more difficult to distinguish between the different colors of smaller microbeads inside the microwells. Therefore, more advanced optical detection should be used in this case. The result for the patterning with 3 μm blue, red and yellow particles on the structures with microwells diameter of 4 μm and pitch of 10 μm is presented in Figure 3.14.
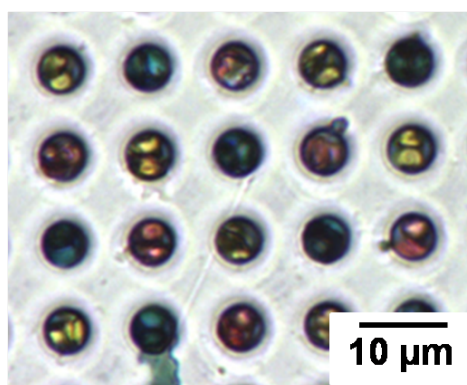
Figure 3.14: Particle pattern generated on the 4 μm cavities and a pitch of 10 μm with 3 μm blue, red and yellow particles.

3.2.2 Pattern Generated with Amino Acid Particles

After realizing the behavior of the microbeads during the deposition and their removal from the microcavities, the particle pattern generation method was considered for peptide arrays synthesis.

As shown in Chapter 3.2, by applying the gold dynamic release layer to the structured surface, the removal of the particles from the microwells becomes more effi-

cient. However, for the peptide synthesis the usage of the additional coating is not possible. The reason is the functionalization of the surface, which is represented by the polymer layer. If the functionalized surface is covered with gold, then all the functional groups, responsible for peptide linking to the surface will be removed during the laser ablation. Nonetheless, without a sacrificial layer, this polymer coating is supposed to stay undamaged, as it is optically transparent to the wavelength of the laser. In order to determine if the functional groups are not destroyed during the ablation process, the proof-of-principle experiment was performed in PhD Thesis of Dr. F. Maerkle and it can be found in more detail in [16].

First of all, the polystyrene particles were deposited on the structured substrate as a first layer in order to reduce contamination. As already shown (Figure 3.12), after the ablation process, without the sacrificial layer, the residue of the polymer stays inside the microcavities and on the top of the structures. Therefore, since the amino acid particles are also made from a polymer, it is possible that the trace of the material would result in impurity. However, the residue of the polystyrene particles in this case do not disturb the synthesis process. Therefore, 4 µm blue polystyrene particles were deposited in the microwells with the diameter of 6 µm. In order to block all possible empty space in the microcavities and, thereby, decrease the possibility of contamination, 1 µm blue polystyrene particles were applied on the top of already deposited 4 µm microparticles.

After the deposition, the microcavities required for the pattern were irradiated with the laser. Subsequently, the emptied microwells were filled with the biotin microparticles, which were fabricated the same way as amino acid microbeads (Chapter 2.2.2). To perform the coupling reaction, the sample was placed in the oven for 90 minutes at 90 ° C. Next, the chemical steps of washing, deprotecting and staining the sample with fluorescent dye were performed, which are described in Appendix 7.2 and 7.3. The resulting fluorescent image in Figure 3.16 shows that the biotin molecules coupled to the surface, which means the functional groups were not destroyed during the ablation process.
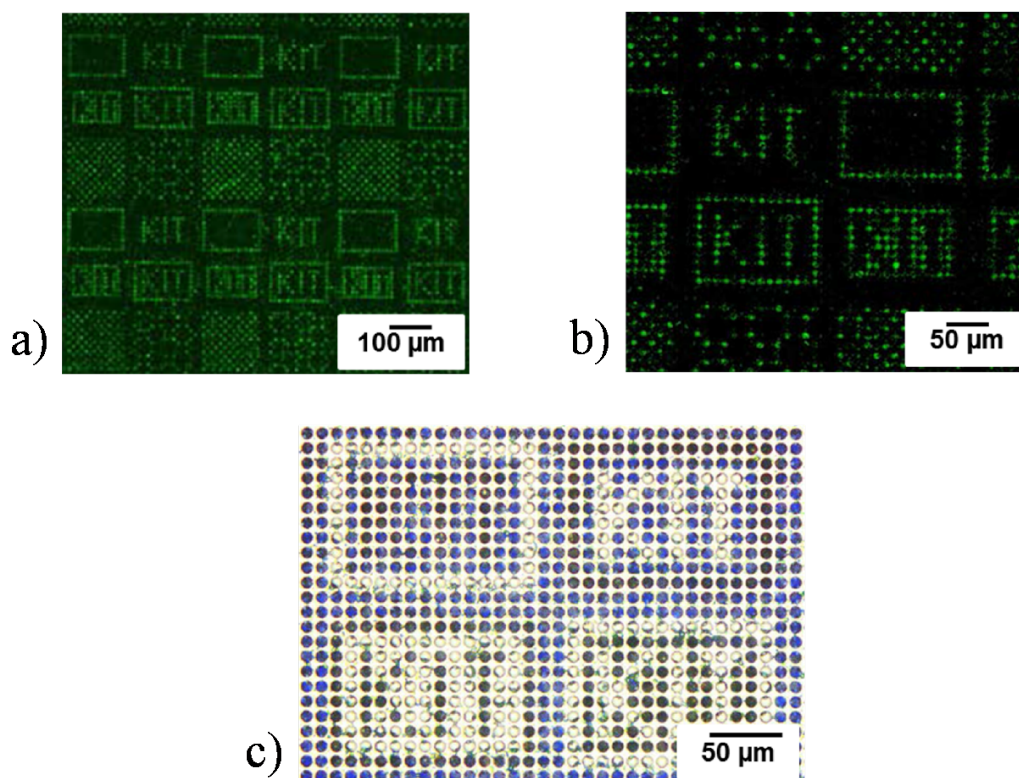
Figure 3.15: Pictures of combinatorial synthesis performed with biotin particles on 6 μm cavity diameter and pitch of 10 μm. a) and b) fluorescent pictures, c) optical microscope image of combinatorial pattern with biotin and polystyrene particles on the structured substrate.[16]

Even though, the described above experiment proves the possibility of generating combinatorial patterns with amino acid particles on the functionalized surface, this technique might not be suitable for the synthesis of the longer chains of amino acids, where the same microcavity should be irradiated up to twenty times. Due to high temperatures, and repeated exposure to high laser intensities, there is always a possibility, that the functionalized polymer layer will be damaged. In order to overcome this problem, the material transfer method was developed.

3.3 Material Transfer Method

As mentioned in the previous chapter, for the combinatorial particle pattern generation method the peptides are synthesized on the same substrate, from which the particles are removed by laser irradiation. Repeated exposure to high laser intensities can destroy the functionalized surface and decrease the efficiency of the method as not all the peptides will be synthesized successfully. Nonetheless, the material transfer method allows combinatorial particle pattern on the substrate to be generated without irradiating it with a laser.[107]

In the material transfer method, the combinatorial pattern is generated by transferring the microbeads from one structured substrate to another. The first substrate is a donor slide, where all the microcavities are filled with the same kind of microparticles. From this donor substrate, the content of the microcavities is transferred to the well-defined microwells on the other substrate, which is called acceptor slide. When the pattern of the first type of particles is generated, the donor slide is changed. This process is repeated until the whole combinatorial pattern with required materials is generated on the acceptor slide. Figure 3.16 shows the principle of particle patterning on the microstructured substrates with the material transfer method.
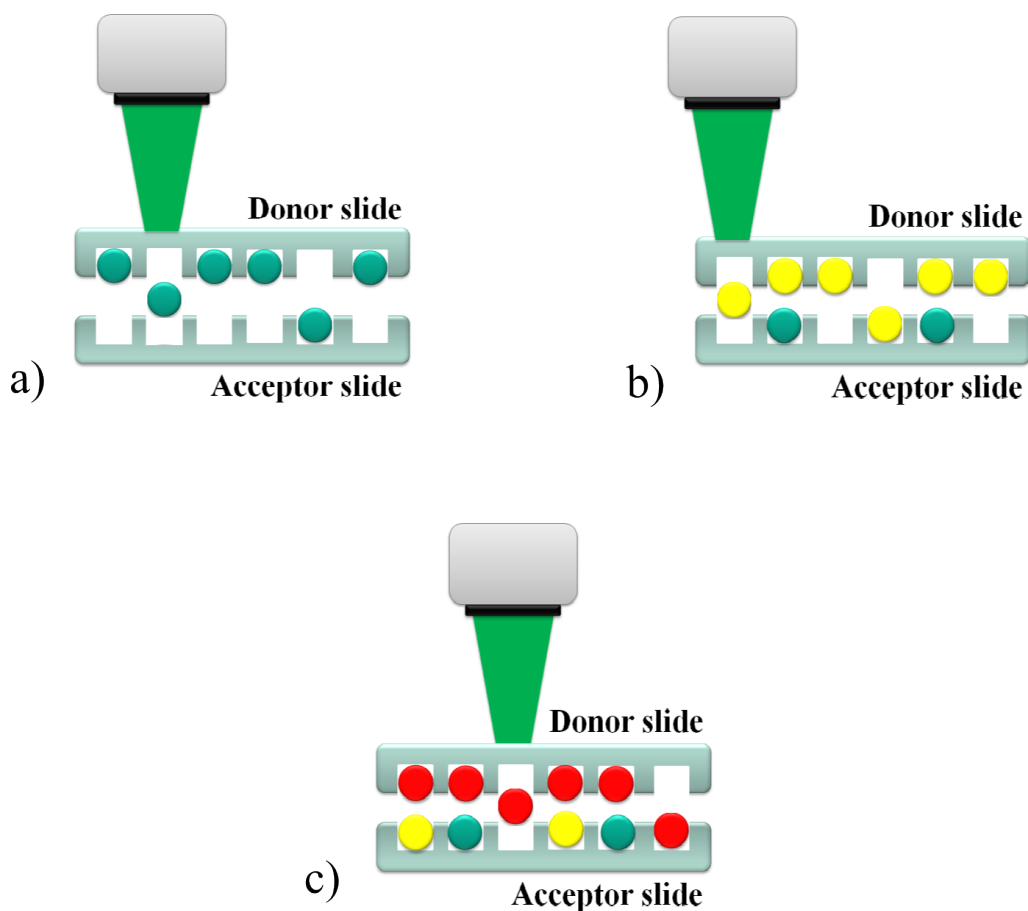
Figure 3.16: Principle of particle patterning with material transfer method. a), b) and c) generation of combinatorial particle pattern by transferring the microparticles from donor slide to acceptor slide using laser irradiation.

Another advantage of this method is that all the donor slides can be prepared in advance to speed up the process. Moreover, it also gives an opportunity to automate the entire process of generating combinatorial patterns, where pre-filled donor slides are loaded and exchanged in the laser system automatically.

3.3.1 Laser Transfer of Polystyrene Microparticles

As the transfer method involves the same principle of removing the material from the microcavities as the particle pattern generation approach, the first experiments were performed based on previous results, described in Chapter 3.2.1. Thus the technique development started with the transfer of polystyrene particles. To prepare the donor slide, the microstructured glass substrate with cavities of 7 μm was covered with 15 nm gold dynamic release layer and subsequently filled with the blue 3 μm polystyrene particles.

The donor and acceptor slides were placed in a specially designed holder, as described in Chapter 2.3, and which allows the microcavities from both slides to be adjusted precisely under each other. The laser parameters for removing the microparticles from the donor slide were 47% laser intensity and 1 pulse.

For the particle pattern generation method, it was not important what happened to the polystyrene particles after their removal from the microcavities. The result of the transfer in Figure 3.17 shows that the microbeads are destroyed. Moreover, previously with the chosen laser parameters, the particles were removed from the microwells completely without any residue left on the surface of the sample. Thus the presence of the polymer material on the top of the donor substrate can be explained by a certain gap between the slides. Debris of the destroyed particles remains in the gap in the double-slide geometry and contaminates the surface.
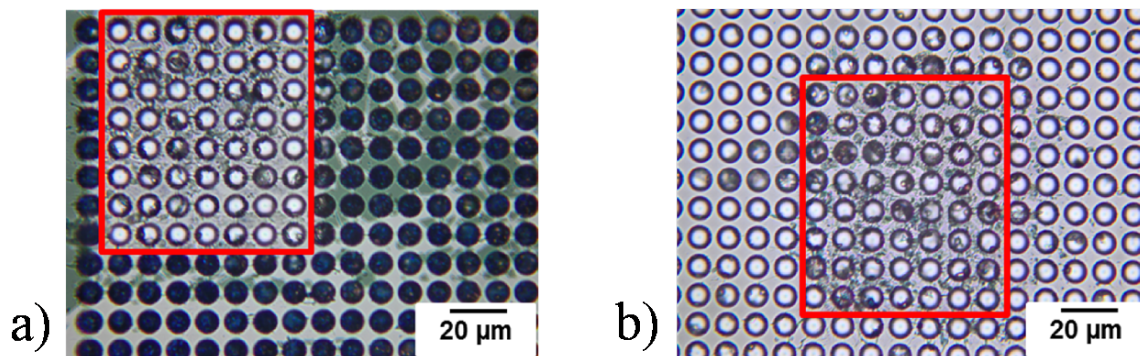
Figure 3.17: Light microscope image of the microcavities after polystyrene particle transfer from donor slide with cavity diameter of 6 μm and pitch of 10 μm to acceptor slide with the same parameters. a) door slide and b) acceptor slide.

3.3.2 Transfer of Amino Acid Particles

In contrast to the monodispersed spherical polystyrene microparticles, amino acid microbeads have a relatively large size distribution. In order to study behavior of

amino acid particles in double-side geometry, several laser transfer experiments were performed proving the possibility of removing and transferring the microbeads from donor to acceptor slides. For the first experiments, the same laser parameters as for polystyrene microbeads as those described in Chapter 3.3.2 were used, namely, 47% laser intensity and 1 pulse. The result is shown in Figure 3.17. In this case, the material was transferred from the donor to acceptor slide. However, not all the micro-cavities were filled with the transferred amino acid particles. Moreover, some of the microwells which were supposed to be empty were contaminated.
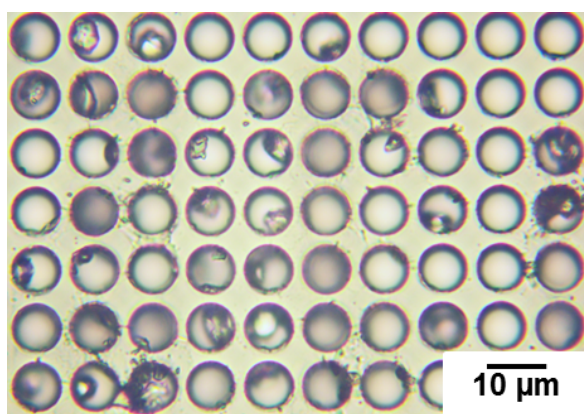
Figure 3.18: Light microscope image of the acceptor slide with 7 μm cavity diameter structures and pitch of 10 μm after the transfer of amino acid particles.

After the repeating the experiment several times, it was found that, during the ablation process, amino acid particles were dispersed. Furthermore, as the donor and acceptor slides had a proximity, the microbeads were also transferred to the contiguous microwells. The reason for this dispersion was that some of the particles were guided through the gap by vapor, generated by the laser ablation. In order to prevent the microbeads from spreading, which could lead to contamination, the amino acid particles were sintered in the oven at 90°C for 10 minutes. After the sintering of the microbeads, the transfer of the material by laser irradiation was significantly improved. As can be seen in Figure 3.19, all the required microwells were filled with the material.
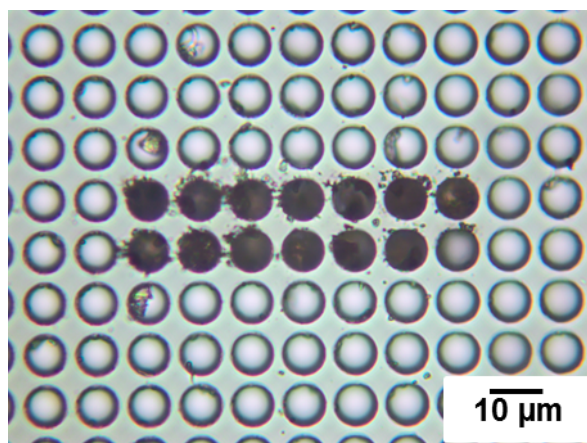
Figure 3.19: Light microscope image of the acceptor slide with 7 µm cavity diameter and pitch of 10 µm after the laser transfer of sintered amino acid particles from the donor slide with the same parameters.

Sintering agglutinates the separate microbeads in a microcavity. The resulting agglomerate behaves as a single particle, which is transferred from the cavity on the donor slide directly to the opposite microwell situated on the acceptor slide. The analysis of the experimental results of material transfer with the sample covered with gold layer (where the transfer was not efficient) and the one with gold layer and sintered particles (where the transferred material completely filled the microcavities) questioned the necessity of applying dynamic release layer (DRL).
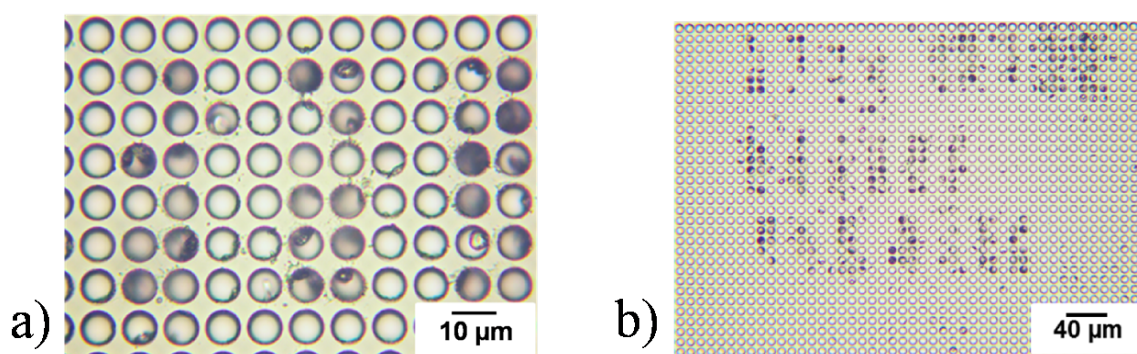
Figure 3.20: Light microscope image of the acceptor slide with 7 µm cavity diameter structures and pitch of 10 µm after the transfer of sintered amino acid particles from the donor slide prepared without the gold layer. a) after transfer of sintered amino acid particles from the donor slide prepared with the gold layer, b) transfer of sintered amino acid particles with variation of the laser parameters.

The next experiment of amino acid particle transfer was performed without gold DRL. Amino acid microbeads were deposited on the donor slide directly and were sintered in the oven. As a result, the transfer was not sufficient (Figure 3.20). Even the variation and increasing of laser intensity, which is shown in Figure 3.20 b), did

not improved the transfer. This emphasizes once again the importance of using the release gold layer.

Thus all other experiments of the transfer material method were performed with the gold release layer and sintered particles. As mention before, these parameters improve the transfer efficiency and significantly reduce contamination. However, the residue of the transferred material was still present. Figure 3.21 a) shows traces of the particles on the top of the structures. One of the reasons for this could be misalignment of the slide holder. For the material transfer method even several hundred nanometers could be a noticeable misalignment. Another reason could be a divergence of the vapor flow during the laser ablation.
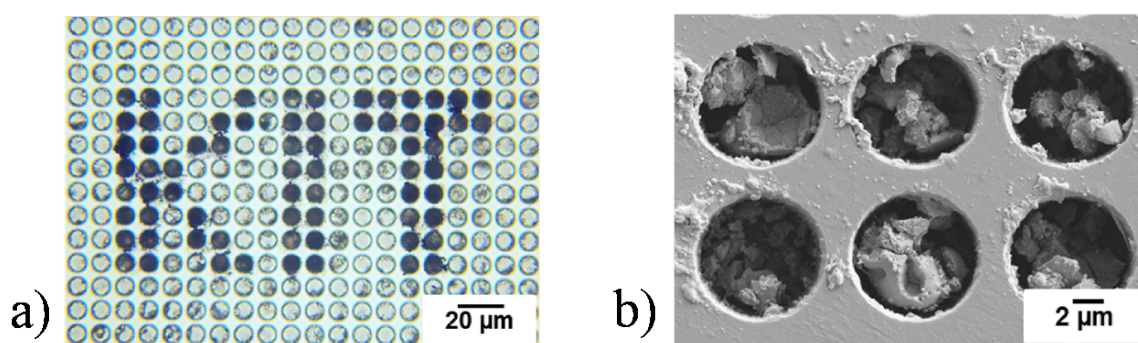
Figure 3.21: Acceptor slide with 7 μm cavity diameter structures and pitch of 10 μm after the transfer of sintered amino acid particles from the donor slide with 7 μm cavity diameter structures and pitch of 10 μm prepared with the gold layer. a) light microscope image of the transferred amino acid particles, b) SEM picture of transferred amino acid particles.
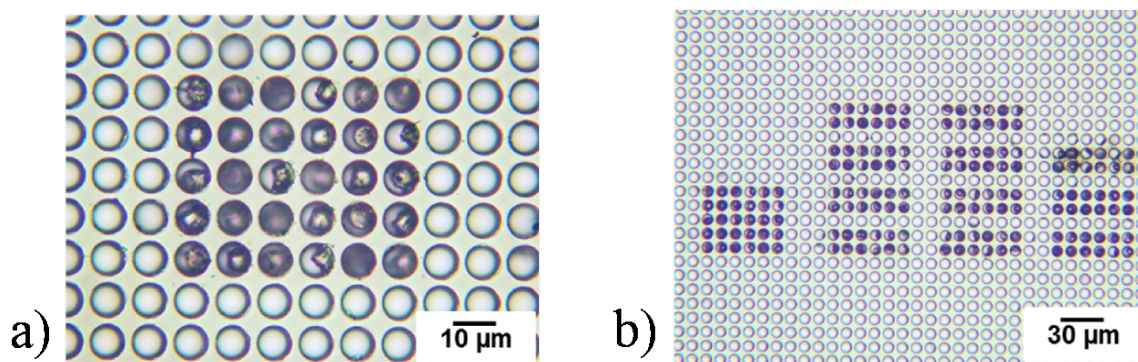
Figure 3.22: Acceptor slide with 7 μm cavity diameter structures and pitch of 10 μm after the transfer of sintered amino acid particles from the donor slide with 5 μm cavity diameter structures and pitch of 10 μm prepared with the gold layer.

Therefore, to reduce the amount of the residue on the surface of the acceptor slide, two structured surfaces with different microwells diameters for donor and acceptor slides were introduced. Thus for the donor slide, microcavities with 5 μm in diame-

ter and for the acceptor 7 μm in diameter were chosen. However the pitch of 10 μm remained the same in both cases. The result of the amino acid particle transfer is presented in Figure 3.22. With this configuration of the microstructured surfaces, the vapor flow fits the size of the microwells on the acceptor slide and possible misalignment does not leave any residue on the top of the substrate.

3.3.3 Array Synthesis Using Material Transfer Method

Based on the result from amino acid particle transfer described in Chapter 3.3.2, the proof-of-principle experiment for peptide synthesis was performed by applying material transfer method.The experiment to generate the combinatorial pattern with amino acid particles using the laser irradiation was made by C. von Bojničić-Kninski and will be described in more detail in [108].

During the experiment for generating the combinatorial pattern of glycine and biotin, two microstructured surfaces with microwell diameters of 5 μm were covered with the 15 nm gold layer. Subsequently, these donor slides were filled with glycine and biotin particles separately. First, the glycine particles were transferred to the acceptor microstructured surface with a microwell diameter of 7 μm and pitch of 10 μm by irradiating the required microcavities with the laser. Subsequently, the additional pattern of biotin particles was transferred onto the same acceptor slide using the same laser parameters. Afterwards, to let the amino acids defuse in matrix material and couple with the functional groups on the surface of the substrate, the sample was placed in the oven for 90 minutes at 90 ° C. Following chemical steps of washing off the matrix material and deprotecting the amino groups can be found in more detail in Apendix 7.2. In order to detect monomers coupled to the functionalized surface, amino acid glycine was stained with fluorescent dye DyLight 650 and biotin with streptavidin DyLight 550 (Appendix 7.3). The result of the synthesis was inspected under the fluorescent microscope and is presented in Figure 3.23. It proves, that, with the transfer material method, it is possible to generate combinatorial molecular arrays with the resolution of 1 million spots per cm^2.
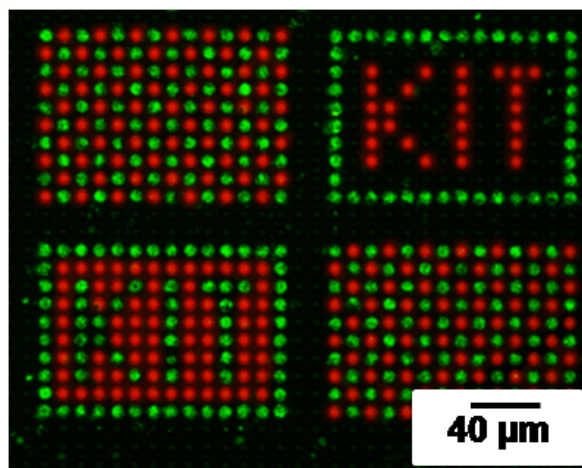
Figure 3.23: Fluorescent picture of proof-of-principle experiment of material transfer method performed on 7 µm cavities with pitch of 10 µm; red fluorescent signal corresponds to glycine and green signal to biotin.[108]

4 Stochastic Particle Pattern Generation

Particle pattern generation and material transfer methods for peptide array synthesis, as described in Chapter 3, require advanced micropositioning techniques in order to be automated. Therefore, increasing the spot density of arrays to above 1 million spots per cm^2 for above mentioned techniques would require significant technical effort. Moreover, following the laser-based methods, the polymer microparticles with embedded amino acids and the functional surface of the substrate are exposed to laser radiation. That might decrease the efficiency of the peptide synthesis. Therefore, to overcome these limitations stochastic method for particle pattern generation is proposed, where the density of the arrays can be increased up to 25 million spots per cm^2.[109]

The main difference between stochastic arrays and arrays fabricated using the laser-based techniques is that, in stochastic approach, it is not possible to predict in advance the position of a specific peptide on the substrate, to be synthesized in the microcavity. However, the position and the sequence of the peptides is known at the end of the synthesis, while in the laser-based techniques, all these parameters are well defined from the beginning of the process.

In stochastic methods, a crucial role is played by particle deposition, following which, microbeads randomly fill the microcavities on a structured surface. To analyze the position of the microbeads, the pictures should be taken after each deposition step. The filling of the microcavities on these photos can be analyzed by image processing software.

In this chapter, a novel stochastic particle deposition method is described. The stochastic method allows combinatorial particle patterns to be fabricated on the substrates structured with different size of the microcavities, even with the pitch less than 2 μm. Moreover, by applying this method the possibility of damaging the particles or functional groups on the surface is minimized.

4.1 Stochastic Deposition of Microparticles

The stochastic deposition method is similar to the particle deposition method described in Chapter 3.1. The main difference is that the microbeads are diluted in liquid at the defined concentration, so that they randomly fill the required percentage of the microwells. Another important requirement is that the diameter of the deposited particles are approximately the same as the diameter of the microcavities. In this case, only one microbead fits the microwell, which removes the possibility of contamination. The schematic representation of the deposition procedure is shown in Figure 4.1. First the required amount of the particles is diluted in water (or other appropriate solution) to make a suspension. Subsequently, the sufficient amount of this solution with microbeads is poured on the structured substrate. After the evaporation of the solvent, microparticles stay inside or on the top of the structures. Some microbeads are removed from the surface and, at the same time, some of them are pushed into the microwells by wiping the substrate with a soft tissue.
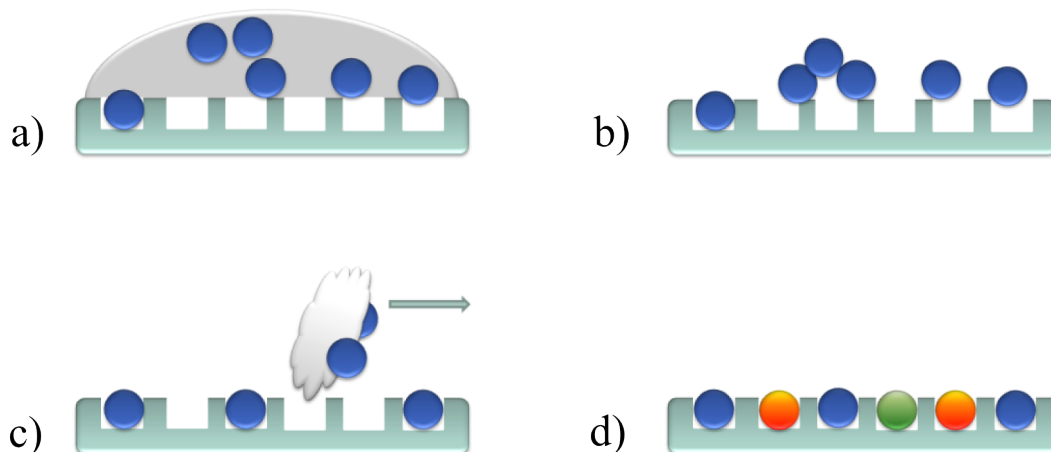
Figure 4.1: Schematic representation of stochastic particle deposition method from liquids. a) solution with well defined particle concentration is applied onto the pre-structured surface, b) self-assembling of the particles after solution evaporation, c) particles distribution and cleaning of the surface by applying a soft tissue, d) repeating the deposition process results the particle pattern generated on the microstructured surface.

The ratio between filled and empty structures depends on the particle concentration in the solution. By varying the concentration of the microbeads, it is possible to fill of 1% to 100% of the microwells. Figure 4.2 shows the microstructures stochastically filled with polystyrene microparticles with different concentrations. Due to the fact that stochastic deposition is a random process, the spatial distribution of the particles in microcavities can be inhomogeneous, where some parts of the sample are filled

more than others (Figure 4.2 d). However, this fact does not limit the performance of the method. In this case filling is calculated as an average. Since the concentration of the particles is always defined, the average amount of filled cavities stays approximately the same for the series of the experiments.
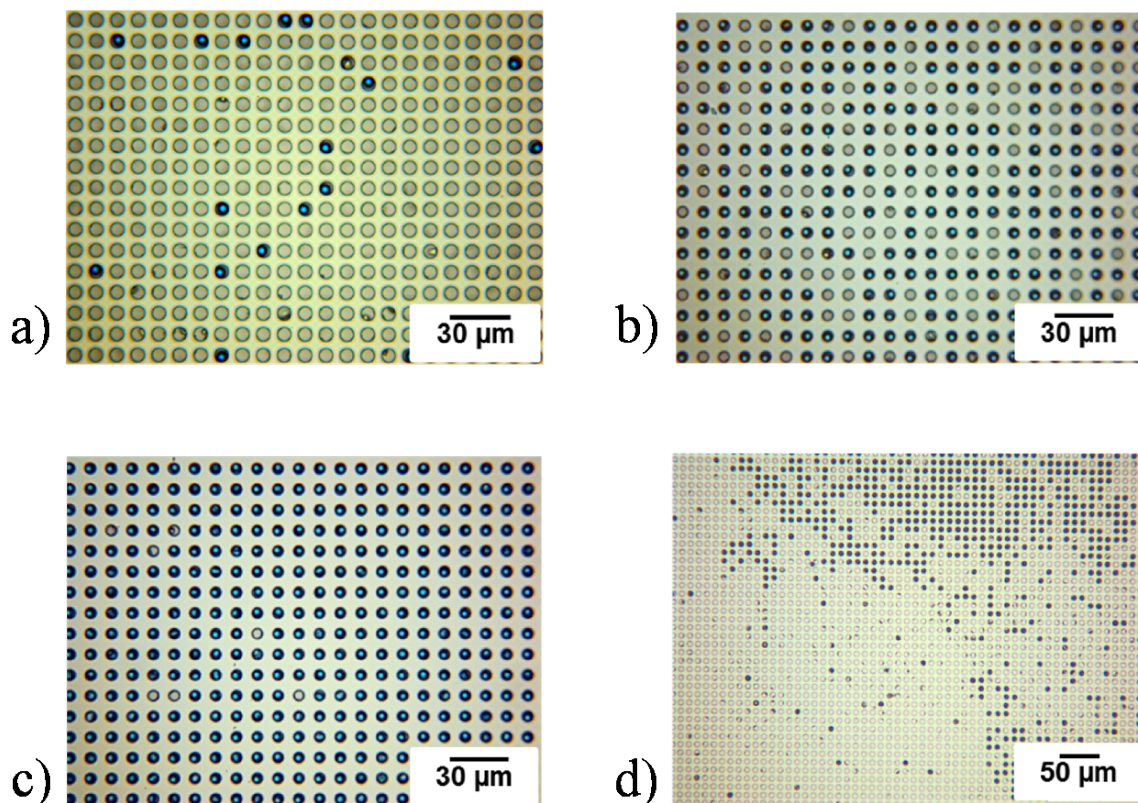
Figure 4.2: Light microscope image of stochastically deposited polystyrene microparticles with different concentrations. a) 0.1 mg of 4 μm particles in 2 ml of water deposited on 6 μm structures, filling of the microwells is 5%, b) 1.5 mg of 4 μm particles in 2 ml of water deposited on 5 μm structures, filling of the microwells is 70%, c) 2.3 mg of 4 μm particles in 2 ml of water deposited on 5 μm structures, filling of the microwells is 99%, d) the particles distributed not evenly on the sample, average filling of micro wells is 23%.

The stochastic deposition method can be applied separately to each kind of microbeads or to a mixture of different kinds with a defined concentration of each. When the particles cannot be differentiated visually the stochastic filling of the microcavities occurs step by step. Figure 4.3 shows the result for the consistent deposition of 3 μm blue, yellow and red polystyrene particles. By applying this particle deposition technique, it is possible to deposit the particles made of different materials and in various sizes (Figure 4.4).
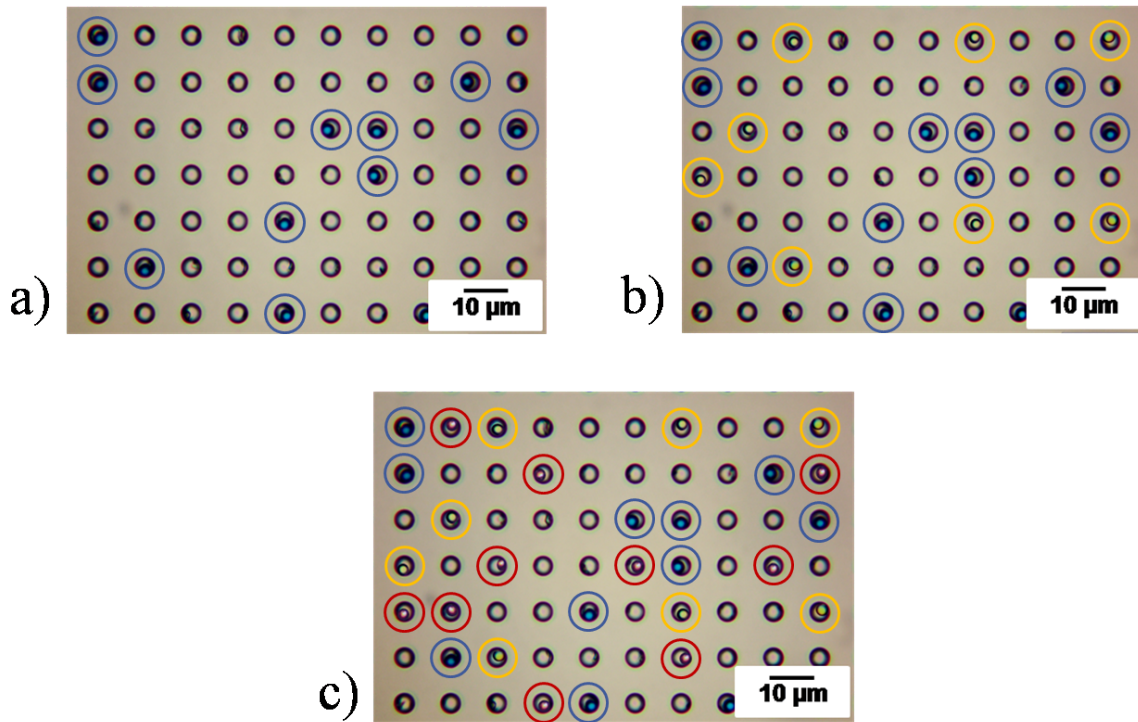
Figure 4.3: Light microscope image of stochastically deposited polystyrene micro particles on 6 µm structures, pitch 10 µm. a) 3 µm blue particles b) 3 µm yellow particles deposited on the sample with already deposited blue polystyrene micro beads, c) 3 µm red particles deposited on the sample with already deposited yellow and blue polystyrene micro beads.
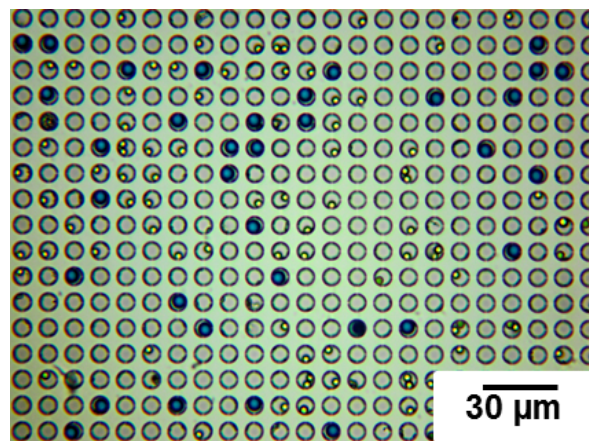
Figure 4.4: Light microscope image of stochastically separately deposited 5 µm blue and 3 µm yellow polystyrene particles on 6 µm structures, pitch 10 µm.

When different kinds of particles can be distinguished from each other, the deposition can be done for all of them at once. Therefore, all the microbeads are mixed together in the required concentration and, subsequently, applied to the microstructured surface. This approach has several advantages. First of all, all kinds of the the microbeads are equally distributed on the sample. Moreover, applying them all at

once speeds up the deposition process. The result of deposition of the mixture of 3 μm red, blue and yellow polystyrene particles in equal concentrations is shown in Figure 4.5 a). The microbeads were distributed evenly on the sample and the colors could be differentiated under the light microscope with 100-times magnification. However, with less magnification, it was not possible to distinguish between the colors of the polystyrene particles.

More information about the stochastic distribution of the microbeads on a larger scale was obtained after deposition of mixture of two kinds of fluorescent melamine particles with diameter of 2.65 μm and excitation wavelengths 510 and 636 nm. The results of this experiment are presented in Figure 4.5 b).
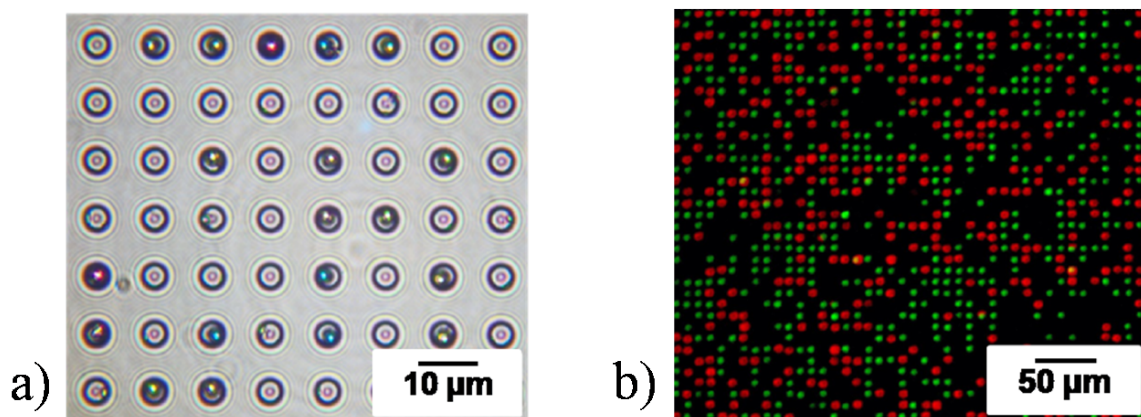
Figure 4.5: Images of stochastically deposited particles. a) 3 μm blue, red and yellow polystyrene particles on 5 μm structures, pitch 10 μm, b) 2.65 μm fluorescent melamine particles with excitation wavelengths of 510 and 636 nm.

The analysis of the light microscope pictures with the stochastically distributed particles in the structured surface for a large number of microwells can be done automatically by using the image processing software. In this work ImageJ with a custom developed plugin is used. This program allows to set a grid with defined diameter of circles, their amount, pitch and correction angle, if necessary. The color intensity inside these circles is analyzed by the software and then the values are given in a table. By realizing the difference in the mean values of filled and empty microcavities, it is possible to obtain the information about the number of each (Figure 4.6).
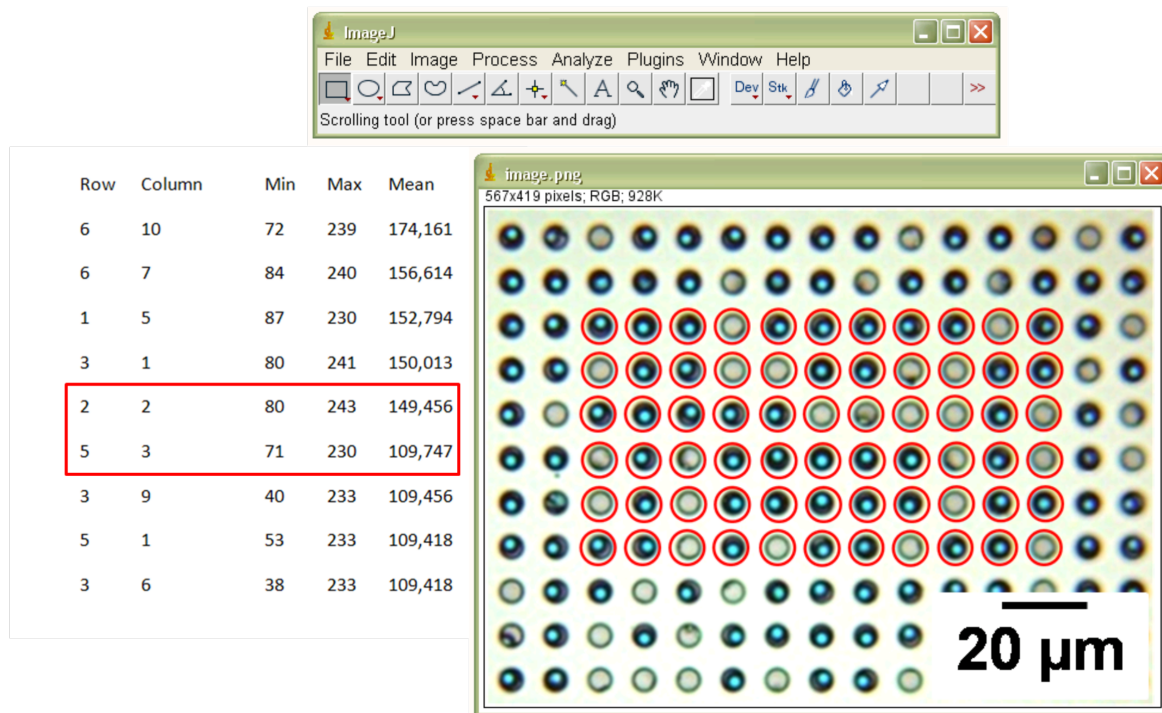
Figure 4.6: Images of the analysis process of the stochastically deposited particles using the ImageJ open source software with a custom developed plugin.

4.2 Stochastic Deposition of Amino Acid Particles

For stochastic amino acid particle deposition, the approach of filling the microcavities from the liquids (Chapter 4.1) is not suitable. First of all, the matrix material in which the amino acids are embedded is hydrophobic and that makes it impossible to prepare the solution for deposition. Deposition from the powder (Chapter 3.1.1) is also not possible, since the defined filling rate of microcavities is required. Moreover, the fact that amino acid microbeads are not monodispersed and have broad size distribution should be taken into account. Therefore, the particle deposition method using the roller was developed.

4.2.1 Stochastic Deposition of Amino Acid Particles Using Roller

Stochastic deposition using the roller has the same working principle as in toner printers. A very thin layer of charged particles is kept on the surface of the roller (developer roller in the toner printer) by the static electricity. Subsequently, the roller is applied to the structured surface. The particles which are fit to the micro cavities are trapped there and others will be carried away from the surface. The schematic representation of this method is shown in Figure 4.7
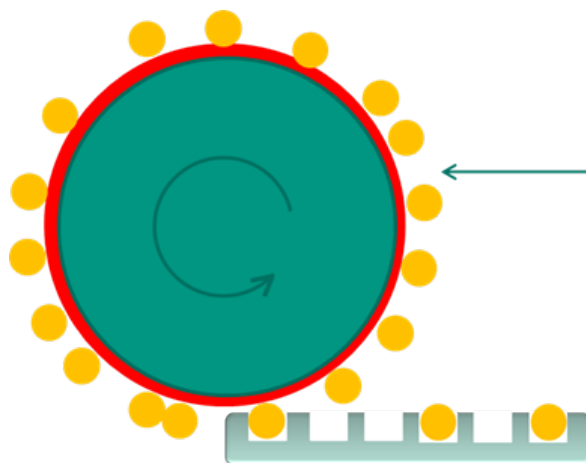
Figure 4.7: Schematic representation of the stochastic deposition of the particles using a roller.

The roller for this method was taken from the toner printer and is represented by a metal stick covered with a rubber material. To obtain the layer of the amino acid particles on the roller surface, the defined amount of the particle powder (measured in grams) is randomly distributed on a flat surface with a spatula (Figure 4.8 a). Due to the weak adhesion, the rubber material cannot retain big clusters of particles on its surface, but only a relatively thin layer of microbeads. Moreover, the inhomogeneous distribution of the powder on the flat surface is an advantage in creating the stochastic pattern with the roller (Figure 4.8 b).
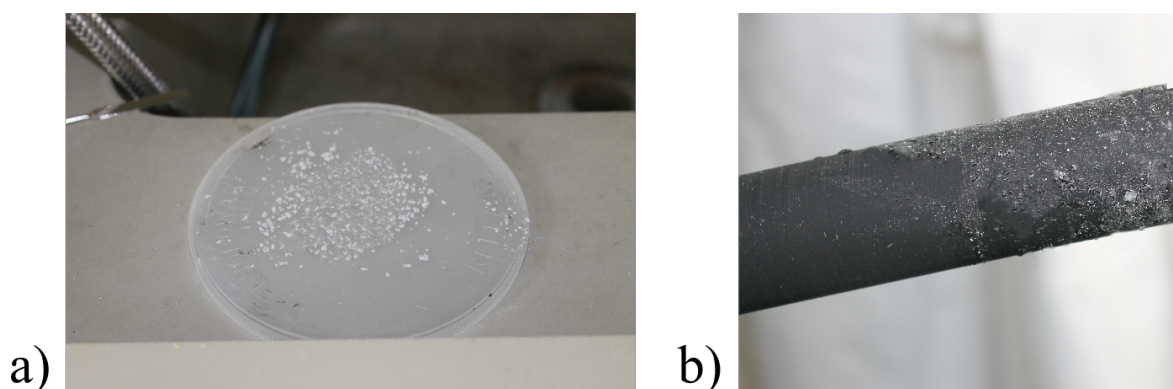
Figure 4.8: Particle deposition method using the roller. a) amino acid particles distributed on the flat surface using the spatula, b) part of the roller with and without the layer of particles.

First, the experiment was performed with the microcavities of 6 µm in diameter and a pitch of 10 µm. The result is shown in Figure 4.9. As can be seen in the picture, by applying the stochastic particle deposition method, it is possible to distribute amino acid particles stochastically. However, due to the particle size distribution, some of the microcavities were not completely filled with the material. Thus it will not be

acceptable for peptide synthesis, due to contamination, as during the second layer deposition, another kind of particles can pack partially filled microwell. It will only be possible to apply the stochastic method on the structures with diameter of 6 μm with monodispersed microbeads of approximately the same size, namely, with diameter of 4 − 5 μm.
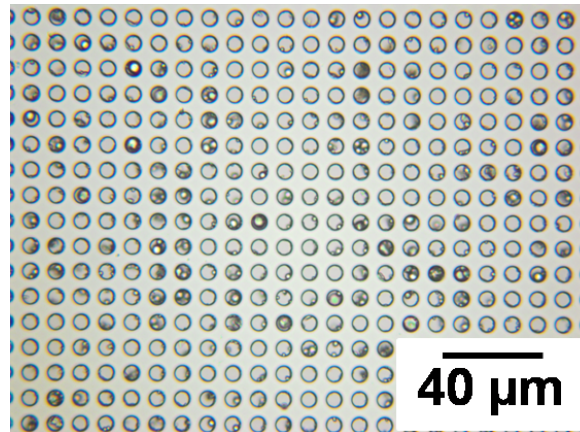
Figure 4.9: Optical image of the structured surface with the micro cavities of 6 μm in diameter and pitch of 10 μm filled with amino acid particles by using the roller.

In the case of the amino particles which are used in the experiments, the only way to avoid contamination is to fabricate the micro structures with the smaller diameter of microcavities. For this, a sample with 1 μm diameter of wells and 2 μm pitch was fabricated on fused silica wafer via etching process (Figure 4.10).
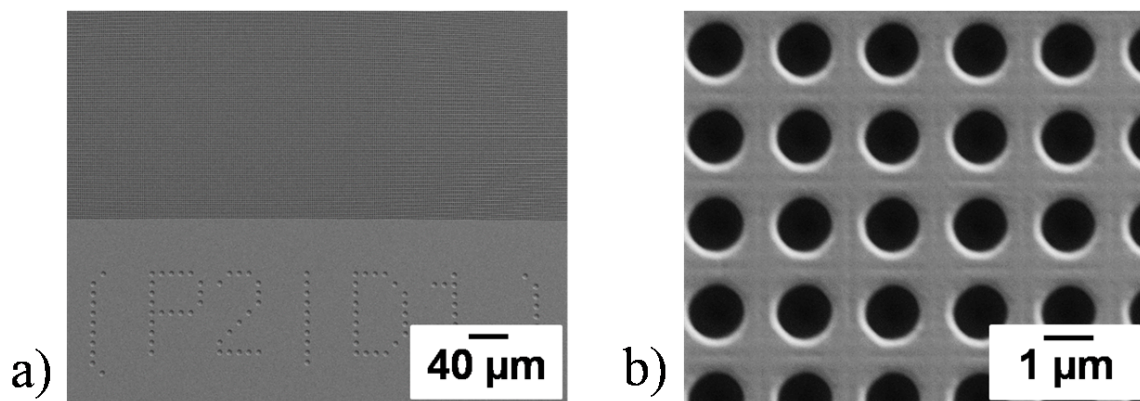
Figure 4.10: The SEM images of structures with 1 μm wells diameter and 2 μm fabricated via plasma etching process by Dr. D. Häringer.

The structures with 1 μm diameter of microcavities and 2 μm pitch was chosen according to the amino acid particle size distribution diagram, which is shown in Figure 4.11. As mentioned in Chapter 3.1 the best filling probability is achieved

when the size of the beads is smaller than, or approximately the same as, the diameter of the microwells. Thus as can be seen in Figure 4.11, only 10.4% of the particles are less than 1 μm in size. These are able to fit the size of the cavities with 1 μm diameter and 2 μm pitch. Therefore, the structures will behave as a filter and the other 89.6% of amino acid particles will be removed.

No	Size (μm)	Mean In%	1*S.D.	No	Size (μm)	Mean In%	1*S.D.
19	0.138	0.00	0.00	36	1.259	2.63	0.00
20	0.158	0.00	0.00	37	1.445	3.38	0.00
21	0.182	0.00	0.00	38	1.660	4.33	0.00
22	0.209	0.08	0.00	39	1.905	5.41	0.00
23	0.240	0.26	0.00	40	2.188	6.52	0.00
24	0.275	0.42	0.00	41	2.512	7.50	0.00
25	0.316	0.62	0.00	42	2.884	8.21	0.00
26	0.363	0.85	0.00	43	3.311	8.51	0.00
27	0.417	1.10	0.00	44	3.802	8.35	0.00
28	0.479	1.29	0.00	45	4.365	7.71	0.00
29	0.550	1.39	0.00	46	5.012	6.69	0.00
30	0.631	1.44	0.00	47	5.754	5.40	0.00
31	0.724	1.46	0.00	48	6.607	4.06	0.00
32	0.832	1.49	0.00	49	7.586	2.78	0.00
33	0.955	1.56	0.00	50	8.710	1.73	0.00
34	1.096	1.75	0.00	51	10.000	0.95	0.00
35	1.259	2.09	0.00	52	11.482	0.02	0.00
					13.183		
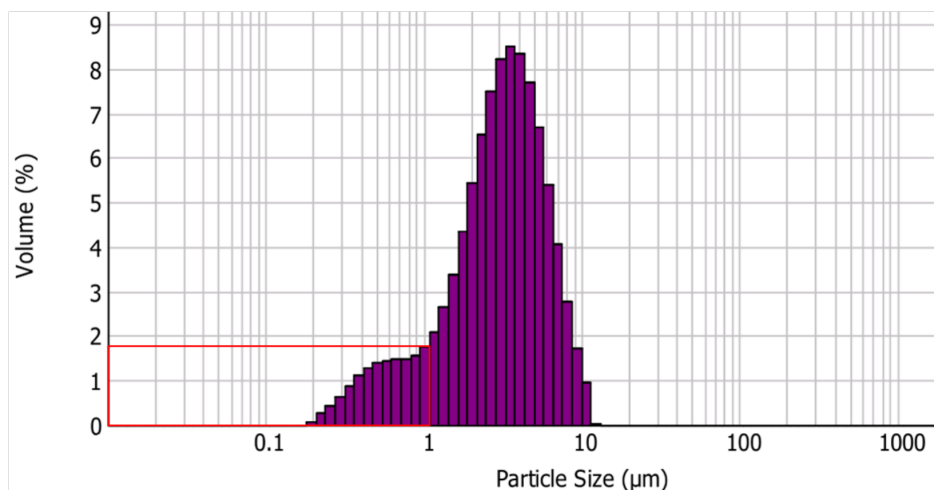
Figure 4.11: The size distribution curve and statistics of amino acid particles which were fabricated via spray drying process.[91]

The results for the deposition of amino acid particles to the microstructures with microwells diameter of 1 μm and pitch of 2 μm using the roller are shown in Figure

4.12. The SEM picture shows that the particles fill the cavities completely and the possibility of contamination is minimal.
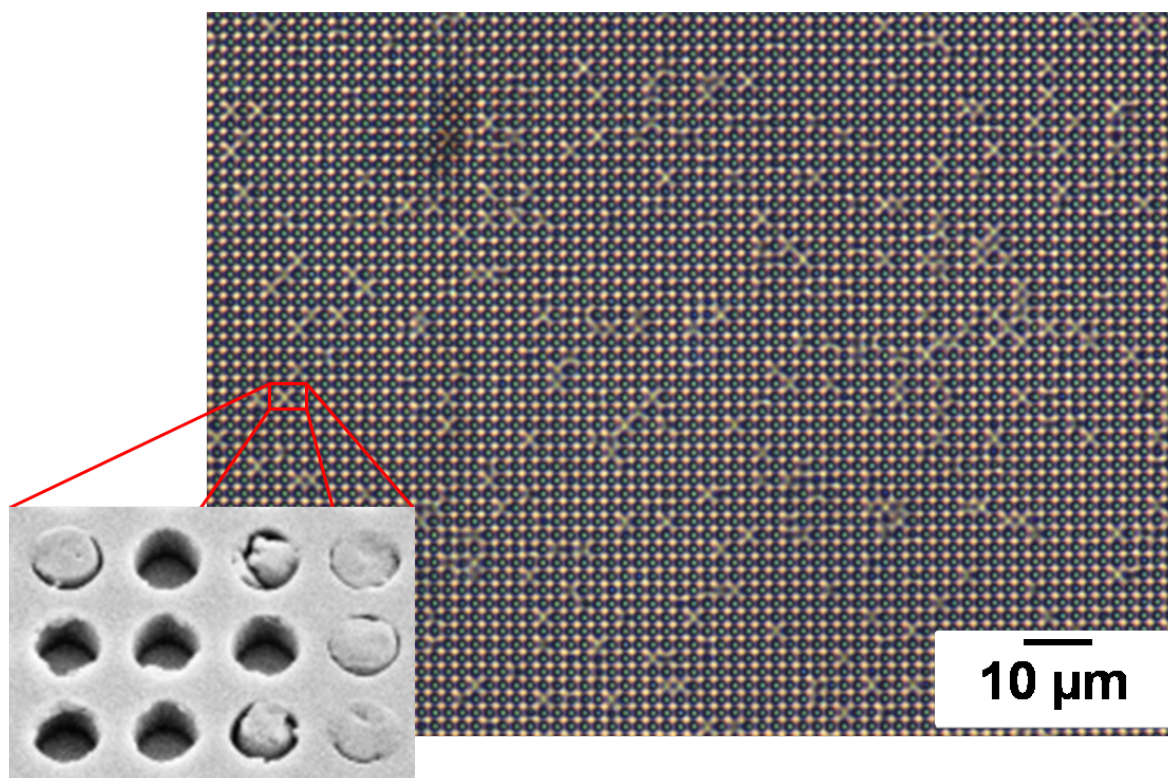
Figure 4.12: Optical and SEM images of structured substrate with 1 μm wells diameter and 2 μm pitch filled with amino acid particles using the roller.

In order to detect the position of themicro cavities in which the amino acid particles were deposited, the microscope pictures should be taken after each deposition step. Subsequently, all other kinds of amino acid particles, which are required for the synthesis, can be applied in the same way. When all the microcavities are filled with the amino acid particles representing stochastic pattern on the structures, the sample is processed with the standard chemical steps, such as coupling in the oven, washing and deprotecting, described in Chapter 1.3.1. After that, the whole process is repeated until the required length of peptides is reached.

However, in case of smaller structures, parameters for washing step from the previous experiments were not sufficient to remove matrix material from the microcavities. Moreover, air bubbles inside the microcavities also prevent the material from being washed away. Therefore, a series of experiments with variation in chemical solvents was carried out to obtain completely clean microwells. In contrast to the old washing protocol, the ultrasonic bath was introduced to remove the air bubbles from the structures and provide better penetration of the solvent into the microwells. At the same

time, it should be kept in mind that processing the sample with ultrasound for too long or too strongly can damage the functional polymer layer inside the microwells where the amino acid sequences are synthesized.

The best result for cleaning the microstructures was achieved when the sample was washed twice in DMF for 1 minute, 1 minute in DCM and twice times for 1 minute in methanol using the ultrasonic bath with 30% power. All other chemical steps stay the same as in previous experiments and are described in more detail in Appendix 7.2 and 7.3.

In principle, for stochastic method there is no limitation for the array spot density. Modern fluorescent methods, such as Stimulated Emission Depletion Microscopy (STED), developed by the Nobel Prize Laureate, Stefan Hell, allow the spots to be detected with a resolution of 10 nm.[110] In other words, with the possibility of fabrication of microstructures with diameter smaller than 1 μm and the availability of the particles with corresponding diameter stochastic method will allow arrays with ultra-high spot density to be fabricated.

Ultra-High Density Dipetide Array

After optimization of deposition parameters of the microparticles on the substrate with wells diameter of 1 μm and 2 μm pitch, the proof-of-principle experiment for stochastic arrays method was performed. The aim of the experiment is to synthesize the, as of today, smallest spots for dipeptide arrays with glycine (Gly) and biotin (Bio) particles. First, Gly particles were deposited on the structures. After the deposition the images of microstructures were taken under the light microscope to detect the positions of the microwells, which were filled with the microbeads (Figure 4.13 Glycine 1). Subsequently, the layer of Bio micro particles was applied and microcavities filled with biotin were detected using the microscope (Figure 4.13 Biotin 1). Afterwards, the sample was placed in the oven at 90° C for 90 minutes to melt the matrix material and to let the amino acid particles couple to the functionalized surface. The next step was the preparation of the sample for the deposition of another layer of Gly and Bio amino acid particles, by washing away the matrix material and deprotecting the NH_2 groups from the coupled monomers. Thus the sample was ready for another cycle of deposition, washing and deprotection. Afterward, the second layer of Gly and Bio microparticles was generated on the sample by the stochastic deposition method with roller and the sample was processed chemically, as previously. After the dipeptide synthesis, the arrays were stained with fluorescent dyes. The full protocol of the ex-

periment can be found in the Appendix 7.2 and 7.3. Some fragments of the amino acid particle deposition and dipeptide staining are shown in Figure 4.13.
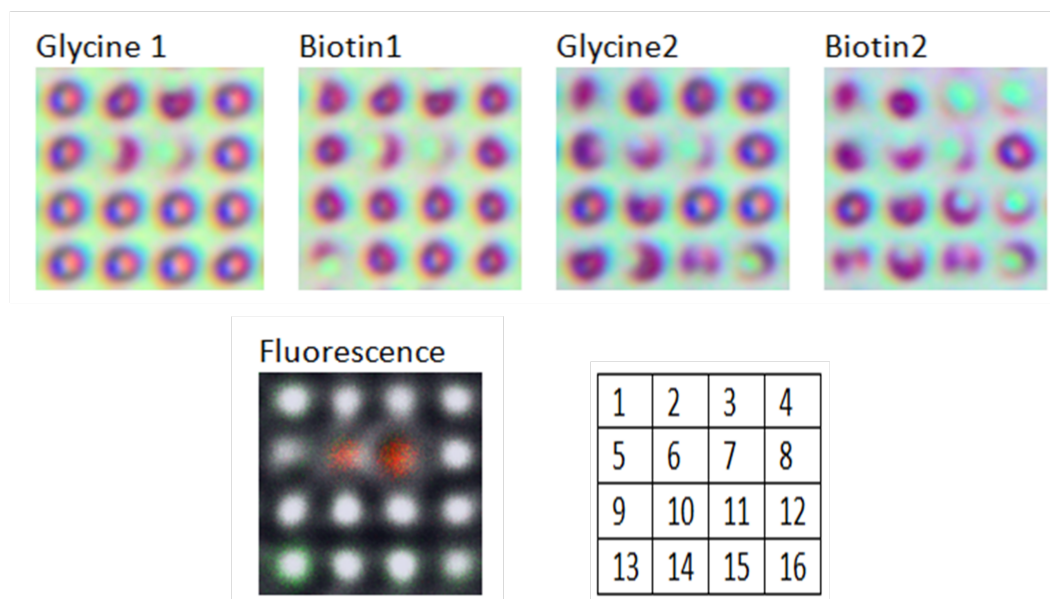
Figure 4.13: Stochastic dipeptide array synthesis, Glycine 1 and Biotin 1 are the pictures of deposited particles of glycine and biotin respectively for the first layer; Glycine 2 and Biotin 2 are the pictures for the second layer of glycine and biotin respectively; Fluorescence is the fluorescent picture of a resulting dipeptide.

The possible combinations of the coupled amino acids and biotin molecules on the functionalized surface are shown in Figure 4.14 a). In the case when no particles of Bio or Gly were deposited in the microcavities as a first layer, the functional groups inside of these microwells were blocked, and thus, no other coupling reaction to the surface was possible. Therefore, no fluorescent signal would be expected from these spots, while with combinations of Bio (first layer deposition), Bio+Bio or Gly+Bio green fluorescent response was expected. The red fluorescent signal was possible only for synthesized Gly+Gly dipeptide. As can be seen from the table in Figure 4.14 b), the experimental fluorescent response completely matches the theoretical expectations presented in Figure 4.14 a). Therefore, by applying the described above method for stochastic deposition with the roller it is possible to synthesize the chain of amino acids with a record resolution of 25 million spots per cm^2.

X	Bio	Gly	X	Bio	X	Bio	Bio	Gly
X	X	X	Gly	Bio	Bio	Bio	Gly	Gly
functionalized surface								

a)

Number	Glycine1	Biotin1	Glycine2	Biotin2	Color(theory)	Color(experiment)
1	-	-	-	-	Black	Black ✓
2	-	-	-	-	Black	Black ✓
3	-	-	-	+	Black	Black ✓
4	-	-	-	+	Black	Black ✓
5	-	-	-	-	Black	Black ✓
6	+	-	+	-	Red	Red ✓
7	+	-	+	-	Red	Red ✓
8	-	-	-	-	Black	Black ✓
9	-	-	-	-	Black	Black ✓
10	-	-	+	-	Black	Black ✓
11	-	-	-	+	Black	Black ✓
12	-	-	-	+	Black	Black ✓
13	-	+	-	+	Green	Green ✓
14	-	-	+	-	Black	Black ✓
15	-	-	+	-	Black	Black ✓
16	-	-	+	-	Black	Black ✓

b)
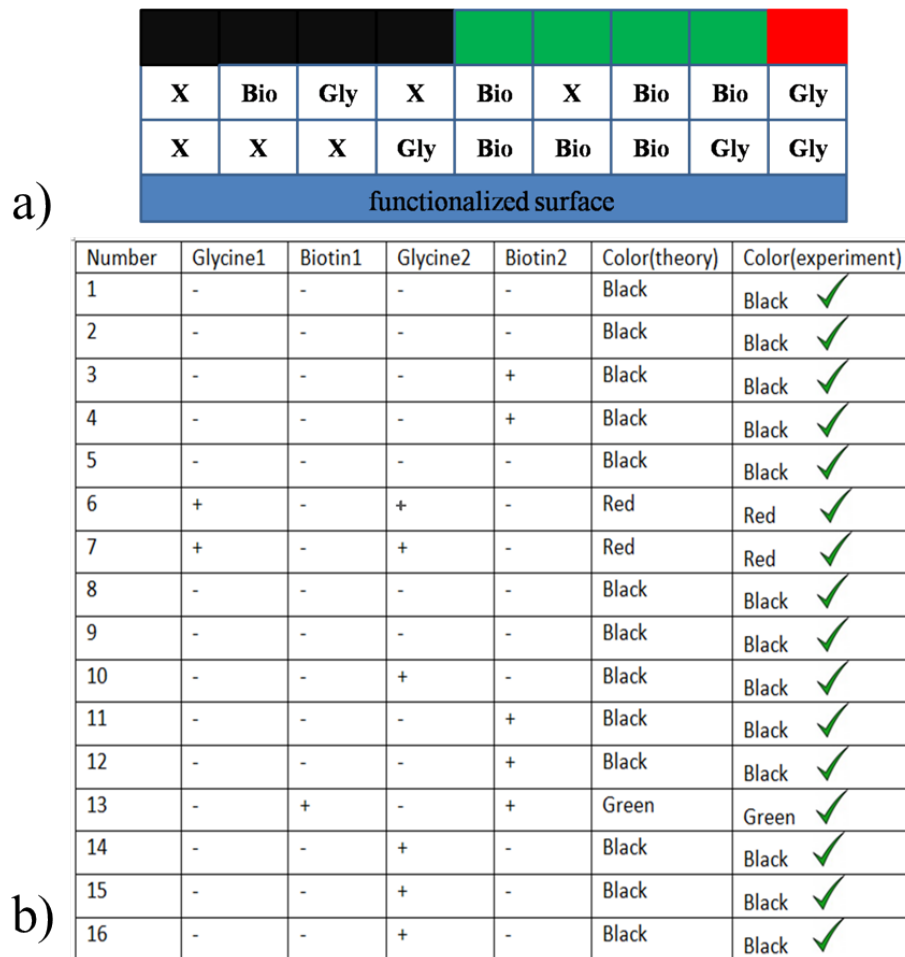
Figure 4.14: Tables to analyze the resulting fluorescent picture of dipeptide synthesis, theoretical expectations and experimental result. Bio-biotin, Gly-glycine

5 Alternative Methods for Pattern Generation

Successful manipulation of microparticles on microstructured surfaces makes it possible to consider the alternative methods for combinatorial deposition of monomers for solid phase synthesis. In this chapter a novel blocking method is described, in which the non-functionalized microparticles are used as corks to selectively block the cavities. In the blocking method, amino acid microparticles are not used. Instead, microwells are filled directly with the amino acids that have been diluted in a solution. The patterning of the blocking microbeads on the structured surface can be performed by both laser-based and stochastic methods described in Chapters 3 and 4.

5.1 Blocking Method for Pattern Generation with Diluted Amino Acids

In the blocking method, the amino acids are deposited directly into the functionalized substrate from the solution. In order to obtain the combinatorial pattern on the structured surface, additional polymer or inorganic particles are used, which are deposited in the microcavities by laser-based or stochastic methods (Chapter 3). These additional microparticles block and, therefore, protect the required microwells from the penetration of the solution with diluted amino acids, generating the pattern. The schematic representation of this method is shown in Figure 5.1.

When amino acid derivatives are diluted in a chemical solution and poured on the functionalised microstructured substrate, they couple with the functional groups on the surface directly. In this case there is no need to place the sample into the oven, as there is no matrix material, which should be melted in order to allow the amino acids to defuse to the (-NH$_2$) amino groups on the surface. However, functionalization of the surface means that (-NH$_2$) amino groups are available on the whole surface of the sample, not only at the bottom of the microcavities. To prevent the synthesis of the peptides outside of the microwells, the functional groups on the surface should be blocked during the first step. For this, all the microcavities should be filled and protected by organic or inorganic particles, capable of preventing capping of (-NH$_2$) groups on the bottom of the structures. In order to determine the correct kind of additional particles, a series of experiments was performed.
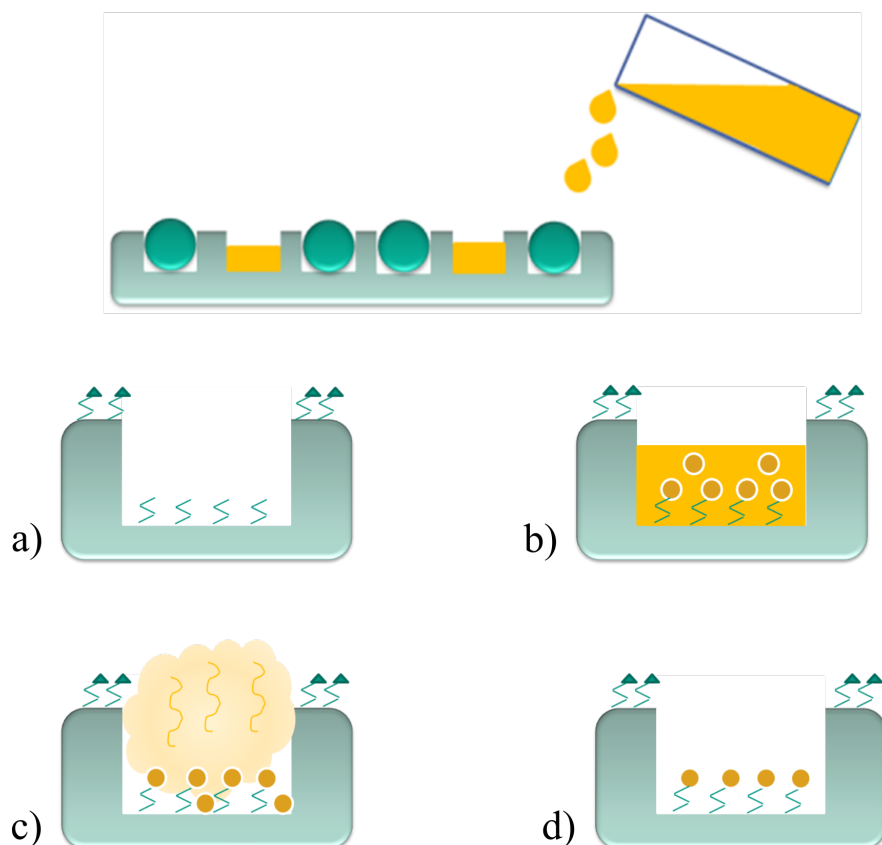
Figure 5.1: Schematic representation of blocking method for pattern generation on microstructured surface. a) functional groups outside of the microcavities are capped, b) solution with amino acids is poured onto the structures, c) amino acids couple to functionalized surface, d) uncoupled amino acids are removed during the washing step.
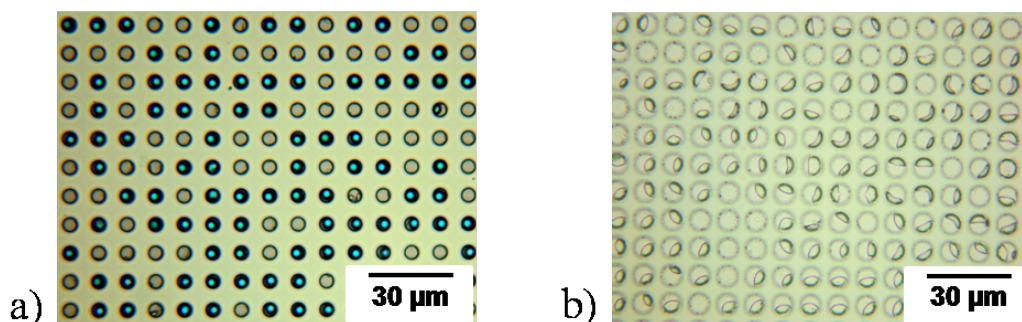
Figure 5.2: Light microscope image of interaction between ESA-DIPEA-DMF solution and polystyrene microbeads. a) deposited polystyrene particles to the microstructures before placing it in ESA-DIPEA-DMF solution, b) sample with polystyrene particles after placing it in ESA-DIPEA-DMF solution for 30 min.

First, microstructures with functionalized surface were filled with the polystyrene blocking particles and placed into the ESA-DIPEA-DMF solution (volume ratio 1:2:7) for 2 hours to block the ($-NH_2$) groups outside of the microcavities. The same capping step is used during peptide array synthesis. Afterward, the sample was washed with

DMF and methanol. In this case of polystyrene particles, the experiment failed, as the polystyrene particles were not resistant to chemical solution (Figure 5.2). Therefore they cannot be used for the blocking method.

Chemically resistant silica particles were chosen next to block microcavities from penetration of the ESA-DIPEA-DMF solution. The same blocking procedure was performed as earlier with polystyrene microbeads, namely, the sample with silica blocking particles was placed in ESA-DIPEA-DMF for two hours and after that washed with DMF and methanol. The substrate was then placed in the ultrasonic bath for 5 minutes to remove the silica microbeads. In order to check if amino groups were capped at the bottom of the microwells, the sample was stained with DyLight 650 fluorescence dye (Appendix 7.3). It was expected that no fluorescent signal would be detected on the surface of the substrate, as all of the functional groups were previously capped. On the other hand, a strong fluorescent signal was expected inside the microcavities. However, as seen in Figure 5.3 b) no fluorescent response was detected on the whole surface of the sample. This meant that during the blocking step, the ESA-DIPEA-DMF solution went through the silica particles and blocked the functional groups on the bottom of the microwells.
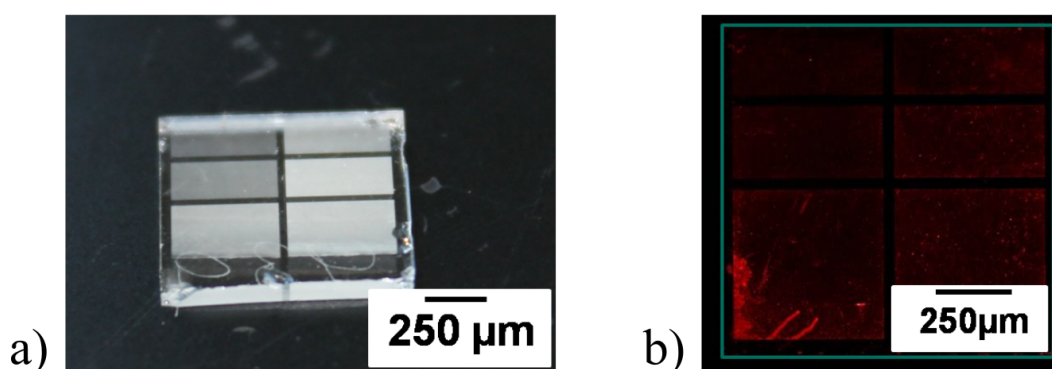
Figure 5.3: Capping of the functional groups on the surface of the micro structures using silica particles. a) glass chip filled with silica particles, b) fluorescent image of the glass chip after the capping of the functional groups on the surface and after staining with fluorescent dye.

In the other experiment, silica particles were replaced by the hydrophobic microbeads with a diameter of 1 μm. Because of the hydrophobic properties of the microbeads, it was expected that the liquids would be stopped from penetrating to the bottom of the structures. Nevertheless, the result of the experiment was the opposite. During the capping step with the ESA-DIPEA-DMF solution, the chemical solvent not only penetrated, but also washed away some of the particles. The resulting fluorescent image is shown in Figure 5.4. It was assumed that the microbeads partially

lost their hydrophobicity in the capping solution and, therefore, could not block the liquid from penetrating the microcavities.
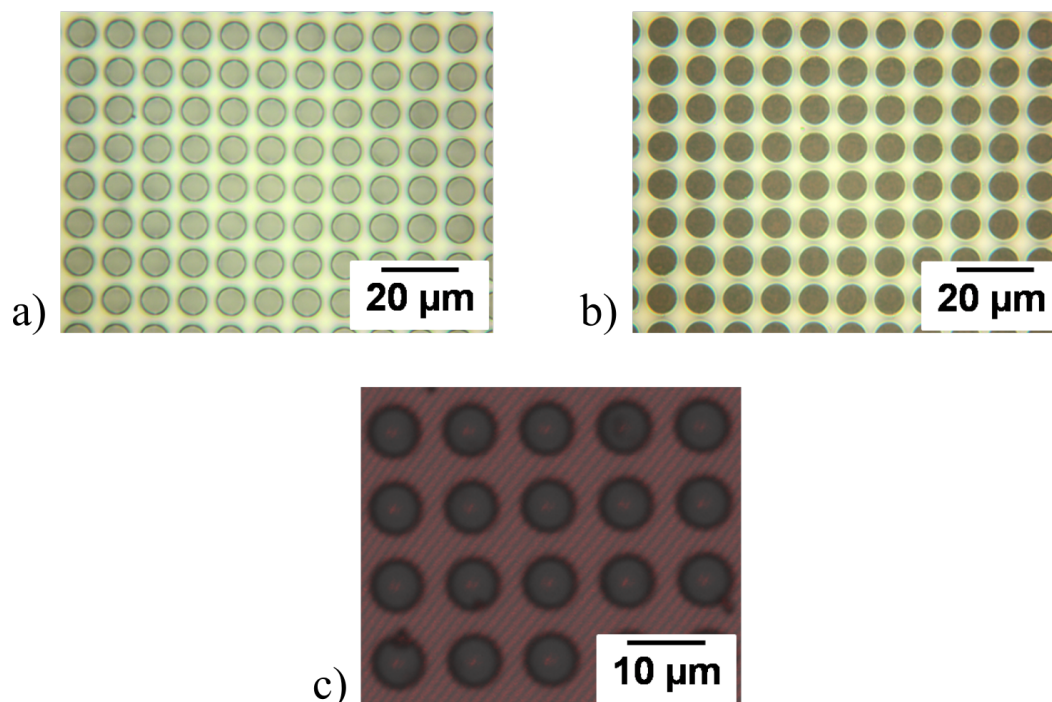
Figure 5.4: Images of micro structures with 10 μm pitch and 10 μm depth blocked with hydrophobic microparticles. a) empty microcavities, b) microcavities filled with hydrophobic particles with a diameter of 1 μm, c) fluorescent image of the microcavities after the capping the functional groups and staining with fluorescent dye.

These experimental results indicate that particles is not able to block the microcavities from penetration by chemical solutions. Therefore, deposition of amino acid derivatives diluted in a solvent is not suitable for peptide arrays synthesis. Thus this technique was modified in such a way that there is no need to perform the capping step anymore.

5.2 Blocking Method with Amino Acids in Matrix Material

The difference of the new approach is that in addition to the amino acid derivatives, matrix material is also dissolved in6 the solvent. This solution is poured on the functionalized structured surface and fills the microcavities. The advantage of using matrix material is that amino acids do not couple with the functional groups immediately, as they are located inside of the polymer. Thus the rest of the material can be removed with a soft tissue and there is no need to block the functional groups on the top of the substrate. This approach is similar to the method of deposition of amino acid particles

described in Chapter 3.1.1. However, in this case, several steps such as fabrication of the microbeads, their functional analysis and post-deposition particle melting (which enables amino acid coupling to the surface) would be skipped.

The solution was prepared by dissolving 65 mg of matrix material in 1.5 ml of dichloromethane (DCM). It was then poured on the substrate structured with microwells. However, not all of the microcavities were filled with the material. The main challenge of this approach was that the DCM evaporated fast and the air got trapped inside the cavities preventing the solvent from going inside the structures. To get rid of the air inside the microwells, the sample was placed in a desiccator and vacuum was applied after pouring matrix material solution on the structures. However, under vacuum the DCM evaporated rapidly leaving behind matrix residue as lumps instead of coating the microwells with uniform layer of matrix (Figure 5.5 a). As a result microwells were not filled with the material.
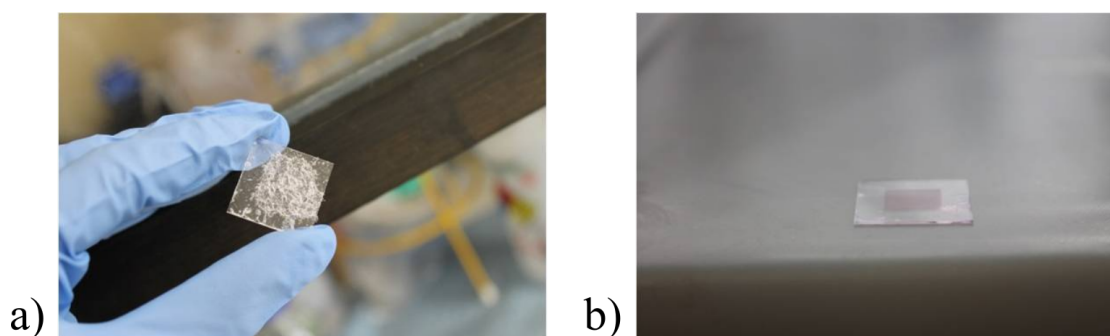
Figure 5.5: Development of blocking method using the vacuum to remove the air from the micro wells. a) sample after deposition of the solution with dissolved matrix material under vacuum, b) sample after cleaning of the surface.

Next option to remove the air from the microcavities was to place empty microstructured substrate into the ultrasonic bath for 3 minutes. After the air was removed from the microcavities, the matrix material solution was poured on the top of the sample. Following this procedure it was possible to fill the microwells with the material. This was proven by observing the sample under the scanning electron microscope (Figure 5.6).

To define the optimal viscosity of the solution for better deposition, the experiments were performed with several concentrations of the matrix material and DCM. The amount of matrix was kept constant at 65 mg, and the amount of DCM was varied from 0.8 ml to 2 ml with steps of 0.2 ml (Figure 5.7). As a result, the viscosity of 0.8 ml solution was too high and with 1.8 ml too low, resulting in almost no material detected inside the microcavities. Therefore, it was determined that the best material

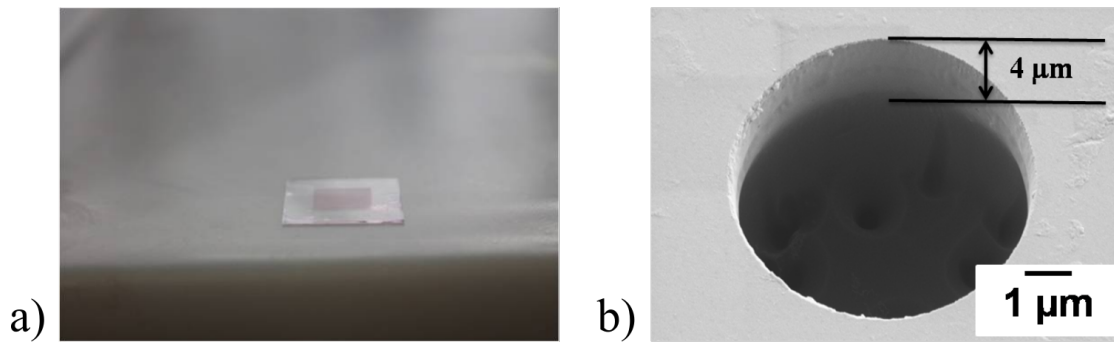deposition was obtained with DCM concentration of 1.2 ml.

Figure 5.6: Development of blocking method using the ultrasonic bath to remove air from the microwells. a) sample after deposition of the solution with dissolved matrix material, b) SEM image of the microwell with depth of 10 μm filled with matrix material.
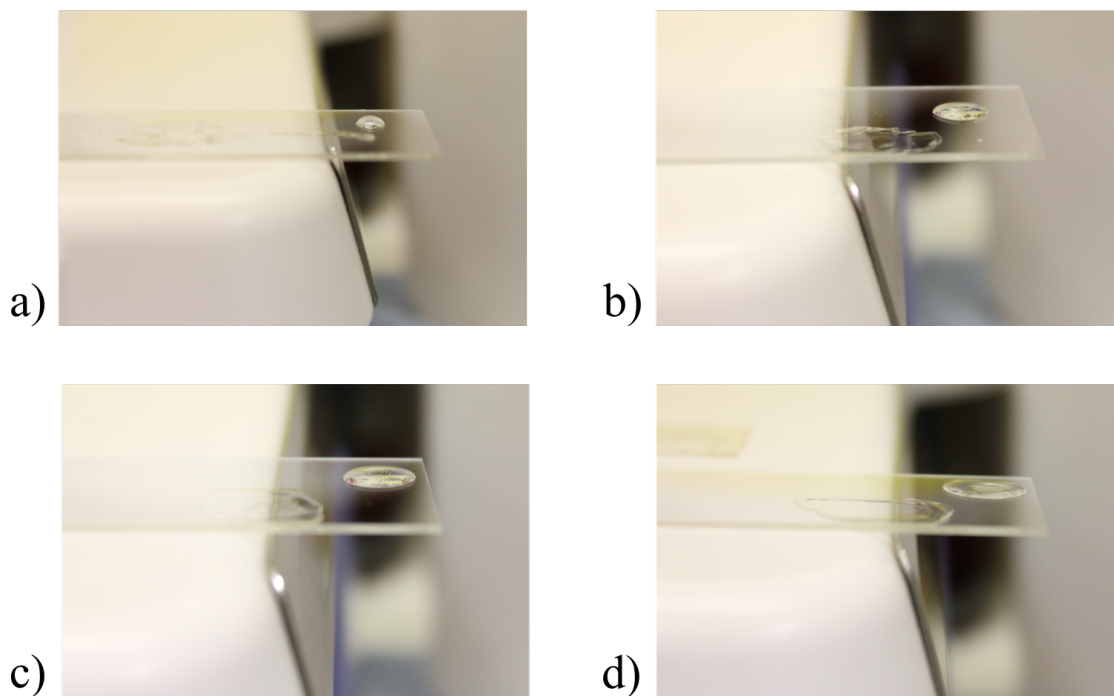
Figure 5.7: Variation of the concentration of matrix material dissolved in DCM. a) 65 mg of matrix material dissolved in 0.8 ml of DCM, b) 65 mg of matrix material dissolved in 1 ml of DCM, b) 65 mg of matrix material dissolved in 1.2 ml of DCM, c) 65 mg of matrix material dissolved in 1.8 ml of DCM.

To investigate the ability of material that is deposited to be transferred or removed from the cavities, the luminescent dye was added into the solution with matrix material. After the deposition of this solution on the structured surface some of the microcavities were processed with laser irradiation to transfer their contents to the flat surface. During the experiment the laser parameters were varied in order to find sufficient energy to remove material from the microwells. For this, 13 blocks of 6x6

matrices were irradiated with the laser (Figure 5.8). The resulting fluorescent image, which is presented on Figure 5.8 b), shows the fluorescent signal on the surface of the flat substrate. That means that it was possible to remove and transfer the material from the microcavities to the flat surface, proving that the microwells were filled with the polymer. Therefore, the deposition of amino acids in the matrix material was considered further for the blocking method.
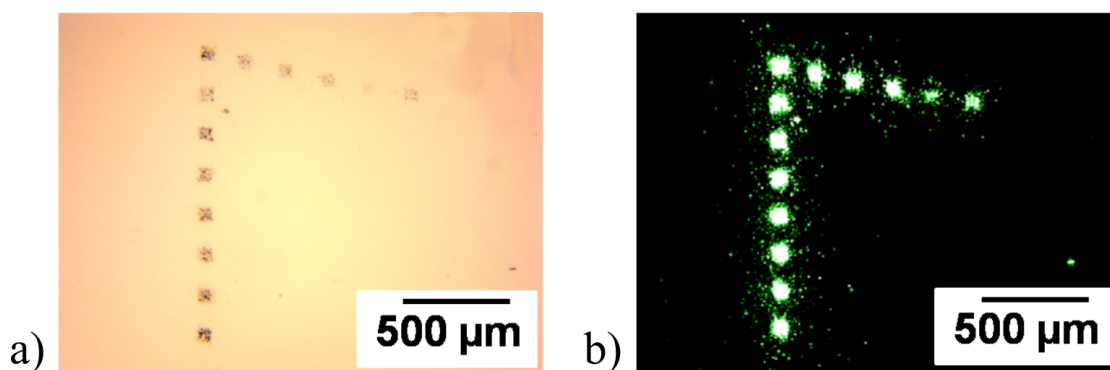
Figure 5.8: Transferred polymer matrix material from the microcavities to flat surface. a) light microscope image of the material transferred by laser irradiation, b) fluorescent image of the material transferred by laser irradiation.

The schematic representation of the blocking method which can be applied for peptide arrays synthesis is shown in Figure 5.9. Matrix material with amino acids that has been dissolved in the DCM is poured on the microstructured surface previously patterned with the blocking particles. Subsequently, the blocking particles are removed from the microwells and the second kind of amino acids is deposited. These steps of filling and washing are repeated until the microcavities are filled with different kind of amino acids in the matrix. As shown in Figure 5.9, a thin layer of another kind of amino acids remains on the top of the previously deposited one. Nevertheless, this will not cause contamination, because during the heating, the amino acids which are closer to the bottom of the microcavities are first to couple to the functional groups. In general, the diffusion rate of the amino acids in the matrix material is low.[91]
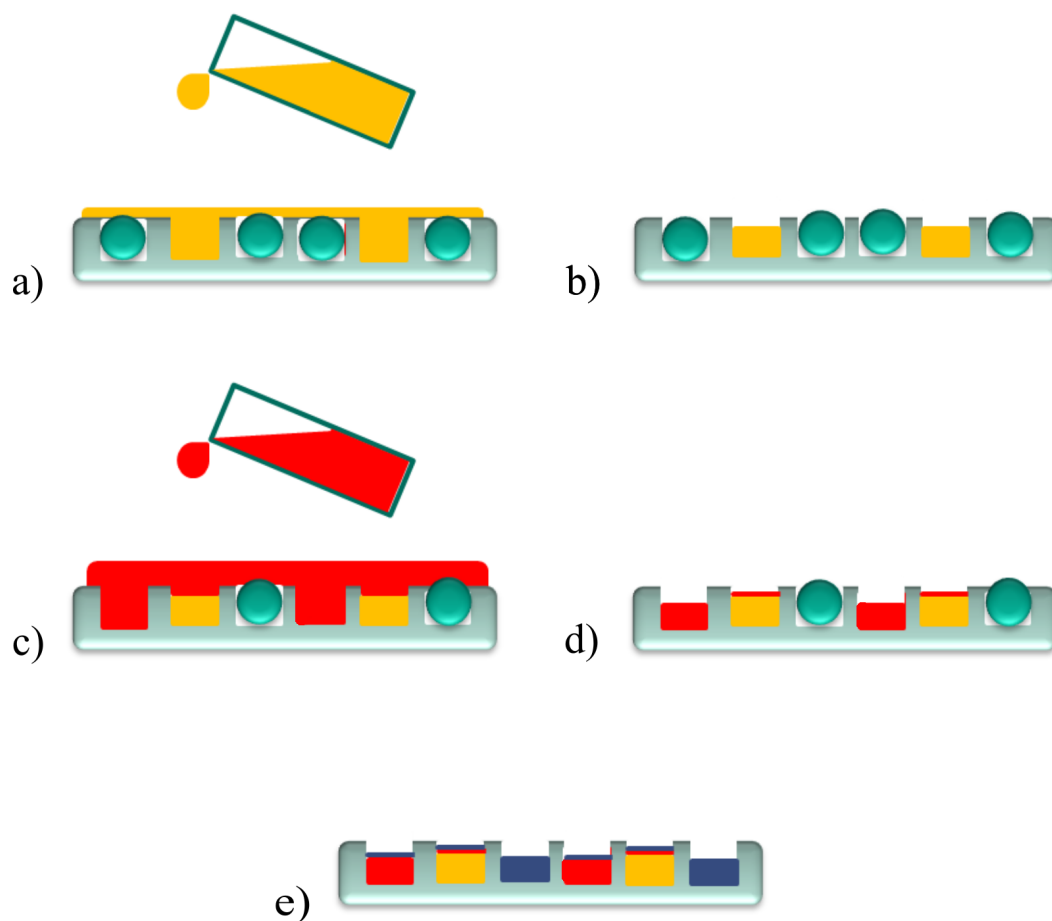
Figure 5.9: Schematic representation of blocking method. a) and c) deposition of amino acid derivatives with matrix material dissolved in DCM on the microstructured substrate patterned with silica particles, b), d) and e) microcavities filled with amino acids in matrix material after DCM evaporation.

To generate the random pattern of the blocking particles on the structured surface, silica microbeads were stochastically deposited from the liquid suspension. In the solution with dissolved matrix material, fluorescent dye Rhodamin was added to make the result of the blocking method more visible. After deposition of the solvent and its evaporation, the sample was cleaned with soft tissue soaked in acetone, so that no matrix material remained on the sample. Afterward, the silica particles were removed from the mocrocavities by placing the sample in the ultrasonic bath for 3 minutes. The result was checked under the light and fluorescent microscope and is presented in Figure 5.10. As a result, a fluorescent signal was detected only from the microwells, which were free from the blocking silica particles.
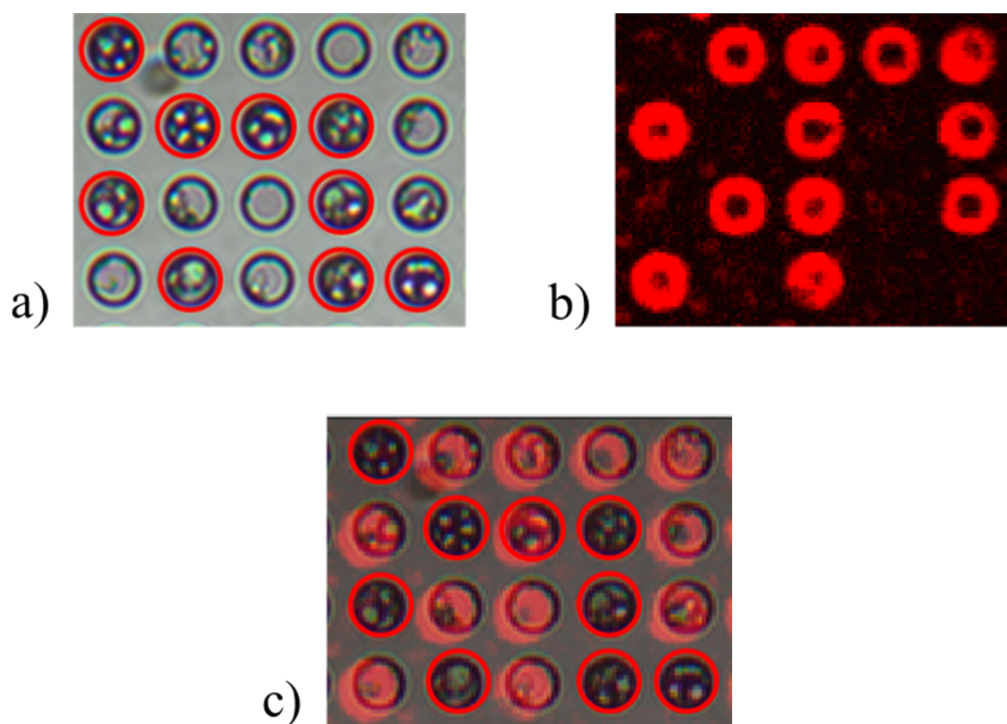
Figure 5.10: Stochastic blocking method performed on microstructures with microcavities diameter of 6 μm and 10 μm pitch. a) light microscope image of the stochastically deposited silica particles, b) fluorescent image of the material filled inside the microcavities where were no silica particles, c) joined picture of a) light microscope and b) fluorescent images.

Thus, possibility of depositing of amino acids in a matrix material gives an additional patterning option. Moreover, combinatorial monomer deposition in a fluid phase leads to a higher coupling efficiency and shorter synthesis steps.

6 Conclusion and Outlook

During this work several novel methods for particle pattern generation were developed in order to obtain arrays with high spot density. In all evolved techniques the particle pattern was generated by using polymer microbeads and structured substrates with cylindrical microcavities. The resolution of the methods in this case was determined by the pitch of the microstructures. In this work, two kinds of structured surfaces were introduced. The first kind contained microwells made of photoresist via a photolithography process. However, due to chemical reactions, it was not possible to use the resist microstructures for peptide array synthesis, as they were not stable in the solvents used for peptide synthesis. Therefore, the second kind of fabrication process, namely, plasma etching of fused silica substrates was applied to make the microwells stable in chemical solutions.

The process of deposition of the microparticles on the microstructured surface was developed based on the self-assembly property of the microspheres that allowed the particles to self-organize on a structured surface due to capillary and mechanical forces. The main advantage of this technique is the ability to deposit any kind of organic and inorganic particles of various sizes without using complicated setup procedures.

To obtain combinatorial patterns on the structured substrates, two laser-based methods were developed. One of them deals with particle pattern generation by removing material from the microwells. The proof-of-principle experiment with this method demonstrated the possibility of applying it to peptide array synthesis with a density of 1 million spots per cm^2.

To increase the automation degree of the particle patterning and reduce the heat transfer of the laser radiation to the synthesis substrate, we advanced the second laser-based method for particle patterning, which involves particle transfer from a structured donor substrate to an acceptor structured substrate. We demonstrated that a dynamic release layer should be applied to the donor slide before particle deposition in order to obtain efficient material transfer without possible particle contamination. In addition, the microparticles deposited on the donor substrate should be sintered before laser transfer. Sintering agglutinates microparticles in a microwell, which

then behave as single agglomerate during the transfer process. Thus the sintering reduces the possibility of contamination as a result of scattering of single particles. We successfully tested the particle transfer between structured surfaces with different microwell diameters to increase the alignment tolerance between donor and acceptor slides and reduce the amount of material scattered on the upper edges of the microwells.

To synthesize the ultra-high density peptide arrays, a stochastic approach for combinatorial peptide array synthesis was developed. This method does not require laser radiation to remove the material, but is mostly based on self-assembly of the particles on a structured surface. According to the stochastic method, the particles were randomly deposited on the structured surface in such a way that only the required percentage of the microcavities was filled. To analyze the position of the microparticles, the microscope images were taken after each deposition step. The filling of the microcavities on these pictures were analyzed by image processing software. Thus using a stochastic method, it was not possible to predict in advance the position of a specific peptide on the structured substrate; it was known only at the end of the synthesis. In the proof-of-principle experiment, we demonstrated the possibility of synthesizing dipeptide arrays with a record resolution of 25 million spots per cm^2.

Successful manipulation of microparticles on microstructured surfaces enables alternative methods for combinatorial deposition of monomers for solid phase synthesis. A novel blocking approach was demonstrated, where the polymer particles are used as corks to selectively block the cavities. The main advantage of this approach is the possibility of combinatorial monomer deposition in a fluid phase, which leads to a higher coupling efficiency and shorter synthesis steps.

In conclusion, all the particle patterning processes developed during this work enable spot densities which were unreachable with previously existing techniques. The methods developed can be automated and scaled up. Moreover, the application of the particle patterning processes on structured surfaces can be extended to other cases where the combinatorial surface patterning is required. One of the examples is fabrication of sensors with combinatorial patterning of particles sensitive to specific reagents. In the future, such sensors will be able to benefit from the densely packed sensitive materials and the small amount of the analyte.

7 Appendix

7.1 Abbreviations

DCM	dichloromethane
DMF	dimethylformamide
DRL	dynamic release layer
ESA	acetic anhydride (Essigsäureanhydrid)
Gly	glycine
IMT	Institute of Microstructure Technology
KIT	Karlsruher Institute of Technology
LIFT	Laser-induced forward transfer
MeOH	methanol
Nd:YAG	neodymium-doped yttrium aluminium garnet
PBS	phosphate buffered saline
RIE	reactive ion etching
SEM	scanning electron microscope
SPPS	solid phase peptide synthesis
UV	ultraviolet light
v/v	volume fraction

7.2 Peptide arrays synthesis

The peptide arrays synthesis consist of several steps, which are repeated for each deposited layer of amino acid particles. The synthesis starts with a coupling of amino acids to functionalized surface. For this purpose, substrate with the deposited amino acid particles is placed in a chamber filled with argon and subsequently baked in the oven. The polymer particles are melted, that allows amino acid derivatives to defuse and couple to the functional groups on the surface. Uncoupled amino acids and matrix material are washed off during the washing step. In case, when not all of the functional groups on the support are bound with amino acids, they are deactivated

through the blocking step in order to avoid synthesis of unwanted sequences. Following deprotecting step removes the protection from N-terminals of amino acids and makes the first layer of coupled amino acids ready for the subsequent cycles of the synthesis.

1. Coupling step:

- 90 min 90° C under argon

2. Washing step:

- 5 min in acetone

- 3 times x 5 min DMF

- 2 times x 3 min MeOH

3. Blocking of free amino groups:

- 2 hours in ESA-DIPEA-DMF, volume ratio 1:2:7

- 3 times x 5 min DMF

- 2 times x 3 min MeOH

- drying with argon gas

4. Deprotecting step:

- 20 min Piperidin (20% v/v) in DMF

- 3 times x 5 min DMF

- 2 times x 3 min MeOH

7.3 Fluorescent labeling

7.3.1 Fluorescent labeling of amino acids

1. Washing step:

-15 min in PBS-T buffer pH 7,4

2. Staining:

-2 hours in DyLight 650 (NHS-Ester)-PBS-T, volume ratio 1:100

3. Washing step:

-1 time x 30 s in PBS-T pH 7,4

-1 time x 1 min in PBS-T pH 7,4

-1 time x 2 min in PBS-T pH 7,4

-rinse in H2O

7.3.2 Fluorescent labeling of biotin molecules

1. Washing step:

-15 min in PBS-T buffer pH 7,4

2. Blocking step:

-30 min in Rockland blocking buffer

3. Washing step:

-1 time x 1 min in PBS-T pH 7,4

4. Staining:

-1 hour in Streptavidin DyLight 550 (NHS-Ester)-PBS-T, volume ratio 1:10.000

7.4 Acknowledgment

Last but not least, I am indebted to my whole family for their love and support during these years of my studying abroad. Particularly, I would like to thank my grandparents, parents, my older brother and dearest nephews for their inspiration and encouragement, for believing in me and for their great patience not to see me for a long time.

Bibliography

[1] D. L. Nelson, M. M. Cox, A. L. Lehninger, and K. Beginnen. *Lehninger Biochemie*. Springer, 2001.

[2] T. Kimmerlin and D. Seebach. 100 years of peptide synthesis: ligation methods for peptide and protein synthesis with applications to beta-peptide assemblies. *J. Peptide Res.*, 65:229–260, 2005.

[3] F. Breitling, C. Schirwitz, T. Felgenhauer, I. Block, V. Stadler, and R. Bischoff. *Epitope mapping by printed peptide librares*, volume 1. Springer, 2010.

[4] A. Fischer. *Entwicklung eines Mikrofluidiksystems zur Inkubation von Peptidarrays mit Antikoerpern*. Diplomarbeit, Karlsruher Institut fuer Technologie, 2014.

[5] B. Hemmer, C. Pinilla, J. Appel, J. Pascal, R. Houghten, and R. Martin. The use of soluble synthetic peptide combinatorial libraries to determine antigen recognition of T cells. *J. Peptide Res.*, 52:338–345, 1998.

[6] R. Paulmurugan and S. S. Gambhir. Combinatorial library screening for developing an improved split-firefly luciferase fragment-assisted complementation system for studying protein-protein interactions. *Anal. Chem*, 79:2346–2353, 2007.

[7] T. Kimmerlin and D. Seebach. Epitope mapping: the first step in developing epitope-based vaccines. *BioDrugs*, 21:145–156, 2007.

[8] E. Fischer and E. Fourneau. über einige derivate des glykocolls. *Berichte der Deutschen Chemischen Gesellschaft*, 34:28682877, 1901.

[9] R. B. Merrifield. Solid Phase Peptide Synthesis. I. The Synthesis of a Tetrapeptide. *Journal of the American Chemical Society*, 85:2149–2154, 1963.

[10] R. Frank. SPOT-synthesis: an easy technique for the positionally addressable, parallel chemical synthesis on a membrane support. *Tetrahedron*, 48:9217–9232, 1992.

[11] R. Frank. SPOT-synthesis technique: Synthetic peptide arrays on membrane supports - principles and applications. *Journal of Immunological Methods*, 267:13–26, 2002.

[12] A. Nesterov-Mueller, F. Maerkle, L. Hahn, T. Foertsch, S. Schhillo, V. Bykovskaya, M. Sedlmayr, L. K. Weber, B. Ridder, M. Soehindrijo, B. Muenster, J. Striffler, F. R. Bischoff, F. Breitling, and F. F. Loeffler. Particle-Based Microarrays of Oligonucleotides and Oligopeptides. *Microarrays*, 3:245–262, 2014.

[13] F. Breitling, A. Nesterov, V. Stadler, T. Felgenhauer, and F. R. Bischoff. High-density peptide arrays. *Molecular BioSystems*, 5:224–234, 2009.

[14] M. Beyer, A. Nesterov, I. Block, K. König, T. Felgenhauer, S. Fernandez, K. Leibe, Torralba G., M. Hausmann, U. Trunk, V. Lindenstruth, F. R. Bischoff, V. Stadler, and F. Breitling. Combinatorial synthesis of peptide arrays onto a microchip. *Science*, 318:1888, 2007.

[15] V. Stadler, T. Felgenhauer, M. Beyer, S. Fernandez, K. Leibe, S. Guettler, M. Groening, G. Torralba, V. Lindenstruth, A. Nesterov, I. Block, R. Pipkorn, A. Poustka, F. R. Bischoff, and F. Breitling. Combinatorial synthesis of peptide arrays with a laser printer. *Angew. Chem.*, 47:7132–7135, 2008.

[16] F. Maerkle, F. F. Loeffler, S. Schillo, T. Foertsch, B. Muenster, J. Striffler, C. Schirwitz, F. R. Bischoff, F. Breitling, and A. Nesterov-Mueller. High-Density Peptide Arrays with Combinatorial Laser Fusing. *Advance Materialces*, 26:3730–3734, 2014.

[17] C. Schirwitz, F. F. Loeffler, T. Felgenhauer, V. Stadler, F. Breitling, and F. R. Bischoff. Sensing immune responses with customized peptide microarrays. *Biointerphases*, 7:1–9, 2012.

[18] S. Schillo. *Prozessentwicklung für die Automatisierung der Herstellung und Anwendung von hochdichten Peptidmicroarrays*. PhD thesis, Karlsruher Institut für Technologie, Karlsruhe, 2014.

[19] V. V. Buchanov, V. A Derzhavin, I. V. Zalesskiy, A. D. Reshetov, and A. I. Sarkisov, O. M. Shushin. Optical manipulators of microparticles using femtosecond laser radiation. *Quantum Electronics*, 40:446–450, 2010.

[20] W. Wang, Y. H. Lin, T. C. Wen, T. F. Guo, and G. B. Lee. Selective manipulation of microparticles using polymer-based optically induced dielectrophoretic devices. *Appl. Phys. Lett.*, 96:113302, 2010.

[21] A. Klini, P. A. Loukakos, D. Gray, A. Manousaki, and C. Fotakis. Laser induced forward transfer of metals by temporally shaped femtosecond laser pulses. *Opt. Express*, 16(15):11300–11309, 2008.

[22] K. Venkatakrishnan, B. Tan, and B. K. A. Ngoi. Femtosecond pulsed laser ablation of thin gold film. *Optics and Laser Technology*, 34:199–202, 2002.

[23] R. Baehnisch, W. Gross, and A. Menschig. Single-shot, high repetition rate metallic pattern transfer. *Microelectronic Engineering*, 50:541–546, 2000.

[24] G. Heise, M. Domke, J. Konrad, S. Sarrach, J. Sotrop, and H. P. Huber. Laser lift-off initiated by direct induced ablation of different metal thin films with ultra-short laser pulses. *J. Phys. D: Appl. Phys.*, 45:1–8, 2012.

[25] V. Dinca, A. Palla-Papavlu, M. Dinescu, J. Shaw Stewart, Lippert T.K., F. Di Pietrantonio, D. Cannata, D. Benetti, and E. Verona. Polymer pixel enhancement by laser-induced forward transfer for sensor applications. *Applied Physics A*, 101:559–565, 2010.

[26] N. T. Kattamis, N. D. McDaniel, S. Bernahard, and C. B. Arnold. Laser direct write printing of sensitive and robust light emitting organic molecules. *Appl. Phys. Lett*, 94:103306, 2009.

[27] J. Shaw-Steward, B. Chu, T. Lippert, Y. Maniglio, M. Nagel, F. Nueesch, and A. Wokaun. Improved laser-induced forward transfer of organic semiconductor thin films by reducing the environmental pressure and controlling the substrate-substrate gap width. *Appl. Phys. A*, 105:713–722, 2011.

[28] M. Colina, P. Serra, J.M. Fernandez-Pradas, L. Sevilla, and J.L. Morenza. DNA deposition through laser induced forward transfer. *Biosens Bioelectron*, 20:1638–1642, 2005.

[29] A. Karaiskou, I. Zergioti, C. Fotakis, M. Kapsetaki, and D. Kafetzopoulos. Microfabrication of biomaterials by the sub-ps laser-induced forward transfer process. *Applied Surface Science*, 208-209:245–249, 2003.

[30] P. Serra, M. Colina, J. M. Fernandez-Pradas, L. Sevilla, and J. L. Morenza. Preparation of functional dna microarrays through laser-induced forward transfer. *Applied Physics Letters*, 85(9):1639–1641, 2004.

[31] M. Duocastella, J. M. Fernández-Pradas, J. Domínguez, P. Serra, and J. L. Morenza. Printing biological solutions through laser-induced forward transfer. *Applied Physics A*, 93(4):941–945, 2008.

[32] B. Hopp, T. Smausz, G. Szabó, L. Kolozsvári, D. Kafetzopoulos, C. Fotakis, and A. Nógrádi. Femtosecond laser printing of living cells using absorbing film-assisted laser-induced forward transfer. *Optical Engineering*, 51(1):014302–1–014302–6, 2012.

[33] S. Genov, D. Riester, T. Hirth, G. Tovar, K. Borchers, and A. Weber. Preparation and characterisation of dry thin native protein trehalose films on titanium-coated cyclo-olefin polymer (COP) foil generated by spin-coating/drying process and applied for protein transfer by Laser-Induced-Forward Transfer (LIFT). *Chemical Engineering and Processing*, 50:558–564, 2011.

[34] A. Dinca, A. Ranella, M. Farsari, D. Kafetzopoulos, M. Dinescu, A. Popescu, and C. Fotakis. Quantification of the activity of biomolecules in microarrays obtained by direct laser transfer. *Biomed Microdevices*, 50:719–725, 2008.

[35] M. Colina, P. Serra, J. M. Fernandez-Pradas, L. Sevilla, and J. L. Morenza. DNA deposition through laser induced forward transfer. *Biosens Bioelectron*, 15:1638–1642, 2005.

[36] R. Fardel, M. Nagel, F. Nu, T. Lippert, and A. Wokaun. Laser forward transfer using a sacrificial layer: Influence of the material properties. *Applied Surface Science*, 254:1322–1326, 2007.

[37] Y. Xie. *The Nanobiotechnology Handbook*. CRC Press, 2012.

[38] J. S. Shaw-Stewart, R. Fardel, M. Nagel, P. Delaporte, L. Rapp, C. Cibert, A. P. Alloncle, F. Nueesch, T. Lippert, and A. Wokaun. The effect of laser pulse length upon laser-induced forward transfer using a trazene polymer as dynamic release layer. *Journal of Optoelectronics and Advanced Materials*, 12:605–609, 2010.

[39] N. T. Kattamis, P. E. Purnick, R. Weiss, and C. B Arnold. Thick film laser induced forward transfer for deposition of thermally and mechanically sensitive materials. *App. Phys. Lett.*, 91:171120, 2007.

[40] A. Palla-Papavlu, V. Dinca, C. Luculescu, J. Shaw-Stewart, M. Nagel, T. Lippert, and M. Dinescu. Laser induced forward transfer of soft materials. *J. Opt.*, 12:1–5, 2010.

[41] S. Williams, A. Kumar, and S.T. Wereley. Electrokinetic patterning of colloidal particles with optical landscapes. *Lab on chip*, 8:1879–1882, 2008.

[42] M. Abasaki, S. Souma, M. Takeda, N. Moronuki, and M. Sugiyama. Selective self-assembly of nanoparticles on trench sidewalls and its relationship with scallop nanostructure. pages 41–44, 2011.

[43] J. Aizenberg, P. V. Braun, and P. Wiltzius. Patterned colloidal deposition controlled by electrostatic and capillary forces. *Physical Review Letters*, 84:2997–3000, 2000.

[44] N. V. Dziomkina and G. J. Vancso. Colloidal crystal assembly on topologically patterned templates. *Soft matter*, 1:265–279, 2005.

[45] B. Gates, B. Mayers, Z. Y Li, and Y. Xia. Fabrication of micro- and nanostructures with monodispersed colloidal spheres as the active components. *Mat. Res. Soc Symp*, 636:D9.15.1, 2001.

[46] S. H. Lee, F. S. Diana, A. Badolato, P. M. Petroff, and E. J. Kramer. Self-assembling nanoparticles into holographic nanopatterns. *J. Appl. Phys.*, 95:5922–5924, 2004.

[47] C. C. Chang, T. Y. Juang, W. H. Ting, M. S. Lin, C. M. Yeh, S. A. Dai, S. Y Suen, Y. L. Liu, and R. J. Jeng. Using a breath-figure method to self-organize honeycomb-like polymeric films from dendritic side-chain polymers. *Materials Chemistry and Physics*, 128:157–165, 2011.

[48] K. M. Chen, X. Jiang, L. C. Kimerling, and P. T. Hammond. Selective self-organization of colloids on patterned polyelectrolyte templates. *Langmuir*, 16:7825–7834, 2000.

[49] B. B. Ke, P. C. Wan, L. S. Chen, L. Y. Zhang, and Z. K. Xu. Tunable assembly of nanoparticles on patterned porous film. *Langmuir*, 26:15982–15988, 2010.

[50] B. B. Ke, L. S. Wan, Y. Li, M. Y. Xu, and Z. K. Xu. Selective layer-by-layer self-assembly on patterned porous films modulated by cassie-wenzel transition. *Phys. Chem. Chem. Phys.*, 13:4881–4887, 2011.

[51] I. Lee, H. Zheng, M. F. Rubner, and P. T. Hammond. Controlled cluster size in patterned particle arrays via directed adsorption on confined surfaces. *Adv. Mater.*, 14:572–577, 2002.

[52] J. Park, Y. S. Kim, and P. T. Hammond. Chemically nanopatterned surfaces using polyelectrolytes and ultraviolet- cured hard molds. *Nano Letters*, 5:1347–1350, 2005.

[53] Y. Lu, Y. Yin, and Y. Xia. Three-dimensional photonic crystals with non-spherical colloids as building blocks. *Adv. Mater.*, 13:415–420, 2001.

[54] Y. Yin, Y. Lu, B. Gates, and Y. Xia. Template-assisted self-assembly: A practical route to complex aggregates of monodispersed colloids with well-defined sizes, shapes, and structures. *J. Am. Chem. Soc.*, 123:8718–8729, 2001.

[55] Y. H. Kim, J. Park, P. J. Yoo, and P. T. Hammond. Selective assembly of colloidal particles on a nanostructured template coated with polyelectrolyte multilayers. *Adv. Mater.*, 19:4426–4430, 2007.

[56] L. S. Wan, J. Lv, B. B. Ke, and Z. K. Xu. Facilitated and site-specific assembly of functional polystyrene microspheres on patterned porous films. *Applied Materials and Interfaces*, 2, 2010.

[57] Y. Zhang and C. Wang. Micropatterning of proteins on 3D porous polymer films fabricated by using the breath-figure method. *Adv. Mater.*, 19:913–916, 2007.

[58] T. Kraus, L. Malaquin, H. Schmid, and W. Riess. Nanoparticle printing with single-particle resolution. *Nature nanotechnology*, 2:570–576, 2007.

[59] A. N. Shipway, E. Katz, and I. Willner. Nanoparticle arrays on surface for electronic, optical, and sensor applications. *ChemPhysChem*, 1:18–52, 2000.

[60] J. Mohr, P. Bley, M. Strohrmann, and Wallrabe U. Microactuators fabricated by the LIGA process. *J. Micromech. Microeng*, 2:234–241, 1992.

[61] A. B. Fraizer and M. G. Allen. Metallic microstructures fabricated using photo-sensitive polyimide electroplating molds. *Journal of Microelectromechanical Systems*, 2:234–241, 1993.

[62] K. Kim, S. Park, J.-B. Lee, H. H. Manohara, Y. Desta, M. Murphy, and C. H. Ahn. Rapid replication of polymeric and metallic high aspect ratio microstructures using PDMS and LIGA technology. *Microsystem Technologies*, 9:5–10, 2002.

[63] A. del Campo and C. Greiner. SU-8: a photoresist for high-aspect-ratio and 3d submicron lithography. *J. Micromech. Microeng.*, 17:81–95, 2007.

[64] C.-H. Lin, G.-B. Lee, B.-W. Chang, and G.-L. Chang. Anewfabricat ion process for ultra-thick microfluidic microstructures utilizing SU-8 photoresist. *J. Micromech. Microeng.*, 12:590–597, 2002.

[65] MicroChem. Processing guidelines. `http://www.microchem.com/pdf/` `SU-82000DataSheet2000_5thru2015Ver4.pdf`.

[66] T. Sikanen, L. Heikkila, S. Tuomikoski, R. A. Ketola, R. Kostiainen, S. Franssila, and T. Kotiaho. Performance of SU-8 microchips as separation devices and comparison with glass microchips. *Anal. Chem.*, 79:6255–6263, 2007.

[67] J. H. Pai, Y. Wang, G. Salazar, C. E. Sims, M. Bachman, G. P. Li, and N. L. Allbritton. A photoresist with low fluorescence for bioanalytical applications. *Anal. Chem.*, 79:8774–8780, 2007.

[68] S. Sinzinger and J. Jahns. *Microoptics*. WILEY-VCH GmbH Co. KGaA, 2003.

[69] W. Menz, J. Mohr, and O. Paul. *Microsystem Technology*. Wiley-VCH GmbH, 2001.

[70] M. J. Madou. *Fundamentals of Microfabrication: The Science of Miniaturization*. CRC Press, 2002.

[71] W. M. Moreau. *Semiconductor lithography principles, practices and materials*. Plenum Press, 1988.

[72] S. Sakawaki. Spin coating process, May 12 1981. US Patent 4,267,212.

[73] D. Meyerhofer. Characteristics of resist films produced by spinning. *J. Appl.Phys.*, 49:3993–3997, 1978.

[74] D.-C. Hu and H.-C. Chen. Humidity effect on polyimide film adhesion. *Journal of Materials Science*, 27(19):5262–5268.

[75] K. L. Mittal. *Adhesion Aspects of Polymeric Coatings*. Springer Science Business Media, 2012.

[76] http://www.microchem.com/pdf/OMNICOAT.pdf.

[77] W.-M. Yeh, R. A. Lawson, L. M. Tolbert, and C. L. Henderson. A study of reactive adhesion promoters and their ability to mitigate pattern collapse in thin film lithography, 2011.

[78] J. Striffler. *Replikation von µ-Peptidarrays*. PhD thesis, Karlsruher Institut of Technologie, Karlsruhe, 2014.

[79] C. S Yoo. *Semiconductor manufacturing technology*. World scientific publishing Co. Pte. Ltd., 2008.

[80] J. R. Sheats and B. W. Smith. *Microlithography:science and technology*. Marcel Dekker, Inc., 1998.

[81] T. Winterstein and H. F. Schlaak. Charakterisierung des schrumpfs von SU-8 für intrinsisch vorgespannte mikrostrukturen. *Mikrosystemtechnikkongress*, pages 5262–5268, 2013.

[82] M. J. Jackson. *Micro and Nanomanufacturing*. Springer, 2007.

[83] M. Stepanova and S. Dew. *Nanofabrication:Techniques and Principles*, volume 7. Springer, 2012.

[84] Heidelbers instruments. User guide, system operation DWL 66FS.

[85] C. Mack. *Fundamental Principles of Optical Lithography: The Science of Microfabrication*. John Wiley Sons, Ltd, 2011.

[86] J. A. Bittencourt. *Fundamentals of Plasma Physics*. Springer, 2004.

[87] M. Sugawara. *Plasma Etching : Fundamentals and Applications: Fundamentals and Applications*. OUP Oxford, 1998.

[88] J. W. Coburn. *Plasma etching and reactive ion etching*. American Institute of Physics, 1982.

[89] R. Anderson, G. Ruhl, N. Sandlin, and M. Buie. Study of the role of Cl_2, O_2 and He in the chrome etch process with optical emission spectroscopy. *SPIE Proceedings*, 4889:641–652, 2002.

[90] Polysciences Inc. http://www.polysciences.com/.

[91] B. Muenster. *Entwicklung von Mikropartikeln für die kombinatorische Synthese hochdichter Peptidarrays durch laserbasierte Verfahren*. PhD thesis, Karlsruher Institut für Technologie, Karlsruhe, 2014.

[92] C. von Bojničić-Kninski. *Automatisierung eines Lasersystems zum ortsgenauen Transfer von Mikropartikeln*. Master thesis, Hochschule Karlsruhe, 2014.

[93] F. Maerkle. *Laserbasierte Verfahren zur Herstellung hochdichter Peptidarrays*. PhD thesis, Karlsruher Institut für Technologie, Karlsruhe, 2014.

[94] F. Breitling, V. Bykovskaya, K. Leibe, F. F. Loeffler, F. Maerkle, A. Nesterov-Mueller, S. Schillo, and C. von Bojničić-Kninski. Method for combinatorial particle manipulation for producing high-density molecular arrays, particularly peptide arrays, and molecular arrays which can be obtained therefrom, 17 2014.

[95] F. Breitling, V. Bykovskaya, K. Leibe, F. F. Loeffler, F. Maerkle, A. Nesterov-Mueller, S. Schillo, and C. von Bojničić-Kninski. Method for combinatorial particle manipulation for producing high-density molecular arrays, particularly peptide arrays, and molecular arrays which can be obtained therefrom, 17 2013.

[96] L. Rapp, C. Cibert, A. P. Alloncle, and P. Delaporte. Characterization of organic material micro-structures transferred by laser in nanosecond and picosecond regimes. *Applied Surface Science*, 255(10):5439 – 5443, 2009.

[97] Y. Ren, C. W. Cheng, J. K. Chen, Y. Zhang, and D. Y. Tzou. Thermal ablation of metal films by femtosecond laser bursts. *International Journal of Thermal Sciences*, 70:32–40, 2013.

[98] M. K. Sharma. *Optimization of Laser Induced Forward Transfer by Finite Element Modeling*. Master thesis, Royal Institute of Technology-KTH, 2013.

[99] Y. Liu, M. Q. Jiang, G. W. Yang, and L. H. Dai. Surface rippling on bulk metallic glass under nanosecond pulse laser ablation. *Appl. Phys. Lett.*, 99:191902, 2011.

[100] M. R. Kasaai, V. Kacham, F. Theberge, and S. L. Chin. The interaction of femtosecond and nanosecond laser pulses with the surface of glass. *Journal of Non-Crystalline Solids*, 319:129–135, 2003.

[101] F. Ferioli. *Experimental characterization of laser induced plasmas and application to gascomposition measurements*. Ph.d. dissertation, University of Maryland, 2005.

[102] A. Palla-Papavlu, V. Dinca, T. Lippert, and M. Dinescu. Laser induced forward transfer for material transfer. *Romanian Reports in Physics*, 63:12851301, 2011.

[103] L. Torrisi, A. Picciotto, L. Ando, s. Gammino, D. Margarone, L. Laska, M. Pfeifer, and J. Krasa. Pulsed laser ablation of gold at 1064 nm and 532 nm. *Czechoslovak Journal of Physics*, 54:421–430, 2004.

[104] X. Zhang, S. S. Chu, J. R. Ho, and D. Grigoropoulos. Excimer laser ablation of thin gold films on a quartz crystal microbalance at various argon background pressures. *Appl. Phys. A*, 64:545–552, 1997.

[105] P. D. Sawant, P. Livingston, and D. V. Nicolau. Microablation of gold nanolayers by direct write lithography. *Journal of Physics: Conference Series*, 34:22–27, 2006.

[106] M. S. Brown and C. B. Arnold. *Laser Precision Microfabrication*, chapter Fundamentals of Laser-Material Interaction and Application to Multiscale Surface Modification. Eds. Springer Berlin Heidelberg, 2010.

[107] V. Bykovskaya, C. von Bojničić-Kninski, F. Maerkle, D. Haeringer, B. Muenster, J. Striffler, L. Hahn, F. Loeffler, F. Breitling, and A. Nesterov-Mueller. Combinatorial laser transfer of polymer particles for microarray fabrication. *Technische Systeme fuer die Lebenswissenschaften*, pages 237–240, 2014.

[108] C. von Bojničić-Kninski. *Mikrostrukturen basierte ultra-hochdichte Peptidarrays*. PhD thesis, Karlsruhe Institute of Technology, Karlsruhe, expected in 2017.

[109] D. Althuon, F. Breitling, V. Bykovskaya, F. F. Loeffler, A. Nesterov-Mueller, R. Popov, B. Ridder, and C. von Bojničić-Kninski. Ultra-hochdichte oligomerarrays und verfahren zu deren herstellung, 15 2015.

[110] J. Hanne, H. J. Falk, F. Goerlitz, P. Hoyer, J Engelhardt, S. J. Sahl, and Hell S. W. STED nanoscopy with fluorescent quantum dots. *Nature Comunication*, 6:1–6, 2015.